ADAS-EU R(12)SU01

ADAS-EU
ADAS for fusion in Europe

Grant: 224607

Hugh Summers, Nigel Badnell, Martin O'Mullane, Francisco Guzman,
Luis Menchero and Alessandra Giunta

SUBC1: Sub-contract specifications, deliverables, integration and analysis

18 Jan 2012

Workpackages : ??-??-??
Category : DRAFT – CONFIDENTIAL

SUBC1: Sub-contract specifications, deliverables, integration and analysis

Hugh Summers, Nigel Badnell, Martin O'Mullane, Francisco Guzman, Luis Menchero and Alessandra Giunta

Department of Physics, University of Strathclyde, Glasgow, UK

Abstract: *The primary set of ADAS-EU sub-contracts, issued in 2009 and 2010, comprised six work packages. The packages were issued to six university groups in Europe and targetted critical specialised data in which these groups had unique capability. The tasks spanned items in heavy element structure, electron impact ionisation and recombinaation and items in charge exchange spectroscopy for medium/heavy elements. Initially scheduled times for task completion proved unrealistic. Extended completion dates were issued and task completions and deliveries began from mid-2011 through to end-2011. This report is a comprehensive document bringing together the objectives of the sub-contracts, the datasets and machinery resulting from them, the analysis, placing and integration of these items into ADAS modelling, and lastly the consequences for fusion plasma modelling. It is anticipated that a further three short duration sub-contracts will be issued in early-2012 for completion by end 2012. These will allow follow-up and extended development of some of the outcomes of the primary sub-contract set of special relance to ITER.*

Contents

Chapter 1

Introduction

The radiation by impurities in plasma driven by collisions with Maxwellian free electrons is an on-going area of importance for fusion. The ADAS Project was targetted, inter alia, on this and has over the years built the atomic datasets and atomic population modelling for sophisticated description of these radiating properties both for plasma modelling and for spectroscopic diagnostic analysis. These datasets grow and the modelling evolves as the impurity species change and new operating scenarios come into play. In this respect, the requirements of ITER has moved the impurity focus away from light elements to very heavy species, especially tungsten, and to lower temperature divertors. A core activity, in the electron collision area, of ADAS and ADAS-EU in the last three years has been the establishment of a confident comprehensive baseline of atomic modelling for these ITER species and scenarios and its associated validation on current machines such as the upgraded JET, AUG and MAST. The details of the baseline creation and its large scale systematic improvement are given in the ADAS-EU report PUBL_3. ADAS-EU sub-contracts in this area have been designed to enable targetted, high precision imnprovements to the baseline guided by the evolving ITER needs.

Tungsten presents special difficulties for atomic physics as the neutral species, W^0, entering the plasma by sputtering from a material surface, such as a divertor strike plate or divertor throat, and then ionises through the W^{+1} and W^{+2} stages. The interpretation of the observed emission in spectral lines of these ions as an element influx needs the theoretical quantities called *photon efficiencies*. W^0 has several metastable states and a complex set of intereacting electronic configurations which lead to hundreds of thousands of levels and millions of transitions. Ab initio calculations of the atomic structure cannot approach the wavelength or transition probability precision required for spectral analysis. ADAS-EU sub-contract 1 was with the atomic physics group of Prof. Biémont at the University of Mons-Hainaut, Belgium. This group has specialised in laser-induced fluorescent spectroscopy of very complex neutral and near neutral atoms of elements such as rare earth and (for the present fusion interest) tungsten. The energy levels and transition probabilities of the neutral and near-neutral tungsten atoms and ions were the target of the ADAS-EU engagement with Mons-Hainaut. The sub-contract objectives are summarised in Appendix A. Crucially, the Mons-Hainaut team analyse and summarise their experimental results using the support vehicle of the atomic structure code of Cowan [**?**]. Optimisation of selected parameters (especially finite nuclear radius and polarisation) with respect to the observational data allows convergence on an acceptable atomic structure, consistent with the most important observed energy levels and transition probabilities, from which the collisional population models can be built. Fortunately, the ADAS baseline data uses the Cowan structure code as a starting point, so the Mons-Hainaut work, in principle, can link directly through to ADAS. Chapter 2 reports on the implementation of sub-contract 1 and the exploitation of these connections.

A second concern is the confident establishment of the ionisation state of low to moderate charge tungsten ions in thermal plasma. First comparative studies with experimental evidence from AUG by Pütterich using the ADAS baseline for the theoretical model indicated a progressive shift, from theory moving downward in ionisation state from $z \sim 25$. Pütterich arbitrarily viewed this as a shift in the recombination coefficients and introduced an experimentally based correction. In the meantime, the newer universal configuration-average-distorted-wave approximation (CADW) for ionisation cross-sections of Pindzola, Loch et al. has become part of ADAS and incorporated into its baseline modelling. Precision measurements of ionisation cross-sections by the Giessen team of Müller and Schippers have recently been focussed on heavy atoms and in generally are compared and contrasted with CADW. For recombina-

tion, most recent theoretical progress has been on so-called low-temperature dielectronic recombination. Previously believed to be of small relevance to the high temperature dielectronic recombination of the fusion plasma, nonetheless, Müller and Schippers measurements of dielectronic recombination do suggest situations in which very large low energy resonance structure is present and can influence the high temperature regime. Such structure is very sensitive to precise energy level structure in the vicinity of the ionisation threshold and, as indicated by Loch and Robicheaux, needs to be handled in the framework of high level population modelling. ADAS-EU sub-contract 2 was placed with the atomic physics group of Prof. Müller at the University of Giessen, Germany. It was designed to clarify these issues for tungsten and to allow ADAS to refine its ionisation and recombination cross-section models appropriately. Chapter 3 reports on the implementation of sub-contract 2 and the exploitation of these connections.

As noted earlier, the ADAS baseline relies on the Cowan program, with default parameters, for complex atom atomic structure. Selective experimental refinement of Cowan parameters for neutral and near neutral tungsten ions was addressed in the first paragraph. From an ab initio theoretical point of view, improvement might be expected for low and intermediate ionisation stages of tungsten by extended handling of configuration interaction beyond the capabilities of the Cowan code - with present computational resources. The atomic physicists of the Institute of Theoretical Physics and Astronomy, University of Vilnius, Lithuania have special capabilties in this regard. The very large configuration interaction (Yutsis approach) of Bogdanovich et al. can address these tunsten ions and would be of particular value to ADAS, extended to include a Born approximation collisional model. The Vilnius team has also special experience and insights into certain characteristic patterns of configuration intereaction which can refine ADAS baseline modelling. Other special capabilities include fully relativisitic structure and multiple ionisation. ADAS-EU sub-contract 3 was placed with the Vilnius team to enable exploitation of these items in tunsten ions for ADAS. Chapter 4 reports on the implementation of sub-contract 3 and the exploitation of these connections. This work was closely linked to the in-house electron impact collision cross-section work of Professor Badnell and there was close collaboration. Additional possibilities for exploitation beyond the present report is one of the concerns of the ADAS-EU Electron Collision Working Party (ECWP) directed by Professor Badnell. Additional information is available in the ECWP report.

The second large on-going area of atomic physics interest for fusion is charge exchange spectroscopy using neutral hydrogen beams. In recent years ADAS has been concerned with extension of charge exchange to heavier, more highly ionised ions as receivers. Based on earlier studies and compilations of state selective charge exchange cross-section data, ADAS implemented a univeral parametric approximation to state selective charge exchange from hydrogen in fast beams for arbitrarily charged receiver ions. An objective in ADAS-EU has been to refine the data available for light element receivers, to validate and make available data for argon ions Ar^{+16}, Ar^{+17} and Ar^{+18} and to validate and refine the universal formulation through to receiver ions as highly charged as W^{+60}. There are special capabilities for theoretical modelling of state selective charge exchange cross-sections from fast neutral hydrogen isotope beam donors in Europe. For ADAS-EU, sub-contracts have been placed with appropriate university groups to procure calculations of selected reference data to the above ends for exploitation in ADAS charge exchange effective emission models. These are summarised in the following paragraphs.

Atomic-orbital-close-coupling (AOCC) is the most sophisticated theoretical method for calculation of charge exchange capture to excited hydrogenic *nl*-shells of bare nucleus receivers from hydrogen isotope donors at beam energies through the key range 10keV/amu - 100keV/amu. Updated code versions in this approach are ideal for filling in precision data for light element ions such as N^{+7} in ADAS, where previously interpolation between adjacent stages was used. Also the updated codes can re-verify the older work for ions such as O^{+8}. These revised codes however employ sophisticated compuational algortihms which now allow more highly ionised systems Ar^{+18} with very many receiver shells to be addressed. ADAS-EU sub-contract 4 was placed with the Technical University Wien (TUW), Vienna, Austria. Katharina Igenbergs of the TUW team has been leading the implementation of parallelised AOCC codes on supercomputers which allow access the required level sets of systems up to Ar^{+18}. The primary sub-contract work related to the the light elements (especially N^{+7} and O^{+8}. But progress was outstanding and Katharina was also able to make available data for Ar^{+18} to ADAS-EU at this time also. This has important implications for the validation of all the ADAS charge exchange data for highly charged ions. Chapter 5 reports on the implementation of sub-contract 4 and outlines the exploitation of the results.

Receivers such as Kr^{+36} are far outside the current scope of AOCC since visible spectroscopic emission following charge transfer occurs from very high n-shells (~ 30). For such systems, the simpler classical-trajectory-Monte-Carlo (CTMC) method only can be used. This method primarily applies to collision energies greater than 100keV/amu. However a modification, called CTMC-improved, developed by the team at the University Autonoma, Madrid, Spain, with a better classical representation of the ground state hydrogen distribution, is believed to remain valid to lower

energies. Divergence of CTMC-improved from the original CTMC at lower energies and higher shells for higher charged states is marked. ADAS-EU sub-contract 5 was placed with the University Autonoma, Madrid, Spain to calculate CTMC-improved state selective capture for Ar^{+18} and Kr^{+36}. Additional objectives included sophisticated calculations for B^{+5} in the molecular-orbital-close-coupling (MOCC). This method, comparable in precision to AOCC is applicable to the low energy regime ¡ 20keV/amu and is matched to CTMC-improved at higher energies.Chapter 6 reports on the implementation of sub-contract 5 and outlines the exploitation of the results. ADAS-EU sub-contracts 4 and 5 are linked amd mutaully reinforcing. The extended exploitation of the ADAS-EU charge exchange sub-contracts is given in the main ADAS-EU report PUBL_1.

Sub-contract 6, the last of the primary set of sub-contracts was with Professor Hoekstra, KVI, Universoity of Groningen. It concerned updating of a range of other hydrogen and proton impact data associated with neutral beams. Changes in direction at KVI meant that it was not possible to complete the work according to the original contract. The contract was terminated with approximately 1/4 completed. The report on this is in preparation and will be added as Chapter 7 when available.

The the light of the success and very productive character of these sub-contracts, it is intended to place follow-up sub-contracts with University of Vilnius and University of Mons-Hainaut. These will enable a large amount of extra data to be added to the ADAS databses exploiting the new methods and links established. These extra data will be of long term general value to fusion. A last sub-contract will be placed with Queen's University, Belfast, Northern Ireland. This will be closely linked to our own in-house electron impact excitation cross-section calculations at the highest level of precision (Rmatrix methods) and for the most complex of the tungsten systems. Greater detail is given in the ECWP report.

Chapter 2

Influx of low ionisation stages of tungsten

The authors of this chapter are Emile Biémont, Patrick Palmeri, Pascal Quinet, Martin O'Mullane and Hugh Summers. It incorporates the brief report on ADAS-EU sub-contract 1 prepared by the Astrophysics and Spectroscopy group, University of Mons, Belgium (E. Biémont, P. Palmeri & P. Quinet) dated 9 November 2011. See also appendix A.

2.1 Background

One of the main goals of the Atomic Data and Analysis Structure (ADAS) Project is to provide, with an appropriate accuracy, all the atomic data required for global modelling and quantitative spectroscopic diagnosis and analysis of fusion plasmas. The system is based on the initial preparation of collections of fundamental atomic transition probability and excitation rate data for specific ions called specific ion files. Several ADAS computer codes then prepare all the derived data (such as net power loss coefficients, spectral line contribution functions, ...) in a form directly usable in experimental analysis and in plasma models. The effectiveness and precision in the applications depends of course on the availability and quality of fundamental data. In that context a specific need is enhanced provision for low ionisation stages of heavy elements up to and including tungsten, this latter element playing a very important role since it will be used in divertor tiles of the ITER tokamak. One of the main sources of spectroscopic properties of such heavy atoms and ions is the Astrophysics and Spectroscopy (ASPECT) group of Mons University (Belgium). This group has developed and systematised methods of atomic structure calculations essentially based on the relativistic Hartree-Fock (HFR) approach of Cowan [1] in which core-polarization has been included [2] giving rise to the so-called HFR+CPOL method. This theoretical approach, combined with a semi-empirical adjustment of the radial parameters in order to minimize the discrepancies between calculated and available experimental energy levels, has been proven to provide reliable transition probabilities in many complex systems such as neutral and lowly ionized atoms belonging to the fifth, the sixth and the lanthanide groups of the periodic table. In a large number of cases, the accuracy of the calculations has been assessed through comparisons with experimental measurements of radiative lifetimes using laser-induced fluorescence (LIF) spectroscopy.

2.2 Atomic structure calculations in W, W^+ and W^{+2} ions

During the last few months, the ASPECT group of Mons University has carried out atomic structure calculations in neutral, singly ionized and doubly ionized tungsten. To do so, the semi-empirical HFR+CPOL method mentioned above has been used with the physical models reported in Table 1. In each case, the accuracy of the computed transition rates was highlighted by the good agreement observed with the LIF measurements available in the literature (for W I) or performed by the ASPECT group in collaboration with Lund University, Sweden (for W II and W III). The final sets of transition probabilities were published in several papers [3-6] and in the DESIRE atomic database [7].

Table 1. Electronic configurations and core-polarization parameters used in atomic structure calculations of W I, W II and W III.

W I		W II		W III	
Even parity	Odd parity	Even parity	Odd parity	Even parity	Odd parity
$5d^46s^2$	$5d^46s6p$	$5d^5$	$5d^46p$	$5d^4$	$5d^36p$
$5d^56s$	$5d^46s7p$	$5d^46s$	$5d^47p$	$5d^36s$	$5d^37p$
$5d^57s$	$5d^56p$	$5d^47s$	$5d^48p$	$5d^37s$	$5d^38p$
$5d^6$	$5d^57p$	$5d^48s$	$5d^36s6p$	$5d^38s$	$5d^26s6p$
$5d^46s7s$	$5d^46s5f$	$5d^36s^2$	$5d^36s7p$	$5d^26s^2$	$5d^26s7p$
$5d^46s6d$	$5d^55f$	$5d^36s7s$	$5d^36s8p$	$5d^26s7s$	$5d^26s8p$
$5d^56d$	$5d^36s^26p$	$5d^36s8s$	$5d^26s^26p$	$5d^26s8s$	$5d6s^26p$
$5d^46p^2$	$5d^36p^3$	$5d^46d$	$5d^26p^3$	$5d^36d$	
$5d^46d^2$	$5d^26s6p^3$	$5d3^6s6d$		$5d^26s6d$	
$5d^36s6p^2$		$5d^36p^2$		$5d^26p^2$	
$5d^26s^26p^2$		$5d^26s^26d$		$5d6s26d$	
W V ionic core :		W IV ionic core :		W VI ionic core :	
α_d = 4.59 a_0^3		α_d = 4.59 a_0^3		α_d = 4.00 a_0^3	
r_c = 1.99 a_0		r_c = 1.77 a_0		r_c = 1.66 a_0	

2.3 Integration of W I-III data into ADAS

Two input files of the Cowan code (ing11 files) per ion, one for the radiative data and a second one for the collision data, containing the optimized radial parameters (Slater, spin-orbit, radiative transition, and Bessel radial integrals) have been transferred to generate higher quality plane-wave Born collision strengths and transition probabilities on the basis of good atomic structures. This part of the work has been performed in collaboration with ADAS-EU staff thanks to visits of Dr. M. OMullane to Mons University who modified the adas8#1 script to use the supplied data as optional input. The ADAS staff will then produce the data (such as photon emissivity coefficients, ...) for transitions of interest for fusion influx spectroscopy.

2.4 Perspectives and recommendations

In view of the large number of new atomic parameters obtained in neutral and lowly ionized tungsten, it is proposed that the Mons group visit the JET facility in order to discuss with spectroscopists working in this laboratory. This would be a good opportunity to compare the the new data with observations made in plasma spectroscopy. It is also proposed that the behaviour of the photon emissivity coefficients (PEC) derived from atomic structure calculations be compared to emipirical data measured in Jlich laboratory. Finally, a similar work will be carried out for other elements of interest for fusion. Among these elements, let us mention Ta I, Ta II, Ta III, Re I and Re II for which atomic structure calculations have already been published [8-12] and higher ionisation stages of tungsten such as W IV, W V and W VI for which calculations are currently in progress. It is worth noting that for these latter three ions, no experimental radiative data are available so that the accuracy of the results obtained will be assessed through comparisons with other theoretical approaches such as the purely relativistic multiconfiguration Dirac-Fock method.

2.5 References

[1] R.D. Cowan (1981) The Theory of Atomic Structure and Spectra, Univ. California Press, Berkeley.
[2] P. Quinet, P. Palmeri, E. Biémont, M.M. McCurdy, G. Rieger, E.H. Pinnington, M.E. Wickliffe, J.E. Lawler (1999) Mon. Not. R. Astr. Soc. 307, 934
[3] P. Palmeri, P. Quinet, V. Fivet, E. Biémont, H. Nilsson, L. Engstrm, H. Lundberg (2008) Phys. Scr. 78, 015304
[4] H. Nilsson, L. Engström, H. Lundberg, P. Palmeri, V. Fivet, P. Quinet, E. Biémont (2008) Eur. Phys. J. D 49, 13
[5] P. Quinet, V. Vinogradoff, P. Palmeri, E. Biémont (2010) J. Phys. B : At. Mol. Opt. Phys. : Special issue on Spectroscopic Diagnostics of Magnetic Fusion Plasmas 43, 144003
[6] P. Quinet, P. Palmeri, E. Biémont (2011) J. Phys. B : At. Mol. Opt. Phys. 44, 145005

[7] http://w3.umons.ac.be/astro/desire.shtml
[8] V. Fivet, P. Palmeri, P. Quinet, E. Biémont, H.L. Xu, S. Svanberg (2006) Eur. Phys. J. D 37, 29
[9] P. Quinet, V. Fivet, P. Palmeri, E. Biémont, L. Engström, H. Lundberg, H. Nilsson (2009) Astron. Astrophys. 493, 711
[10] V. Fivet, E. Biémont, L. Engström, H. Lundberg, H. Nilsson, P. Palmeri, P. Quinet (2008) J. Phys. B: At. Mol. Opt. Phys. 41, 015702
[11] P. Palmeri, P.Quinet, E. Biémont, S. Svanberg, H.L. Xu (2006) Phys. Scr. 74, 297
[12] P. Palmeri, P. Quinet, E. Biémont, H.L. Xu, S. Svanberg (2005) Mon. Not. R. Astr. Soc. 362, 1348

Chapter 3

Electron-ion recombination and electron-ion impact ionisation of many-electron atomic ions

The authors of this chapter are Alfred Müller, Stefan Schippers, Martin O'Mullane and Hugh Summers. It incorporates the brief report on ADAS-EU sub-contract 2 prepared by the Institut für Atom- und Molekülphysik, Justus-Liebig-Universität Giessen, Germany (Alfred Mller and Stefan Schippers) dated 30 July 2011. See also appendix B.

3.1 Background

Colliding-beams measurements of cross sections for electron-impact ionization and electron-ion recombination of many-electron ions have been performed and are discussed in the light of available theoretical results. In the recombination of ions such as W20+ and Au25+ very large cross sections were observed for dielectronic recombination at low energies. Peak features seen in the cross sections for these ions suggest the presence of large numbers of unresolved, possibly unresolvable resonances. Ionization of xenon ions was studied for charge states q between 1 and 25. Even for the very high charge states, where the distorted wave approximation is expected to provide good results, the calculated cross sections are found to be about 30 to 50 % below the experimental data. Important processes appear to be missing in the theoretical treatments. It is suggested that resonant cross section contributions have to be considered in addition to direct ionization and excitation-autoionization. Within the frame of the ADAS-EU sub-contract the Giessen group has investigated electron- ion processes involving complex, multi-electron ions. The main findings are summarized in this final report.

3.2 Electron impact ionization of many-electron ions up to high charge states

Cross section measurements for electron impact single and multiple ionization of a number of xenon ions in different charge states have been published previously. A comprehensive theoretical study of electron impact single ionization covering all charge states of the xenon atom has previously been reported by Loch et al. [1]. However, prior to the present study no comprehensive systematic experimental investigation has been undertaken. The highest xenon ion charge state for which experimental data from crossed-beams experiments were available in the literature is Xe10+. In contrast, the present study covers all xenon ion charge states from q=1 to q=25. A previous experimental study of the ionization of Xe43+ ions has been carried out with an electron beam ion trap [2] resulting in the determination of relative cross sections that were put to an absolute scale by normalization. For the present measurements, a well-established electron-ion crossed beams technique was employed. High quality absolute cross section data and high-resolution energy-scan spectra were obtained for the investigated xenon ions. The Giessen group has also started to study ionization of tungsten ions. Cross sections for several charge states up to q=17 are now available.

It is interesting to note the discrepancy between experiment and theory for the ionization of Xe2+ ions. Griffin et al. [3] provided a configuration average distorted wave (CADW) calculation including direct ionization and excitation-autoionization processes. The resulting cross section is shown in Fig.1 together with the present experimental data. At energies below 80 eV the calculation significantly underestimates the measured cross section. There is a number of reasons that can be responsible for this discrepancy. Already the (4d105s25p4) ground state configuration of Xe2+ involves long lived excited states with excitation energies up to about 4.5 eV [4]. The experimental cross sections indicate the presence of initial states excited by up to about 15 eV. Configurations with such states comprise (4d105s25p4),

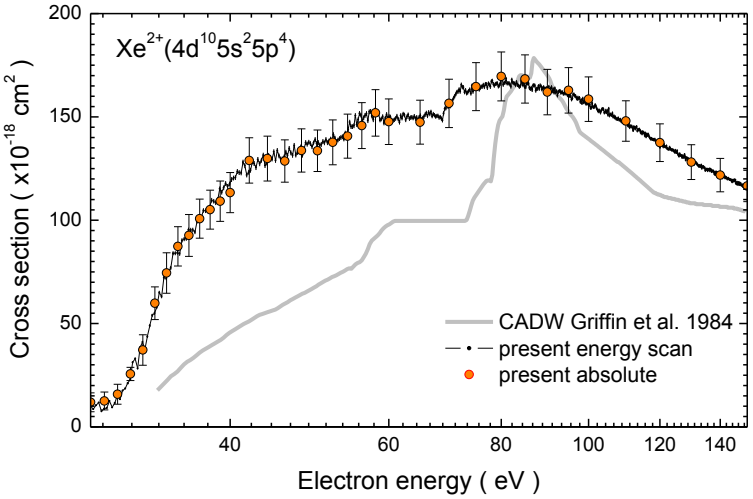

Figure 3.1: Cross sections for electron impact single ionization of Xe2+ ions [6]. The solid gray line is the configuration averaged distorted wave (CADW) calculation carried out in 1984 by Griffin et al. [3]. The circles are absolute Giessen measurements and the dots connected by thin solid lines represent the energy scan data.

(4d105s5p5), (4d105s25p35d), and (4d105s25p36s). There is no experimental access to the fractions of the many different states that can be present in the parent ion beam. Calculations for direct single ionization of these excited states using the Los Alamos Atomic Physics Codes (http://aphysics2.lanl.gov/tempweb/lanl/) compared with the experimental observations yield metastable contents of the primary ion beam of the order of 10 to 15codes one finds that excitation of a 5s electron in (4d105s25p35d) produces autoionizing states with large collision strengths at energies just above the ground-state ionization threshold. Such excitations can partly fill up the gap between the measured and calculated cross sections shown in Fig. 1. Another reason, that might be responsible for the differences between theory and experiment in Fig. 1, is that resonances in the different excitation channels have not been taken into account in the calculations. It is well known, however, that electron impact excitation is often dominated by resonances [5].

The general wisdom about the theoretical description of electron impact ionization of ions has been that theory becomes more reliable when the ion charge state increases. Electron-electron interactions become less important in comparison with electron-nucleus interactions. As a result one would expect CADW theory to be quite reliable for charge states q beyond approximately 10. The present study on Xeq+ ions shows that this is not necessarily the case.

As an example of the new data obtained for higher xenon charge states Fig. 2. shows the cross section for electron impact single ionization of Xe22+ ions [6]. The experimental data are compared with theoretical results of Mandelbaum et al. [7]. The most important contributions of excitation-autoionization (EA), i.e., non-resonant excitation of an electron from the 3d and 3p subshells with subsequent autoionzation have been taken into account. The cross sections calculated for EA channels greatly exceed those for direct ionization. Given the present state of the analysis, conservative error bars are provided for the absolute experimental data points. The comparison shown in Fig. 5. indicates a substantial discrepancy between theory and experiment. Considering the rich resonance structure found in the experimental energy-scan data, this discrepancy might be explained by the contribution of indirect ionization proceeding via resonant excitation of an inner shell electron (with simultaneous capture of the incident electron) and subsequent emission of two electrons.

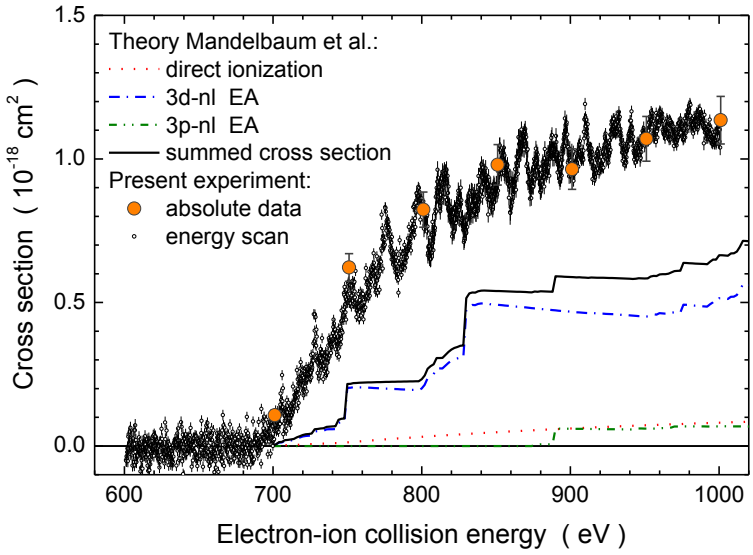

Figure 3.2: Electron impact ionization of Xe22+ ions: present preliminary experimental results [6] with conservative error bars and theoretical calculations by Mandelbaum et al. [7] including indirect ionization through non-resonant excitation-autoionization (EA) of 3p and 3d subshells.

Summarizing this investigation of electron-impact ionization of xenon ions, we have significantly extended the range of charge states accessible to crossed beams measurements. The experimental data tend to substantially exceed theoretical predictions based on the separate treatment of direct ionization and excitation-autoionization contributions. The distinct threshold step features obtained by theory for excitation-autoionization of Xeq+ ions are almost never seen in the experiments (few indications may be visible in Fig. 1.) where steps appear to be washed out to an extent that makes them mostly undetectable. This effect cannot be explained by limited energy resolution of the experiments. The present setup is characterized by energy spreads of less than 0.5 eV below 100 eV electron energy and less than 3 eV below 1 keV. With this low energy spread detailed scan measurements were carried out for all cross sections measured. Especially for the highest charge states large resonance features have been found. The large number of resonances that can be expected in ions as complex as the ones studied here certainly cannot be individually distinguished even with the relatively good resolution of the present experiment. The resonance features seen in the measured cross sections must rather be regarded as the remaining structure obtained when large numbers of individual resonances are smeared out with a given energy distribution function. The individual resonances only leave a trace in this convolution because they are not evenly distributed across the collision energy axis and because they have vastly different widths and sizes. What the experiment can resolve must therefore be the ”tips of icebergs”. Thus, the resonance contributions may be of much greater importance for electron impact ionization than usually expected. So far it has been assumed that distorted wave calculations should deliver increasingly better results as the charge state of the ions increases. This expectation may have to be revised after the present experimental study. Another complex task arising in the theoretical modeling of experimental data on ionization of ions is due to the presence of unknown fractions of metastable ions in the parent ion beams used in the experiments. There is no general solution of this problem. Even in ion storage rings or traps, highly excited states may survive accessible storage times and contribute to the signals measured. The Giessen group will continue to help resolve these issues by carrying out both crossed-beams and storage ring merged-beam experiments on electron impact ionization of ions. Close interaction with ADAS-EU representatives on this subject will continue.

3.3 Recombination of many-electron ions with electrons

Early experiments on electron-ion recombination revealed unexpected features in the cross sections at low energies. Huge recombination rates were observed at electron-ion collision energies below 1 eV for many-electron ions such

as U28+ [8] and Au25+ [9]. The origin of enhanced recombination rates has been investigated in numerous merged-beam experiments. One effect, that can even be observed with completely ionized parent ions such as C6+ [10], Cl17+ [11] and U92+ [12] originates from the merged-beam technique itself. For the merging of a beam of fast ions with energetic electrons magnetic fields are required that induce motional electric fields in the rest frame of the ions. The time dependence of these fields in conjunction with relaxation processes in the electron-ion complexes leads to enhanced recombination at energies in the meV range. Actually, by these effects the recombination threshold is softened and below-threshold states play a role in the recombination processes. This is similar to the situation in a finite density plasma as discussed recently by Robicheaux et al. [13]. Fig. 3. shows an example.

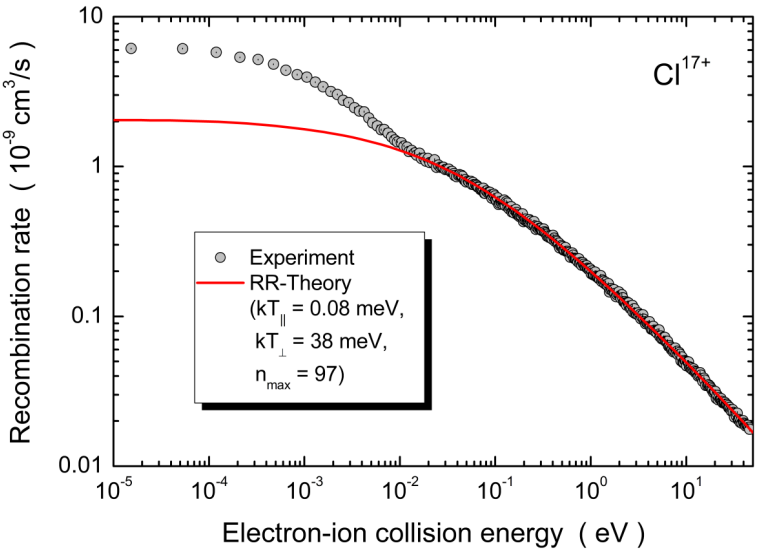

Figure 3.3: Storage ring recombination rate coefficient measured for Cl17+ ions [11] in comparison with the theoretical result for radiative recombination at the indicated electron beam temperatures and the maximum principal quantum number (97) of the recombined ion in the experiment. The rate enhancement factor at energies below 1 meV is approximately 3.

The second effect producing very high recombination rates at low energies is found mainly with many-electron ions. Ions with several electrons in open subshells have densely spaced excited levels. Each of these excited levels is associated with a Rydberg series of states in the recombined ion. With the high density of resonant states, there is a high probability for resonances to occur at low electron-ion collision energies E. The cross sections for resonant recombination scale by a factor 1/E so that greatly enhanced recombination rates can result. An example is provided in Fig. 4 which shows the merged-beam recombination rate coefficient of U28+ [8]. Resonances at very low energies result in an enhancement over plain radiative recombination by almost a factor 100.

In some cases the density of excited states in the threshold region is exceptionally high. A first example of that kind was found to be the Xe-like Au25+ ion with the ground state

configuration 4s24p64d104f8. For this ion the merged-beam recombination rate coefficient found experimentally at electron-ion collision energies below about 10 meV even reaches a maximum of 72010-9 cm3/s. Moreover, the resonances are apparently so densely spaced that little structure remains in the energy dependence of the rate coefficient. This is demonstrated by Fig. 5. It is difficult to handle such ions in storage rings since the electron cooling leads to a very rapid exponential loss of the stored ion beam by electron-ion recombination at cooling energy, i.e. at E=0.

The rate enhancement characteristic for all electron-ion merged-beam experiments in the meV energy range is illustrated by inset a) of Fig. 5. A feature similar to the one in Fig. 3 is seen also for Au25+. Inset b) shows the large peak features probably consisting of very many unresolvable dielectronic recombination resonances. The rate coefficients at each peak

maximum reach almost a size of 10-8 cm3/s. At these energies radiative recombination is already down below 10-11 cm3/s.

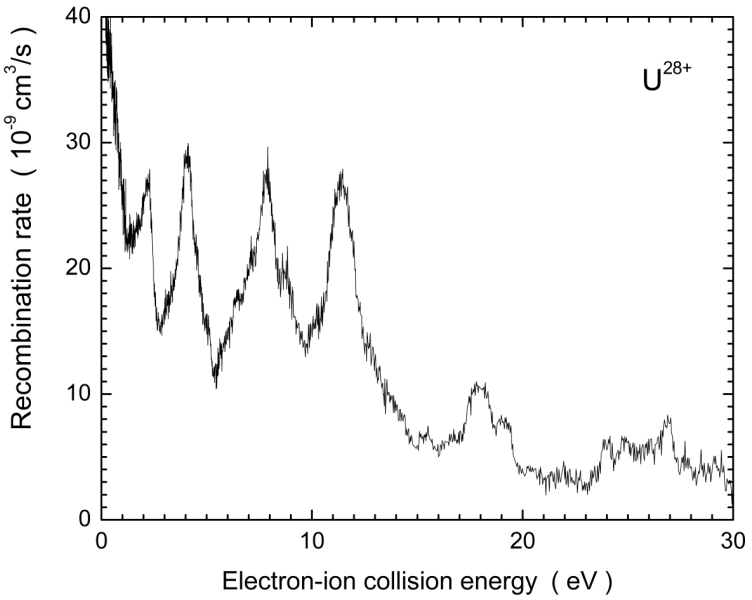

Figure 3.4: Merged-beam recombination rate coefficient measured for U28+ ions [8]. The ordinate units are the same as in Fig. 3. At energies below 1 eV a maximum rate coefficient of 20010-9 cm3/s was observed which is more than 30 times above that of Cl17+ ions.

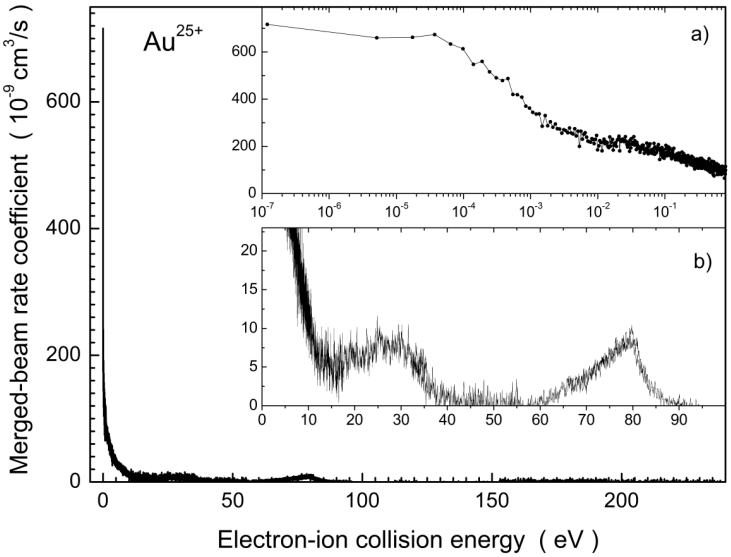

Figure 3.5: Merged-beam recombination rate coefficient measured for Au25+ ions [9]. The ordinate units are the same as in Figs. 3 and 4. Because of the huge recombination rate at zero energy, the comparatively big peak features at around 25 eV and 75 eV are optically suppressed. The insets a) and b) show parts of the data on different scales, magnifying features that are not seen in the main frame of the figure. The scale units are unchanged. Inset a) shows the variation of the rate in the threshold region. Inset b) amplifies the features seen at higher energies.

Excessive recombination rates have been found in several other ion species at cooling energy, i.e., at E=0. Among these are Cu-like Pb53+ [12] and Au50+ [13] both with recombination rates at cooling yet another order of magnitude higher than the one seen in Au25+. The most recent example of that kind is W20+ [14]. The result of our storage-ring merged-beam experiment is shown in Fig. 6. At electron-ion collision energies close to the threshold (E=0) the merged- beam recombination rate coefficient is now more than 500010-9 cm3/s. It exceeds that of plain radiative recombination by almost a factor 2000.

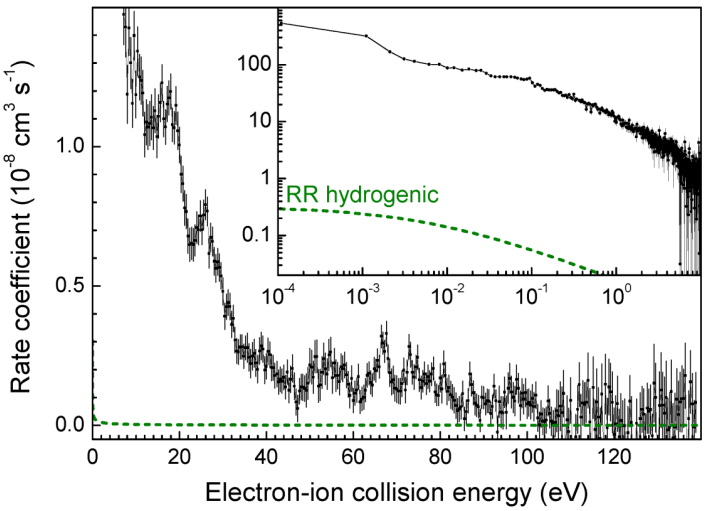

Figure 3.6: Storage-ring merged-beam recombination rate coefficient measured for Xe-like W20+ ions [14]. The short-dashed curve is the rate coefficient for radiative recombination (RR) calculated by using a hydrogenic approximation. The inset shows the same data in a log-log representation and with finer energy bins emphasizing the rate coefficient at very low energies.

The very large feature at zero energy decreases as the electron-ion collision energy increases. It reaches a sort of a base value of about 210-9 cm3/s at an energy of approximately 30 eV. When this result is converted to a plasma rate coefficient the zero energy feature turns out to be so large that it influences the recombination inside a collisionally ionized plasma even at the temperatures corresponding to about 200 eV where W20+ is formed. It exceeds the plasma recombination rate coefficient used for current plasma modelling by at least a factor of 4 in that temperature range.

There is an apparent deficit in the theoretical description of electron-ion recombination processes involving complex many-electron ions. Further work will be necessary to develop suitable approaches that can be used in plasma modeling calculations. The experimental data that have been obtained in our group partly in collaboration with colleagues from the Max- Planck-Institute for Nuclear Physics in Heidelberg and the Columbia Astrophysics Laboratory in New York will provide a basis for further theoretical developments. It is planned to continue the fruitful collaboration with ADAS-EU on electron-impact ionization and electron- ion recombination of multiply charged many-electron atoms.

3.4 References

[1] S. D. Loch,M. S. Pindzola, D. C. Griffin (2008) Int. J. Mass Spectrom. 271, 68.
[2] D. Schneider, D. Dewitt, M. W. Clark, R. Schuch, C. L. Cocke, R. Schmieder, K. J. Reed, M. H. Chen, R. E. Marrs, M. Levine, R. Fortner (1990) Phys. Rev. A 42, 3889.
[3] D. C. Griffin, C. Bottcher, M. S. Pindzola, S. M. Younger, D. C. Gregory, D. H.Crandall (1984) Phys. Rev. A 29 1729.
[4] Y. Ralchenko, A. E. Kramida, J. Reader, NIST ASD Team, NIST Atomic Spectra Database (version 3.1.5), National Institute of Standards and Technology, Gaithersburg, MD, available: http://physics.nist.gov/asd3

[5] A.Müller (2008) Adv. At. Mol. Phys. 55, 293.
[6] A.Borovik, S.Schippers, A.Müller Atomic and Plasma-Material Interaction Data for Fusion Series, IAEA - in preparation.
[7] P. Mandelbaum, M. Cohen, J. L. Schwob, A. Bar-shalom (2005) Eur. Phys. J. D 33 2130.
[8] D. M.Mitnik, M. S.Pindzola, F.Robicheaux, N. R.Badnell, O. Uwira, A. Müller, A. Frank, J. Linkemann, W.Spies, N. Angert, P. H. Mokler, R. Becker, M. Kleinod, S. Ricz, L. Empacher (1997) Phys. Rev. A 54, 4365 .
[9] A. Hoffknecht, O. Uwira, S. Schennach, A. Frank, J. Haselbauer, W. Spies, N. Angert, P. H. Mokler, R. Becker, M. Kleinod, S. Schippers, A. Müller (1998) J. Phys. B: At. Mol. Opt. Phys. 31, 2415.
[10] G. Gwinner, A. Hoffknecht, T. Bartsch, M. Beutelspacher, N. Eklöw, P. Glans, M. Grieser, S. Krohn, E. Lindroth, A. Müller, A. A. Saghiri, S. Schippers, U. Schramm, D. Schwalm, M. Tokman, G. Wissler, A. Wolf (2000) Phys. Rev. Lett. 84, 4822.
[11] Hoffknecht A., Schippers S., Müller A., Gwinner G., Schwalm D., Wolf A. (2001) Phys. Scripta T92, 402.
[12] W. Shi, S. Böhm, C. Böhme, C. Brandau, A. Hoffknecht, S. Kieslich, S. Schippers, A. Müller, C. Kozhuharov, F. Bosch, B. Franzke, P. Mokler, M. Steck, T. Stöhlker, Z. Stachura (2001) Eur. Phys. J. D 15, 145.
[13] F. Robicheaux, S. D. Loch, M. S. Pindzola, C. P. Ballance (2010) Phys. Rev. Lett. 105, 233201.
[14] S. Schippers, D. Bernhardt, A. Müller, C. Krantz, M. Grieser, R. Repnow, A. Wolf, M. Lestinsky, M. Hahn, O. Novotný, D. W Savin. (2011) Phys. Rev. A 83, 012711.

Chapter 4

Atomic structure and electron data for heavy element ions

The authors of this chapter are Alicija Kupliauskiene, Pavel Bogdanovich, Olga Rancova, Valdez Jonauskas, Romas Kiselius, Nigel Badnell and Hugh Summers. It incorporates the brief report on ADAS-EU sub-contract 1 prepared by the Institute of Theoretical Physics and Astronomy, University of Vilnius, Lithuania (A. Kupliauskiene) dated 30 November 2011. See also appendix C.

4.1 Introduction

The work consisted of four parts: ab initio structure and transition probability calculations in the large scale multi-configurational approach with virtual excitations and transformed radial orbitals; global characteristics and CI prescriptions; Auger/cascade pathways and multiple ionisation; selected Dirac-Fock calculations for neutral/near-neutral very heavy systems. The tasks were as follows:

- A benchmark study for W I, W II, and W III using the Bogdanovich quasi-relativisitic (QRHF) approach. The structure and transition probability studies will be extended to implement plane-wave Born cross-sections so that delivery can be in the form of ADAS adf04 datasets. Professor N. R. Badnell from ADAS-EU will collaborate with Professor P. Bogdanovich and his co-workers and provide support procedures and sub-routines so that the link from the structure to the plane-wave Born can be made.
- A benchmark study in Dirac-Fock approximation of a selected lanthanide-like ion in a low charge state ($\sim 6-12$). The study is designed to assess the possibility of more extensive use of such heavy elements as markers (observed in low ionisation stages in divertor regimes) and edge transport studies and cross-reference other approximate studies of low charge state tungsten ions. Suitable ions would be W^{+8} (Dy-like).
- Multiple electron ionisation rate coefficients, with special emphasis on 4d, 4f and 5d, 5f open-shell systems. The study should be based on contiguous sets of iso-nuclear ions of selected elements from which approximate general prescriptions can be inferred. This will include design of an extension of ADAS data formats adf23 and adf07.
- Exploitation of ITPA special studies of key complex ion configuration interactions (such as symmetric exchange of symmetry) by inclusion in ADAS data format adf54, tuned to primary resonance line spectroscopy, with special emphasis on 4d, 4f and 5d, 5f open-shell systems.

Integration of data into the ADAS system will be executed by staff of ADAS-EU.

4.2 Electron-impact excitation of tungsten ions

4.2.1 Energy spectra calculation in quasirelativistic approach

The software exploited is created for ab initio calculations of spectra of atoms and ions within the quasirelativistic approach. This approach significantly differs from the widely known program based on methods described in the monograph by R.D. Cowan [1]. The quasirelativistic equations used to obtain the radial orbitals(RO) are of thefollowing form:

$$\left\{\frac{d^2}{dr^2} - \frac{l(l+1)}{r^2} - V(nl|r) - \varepsilon_{nl}\right\} P(nl|r) - X(nl|r) + \frac{\alpha^2}{4}\left(\varepsilon_{nl} + V(nl|r)\right)^2 P(nl|r) + \frac{\alpha^2}{4}\left(\varepsilon_{nl} + V(nl|r)\right) X(nl|r) + \frac{\alpha^2}{4}\left(1 - \frac{\alpha^2}{4}\left(\varepsilon_{nl} + V(nl|r)\right)\right)^{-1} D(nl|r)P(nl|r) = 0. \quad (4.1)$$

The first part of the equation coincides with the usual Hartre-Fock equations, where $X(nl|r)$ denotes the exchange part of the potential, and $V(nl|r)$ denotes the direct part of it including an interaction of an electron with a nucleus $U(r)$ and with other electrons. The finite size of a nucleus is taken into account within the interaction with a nucleus potential $U(r)$ [7] thus enabling us to derive a simple expansion of RO in powers of the radial variable in the nucleus region. Two terms containing the multiplier $(\varepsilon + V(nl|r))$ squared and that in the first order describe the relativistic correction of the mass dependence on the velocity. The last term on the left side of the equation (1) describes the potential of the contact interaction of the electrons with the nucleus. Here the contact interaction with the nucleus is taken into account not only for s-electrons, but also for some part of p-electrons:

$$D(nl|r) = \left(\delta(l,0) + \frac{1}{3}\delta(l,1)\right)\frac{dU(r)}{dr}\left(\frac{d}{dr} - \frac{1}{r}\left(\alpha^2 Z^2 \delta(l,1)\left(-\frac{37}{30} - \frac{5}{9n} + \frac{2}{3n^2}\right) + 1\right)\right). \quad (4.2)$$

Special features of the equation (1) are described in details in [8], [9], and their solution technique can be found in [10], [11].

Energy spectra are calculated within Breit-Pauli approach adjusted for the application of the quasirelativistic radial orbitals (RO). A single joint integral [12] is used to describe the one-electron interactions, both the non-relativistic and the relativistic ones, independent of the total angular momentum J:

$$\begin{aligned} L_{\mathrm{QR}}(n'l, nl) = &- \int_0^\infty P(n'l|r)U(r)P(nl|r) \\ &+ \int_0^\infty \left(1 - \frac{\alpha^2}{4}\left(\varepsilon_{nl} + V(nl|r)\right)\right)^{-1} P(n'l|r)\left\{\frac{d^2}{dr^2} - \frac{l(l+1)}{r^2}\right\} P(nl|r)dr \\ &+ \frac{\alpha^2}{4}\int_0^\infty \left(1 - \frac{\alpha^2}{4}\left(\varepsilon_{nl} + V(nl|r)\right)\right)^{-2} P(n'l|r)D(nl|r)P(nl|r)dr. \end{aligned} \quad (4.3)$$

Here one must apply the symmetrization procedure for the integrals within the interconfiguration matrix elements because of their non-symmetric form:

$$L_{\mathrm{S}}(n'l, nl) = \frac{1}{2}\left(L_{\mathrm{QR}}(nl, n'l) + L_{\mathrm{QR}}(n'l, nl)\right). \quad (4.4)$$

Special features of the quasirelativistic RO and the finite size of the atomic nucleus are taken into account while evaluating the spin-orbit interaction. This results in the spin-orbit interaction parameter acquiring the following form [9]:

$$\eta_{\mathrm{QR}}(nl) = \frac{\alpha^2}{8}\int_0^\infty \frac{P(nl|r)\frac{1}{r}\frac{dU(r)}{dr}P(nl|r)}{1-\frac{\alpha^2}{4}\left(\varepsilon_{nlj}+V(r)\right)}dr. \tag{4.5}$$

All two-electron interactions are taken into account in the same way as it is usually done within the Breit-Pauli approach. This similarity with the conventional approach enabled us to use the program [13] for calculation of the angular integrals of the energy operator matrix elements, and the program [14] for calculations of the electron transition characteristics along with the program [15] upgraded for the use of the quasirelativistic RO. Our own original codes are used in the remaining calculations.

To take into account the correlation effects, the transformed radial orbitals (TRO) are used to describe the virtually excited electrons. The TRO were initially introduced for non-relativistic calculations [16] and their advantages are confirmed by numerous non-relativistic researches (see for example [17],[18],[19],[20] and references therein). The TRO with two free parameters k and B are utilized within the present calculations:

$$\begin{aligned} P_{\mathrm{TRO}}(nl|r) = N\Big(r^{l_0-l+k}\exp(-Br)P(n_0l_0|r) \\ -\textstyle\sum_{n'<n}P(n'l|r)\int_0^\infty P(n'l|r)r^{l-l_0+k}\exp(-Br)P_{\mathrm{QR}}(n_0l_0|r)dr\Big). \end{aligned} \tag{4.6}$$

These parameters are varied in order to ensure the maximum of the averaged energy correction to the energy of the configuration under research expressed in the second order of the perturbation theory. The same set of RO is used to describe both even and odd configurations thus avoiding any problems caused by the non-orthogonality of RO while calculating the transition characteristics.

Employing the TRO one can generate a very large basis of radial orbitals. Consequently, the number of possible admixed configurations increases rapidly. Therefore it becomes necessary to select the admixed configurations that have the largest influence on the configuration being adjusted. The mean weight of the admixed configuration within the wave function of the adjusted configuration expressed in the second order of perturbation theory is used as a selection criterion

$$W_{\mathrm{PT}}(K_0,K') = \frac{\sum_{TLST'}(2L+1)(2S+1)\langle K_0TLS||H||K'T'LS\rangle^2}{g(K_0)\left(\bar{E}(K')-\bar{E}(K_0)\right)^2}. \tag{4.7}$$

Only the configurations having $W_{PT}(K_0,K')$ larger than a specified small parameter S are used in the calculations. This method coincides completely with the one exploited in the non-relativistic calculations [17], [21], [22]. The configuration state functions of the selected configurations were utilized to form the energy operator matrices. The approach employed is more thoroughly described in [12] and references therein. The examples of applications of the approach are available in [23], [24].

4.2.2 Electron-impact excitation of ions

We adopt the Born approximation [25] to determine electron-impact excitation of atoms and ions. The calculation consists of two parts. First of all, we determine the angular integrals for all required matrix elements. For this purpose we employ the computer code [14] which determines angular integrals for the matrix elements of radiative transitions. Secondly, the special code to calculate the parameters for the electron-impact excitation in Born approximation was created. This program employs the eigenvalues and eigenvectors obtained from the Hamiltonian matrix in quasirelativistic approach (as it was described in the previous section **??**) to compute the excitation cross-sections and collision

Table 4.1: Excitation cross-sections (in 10^{-17} cm^2) for 1s – 2p transitions in hydrogen atom

E (eV)	BE-sc [29]	CCC [30]	QR	BP
11	1.5876		1.58028	1.58029
15	3.9256	4.021	3.91899	3.91904
20	5.2779	5.163	5.27045	5.27053
45	6.5130	6.499	6.50485	6.50497
100	5.3369	5.485	5.32992	5.33003
200	3.7771	3.912	3.77141	3.77149
500	2.0807	2.126	2.07619	2.07624
1000	1.2463	1.261	1.24211	1.24214
2000	0.7236		0.71936	0.71937
3000	0.5214		0.51708	0.51710

strengths in multiconfigurational approximation. The main task of this code is to calculate the radial integrals containing the spherical Bessel functions. In our code these integrals are calculated for each electron energy in order to avoid possible computating errors. We apply a logarithmic step for the numerical integration of radial integral over the wave-vector to reduce computing time. The analysis of computed integral values have demonstrated that it is enough to employ only 25 integration points. In order to check the calculated results and to analyze the influence of the quasirelativistic approach, an absolutely identical computer code was created to calculate excitation parameters in the same Born approximation by exploiting the non-relativistic radial orbitals.

We use cross-section values for the light elements extracted from NIST database [27] to certify our calculated results. In Table 4.1 we compare electron-impact excitation $1s - 2p$ cross-sections for the hydrogen atom. In the first column of Table 1 we present incident electron energies in eV, and the cross-sections (in 10^{-17} cm^2) are given in the next four columns. Since the values of cross-sections presented in database [27] are scaled according to the method applicable for the neutral ions and described in [28], our results were scaled accordingly. These results are compared with the theoretical data obtained in Plane-Wave-Born (PWB) approximation from (BE-sc) [29] by applying reduction method [28] for the hydrogen, helium and lithium atoms. These data are fully-relativistic since Dirac-Fock radial orbitals were employed to describe atomic electrons. We have scaled PWB cross-sections to calculate the dipole- and spin-allowed excitation from the ground state of neutral hydrogen. The results obtained by convergent close-coupling calculations (CCC) from [30] are presented too. These data are compared with our results obtained using quasirelativistic RO (QR) and non-relativistic RO in Breit-Pauli approximation (BP). One can see from Table 4.1 that our results match each other very well since relativistic effects are very small for these atoms. For very same reason the agreement with fully-relativistic data from [29] is remarkable. The deviations from CCC data, although more noticeable, are still insignificant.

We present the comparison of our theoretical data with the results from other studies in Table 4.2. On top of the above mentioned two theoretical data sets, we present the experimental data [31],[32], [33] and recommended values from [34]. Similarly to Table 4.1, we present our quasirelativistic and non-relativistic data scaled according to [28]. In this case, our calculations were performed both in the single-configuration (SC) and in the configuration interaction (CI) approach. Similarly to Table 4.1, our QR and BP calculation data demonstrate an excellent agreement. Our CI data almost always agree very well with the recommended values from [34]. Only at the lowest energy point where electron-impact energy is just 3.8 eV higher than the excitation threshold, the deviation from the recommended cross-section value is significant. For the higher energies our data are in much better agreement with the recommended values comparing to other theoretical data.

The electron-impact cross-sections for the lithium are presented in Table 4.3. As one could expect, our QR and BP results are in good agreement. The inclusion of correlation effects for lithium atoms has a significantly lower effect comparing to helium atoms because the transitions affect a single electron outside the strongly-bound core. The deviations of our results from the other theoretical and experimental data are insignificant. They become noticeably

Table 4.2: Excitation cross-sections (in 10^{-17} cm^2) for 1s – 2p transitions in helium atom

E (eV)	BE-sc [29]	CCC [30]	Exp [31]	Exp [32]	RV [34]	Exp [33]	QR SC	BP SC	QR CI	BP CI
25	0.293	0.223		0.117	0.120		0.401	0.401	0.327	0.327
50	0.790	0.819	0.820	0.837	0.850		1.111	1.111	0.876	0.869
100	0.906	1.087	1.010	0.974	1.010		1.263	1.263	0.997	0.991
200	0.772	0.905	0.830	0.775	0.810	0.920	0.920	1.071	0.844	0.842
500	0.489	0.554	0.507	0.458		0.519	0.675	0.675	0.531	0.533
1000	0.312		0.314	0.290			0.429	0.429	0.337	0.339
2000	0.189		0.185	0.175			0.258	0.258	0.203	0.204
3000	0.138						0.189	0.189	0.148	0.149

Table 4.3: Excitation cross-sections (in 10^{-16} cm^2) for 2s – 2p transitions in lithium atom

E (eV)	BE-sc [29]	CCC [35]	Exp [36]	Exp [37]	Exp [38]	QR SC	BP SC	QR CI	BP CI
2	14.594					15.482	15.477	15.087	15.036
4	38.978	36.08	38.796			40.486	40.486	40.233	40.214
5	41.474		41.084			43.032	43.033	42.793	42.777
10	41.072	38.33		44	38.0	42.510	42.512	42.328	42.319
20	32.984	31.36		36	33.1	34.077	34.079	33.956	33.952
60	17.739			28	17.5	18.294	18.295	18.241	18.241
100	12.387	12.90			12.4	12.767	12.768	12.733	12.733
200	7.296	7.66			7.6	7.515	7.515	7.496	7.496
600	2.970	3.08				3.055	3.055	3.048	3.048
1000	1.927	2.01				1.979	1.979	1.975	1.975
2000	1.061	1.08				1.087	1.087	1.084	1.085
3000	0.746					0.762	0.762	0.760	0.760

smaller with the increase of ionization degree.

The ADAS implies an appropriate formatting to present calculated results. Therefore we have created a driver code to present our data in a form suitable for ADAS. In this case we don't apply any of scaling methods. An output file example for the lithium atom is presented in Table 4.4.

The initial lines describe parameters of the levels participating in the excitation process. The first line of the main table provides the ionization degree in spectroscopic notation and the energy coefficients. The incident electron energy can be calculated by multiplying the excitation energy by this coefficient. The column with the coefficient equal to 1 gives the emission transition rates in s^{-1}. The further columns provide the excitation collision strengths. The last column (with the energy coefficient absent) gives collision strengths for the infinite electron energy. If the multiplicity of transition is equal to 1, these collision strengths are equal to 4/3 of the corresponding oscillator strengths and set to have a negative sign. In all other cases an additional cross-section is calculated for the energy coefficient equal to 1000, and the necessary value is obtained by interpolating over the 5 calculated collision strengths.

The first two columns of the main output table give the numbers of levels involved in transition followed by above-mentioned transition data. At the bottom of table we provide comments about the calculation method, the maximum excitation multiplicity (LAMDmax) and the number of configurations involved to describe the initial and final levels. A demonstration of the obtained output files we give in Table 4.5 for QR results and in Table 4.6 for BP results. Our collision strengths presented for Fe^{+21} ions in these tables agree well with the data from fully-relativistic calculations available from ADAS files.

Table 4.4: Quasirelativistic results of lithium atom for ADAS

```
Li+ 0         3         1
    1 1s2 2s1           (2)0( 0.5)              0.00000
    2 1s2 2p1           (2)1( 0.5)          14902.10862
    3 1s2 2p1           (2)1( 1.5)          14902.32810
   -1
 1.00    1       1.10+00 1.20+00 1.55+00 2.00+00 3.00+00 5.50+00 1.00+01 2.00+01 5.50+01 1.00+02
   2   1 3.76+07 8.39+00 1.16+01 1.82+01 2.34+01 3.06+01 4.04+01 4.98+01 6.04+01 7.57+01 8.47+01-1.50+01
   3   1 3.76+07 1.68+01 2.33+01 3.65+01 4.68+01 6.11+01 8.09+01 9.96+01 1.21+02 1.51+02 1.69+02-2.99+01
  -1
  -1  -1
C-----------------------------------------------------------------------------
C
C QUASIRELATICISTIC PLANE-WAVE BORN LAMDmax= 1    138 INIT.CONF. ->  120 FIN.CONF.
C
C NAME: BOGDANOVICH P.
C DATE: 03/11/11
C
C-----------------------------------------------------------------------------
```

Table 4.5: Quasirelativistic results of Fe^{+21} ion for ADAS

```
Fe+21        26        22
    1 2s2 2p1           (2)1( 0.5)              0.00000
    2 2s2 2p1           (2)1( 1.5)         117248.83989
    3 2s1 2p2           (4)1( 0.5)         399818.92810
    4 2s1 2p2           (4)1( 1.5)         455543.97830
    5 2s1 2p2           (4)1( 2.5)         508875.21860
    6 2s1 2p2           (2)2( 1.5)         735696.11440
    7 2s1 2p2           (2)2( 2.5)         758860.56534
    8 2s1 2p2           (2)1( 0.5)         854434.96762
    9 2s1 2p2           (2)0( 0.5)         979294.96857
   10 2s1 2p2           (2)1( 1.5)         993487.51568
   11 2p3               (4)0( 1.5)        1249638.56350
   12 2p3               (2)2( 1.5)        1392723.73861
   13 2p3               (2)2( 2.5)        1423160.48177
   14 2p3               (2)1( 0.5)        1566697.77464
   15 2p3               (2)1( 1.5)        1624688.90051
   -1
22.00    1       1.10+00 1.20+00 1.55+00 2.00+00 3.00+00 5.50+00 1.00+01 2.00+01 5.50+01 1.00+02
   2   1 1.45+04 2.63-04 3.87-04 7.22-04 1.09-03 1.83-03 3.46-03 5.83-03 9.36-03 1.37-02 1.48-02 1.51-02
   3   1 8.24+07 1.97-03 2.74-03 4.29-03 5.43-03 6.88-03 8.56-03 9.86-03 1.11-02 1.29-02 1.39-02-1.70-03
   3   2 1.34+07 9.28-04 1.29-03 2.02-03 2.57-03 3.28-03 4.12-03 4.77-03 5.39-03 6.21-03 6.68-03-7.82-04
   4   1 1.91+06 6.13-05 8.50-05 1.33-04 1.68-04 2.12-04 2.63-04 3.03-04 3.42-04 3.97-04 4.29-04-5.32-05
   4   2 8.33+06 6.66-04 9.25-04 1.45-03 1.84-03 2.34-03 2.93-03 3.38-03 3.82-03 4.40-03 4.74-03-5.66-04
   5   1 0.00+00 0.00+00 0.00+00 0.00+00 0.00+00 0.00+00 0.00+00 0.00+00 0.00+00 0.00+00 0.00+00 0.00+00
   5   2 7.02+07 5.38-03 7.47-03 1.17-02 1.48-02 1.88-02 2.34-02 2.69-02 3.04-02 3.52-02 3.80-02-4.61-03
   6   1 1.05+10 7.67-02 1.06-01 1.65-01 2.07-01 2.59-01 3.18-01 3.65-01 4.15-01 4.87-01 5.29-01-6.96-02
   6   2 2.45+07 3.05-04 4.23-04 6.58-04 8.28-04 1.04-03 1.28-03 1.47-03 1.67-03 1.95-03 2.11-03-2.72-04
   7   1 0.00+00 0.00+00 0.00+00 0.00+00 0.00+00 0.00+00 0.00+00 0.00+00 0.00+00 0.00+00 0.00+00 0.00+00
   7   2 5.89+09 9.84-02 1.36-01 2.12-01 2.67-01 3.35-01 4.12-01 4.73-01 5.37-01 6.27-01 6.80-01-8.80-02
   8   1 3.80+10 8.66-02 1.20-01 1.85-01 2.32-01 2.90-01 3.55-01 4.08-01 4.66-01 5.48-01 5.97-01-8.01-02
   8   2 8.16+07 2.99-04 4.14-04 6.43-04 8.09-04 1.01-03 1.25-03 1.43-03 1.63-03 1.90-03 2.06-03-2.68-04
   9   1 2.23+09 3.33-03 4.60-03 7.11-03 8.90-03 1.11-02 1.36-02 1.56-02 1.79-02 2.11-02 2.30-02-3.13-03
   9   2 3.35+10 7.42-02 1.03-01 1.59-01 1.99-01 2.48-01 3.04-01 3.50-01 4.00-01 4.70-01 5.12-01-6.88-02
  10   1 6.17+09 1.75-02 2.42-02 3.74-02 4.67-02 5.81-02 7.11-02 8.20-02 9.39-02 1.11-01 1.21-01-1.66-02
  10   2 4.41+10 1.86-01 2.57-01 3.98-01 4.99-01 6.22-01 7.61-01 8.76-01 1.00+00 1.18+00 1.28+00-1.73-01
  11   1 5.93+03 2.27-05 3.26-05 5.54-05 7.49-05 1.01-04 1.27-04 1.37-04 1.39-04 1.39-04 1.40-04 1.40-04
  11   2 5.53+03 1.89-05 2.70-05 4.57-05 6.15-05 8.22-05 1.00-04 1.05-04 1.06-04 1.06-04 1.06-04 1.07-04
  12   1 3.12+04 2.27-04 3.24-04 5.45-04 7.28-04 9.64-04 1.18-03 1.25-03 1.26-03 1.27-03 1.27-03 1.27-03
  12   2 1.57+04 9.42-05 1.35-04 2.27-04 3.05-04 4.06-04 4.99-04 5.30-04 5.36-04 5.38-04 5.38-04 5.39-04
  13   1 9.39+03 1.05-04 1.49-04 2.51-04 3.34-04 4.40-04 5.34-04 5.65-04 5.71-04 5.73-04 5.73-04 5.74-04
  13   2 2.74+04 3.95-04 5.65-04 9.56-04 1.29-03 1.72-03 2.13-03 2.28-03 2.31-03 2.32-03 2.32-03 2.33-03
  14   1 2.42-07 8.33-05 1.18-04 1.92-04 2.48-04 3.09-04 3.48-04 3.54-04 3.55-04 3.57-04 3.57-04 3.55-04
  14   2 3.83+04 9.93-05 1.42-04 2.37-04 3.16-04 4.16-04 5.04-04 5.33-04 5.39-04 5.40-04 5.40-04 5.41-04
  15   1 4.29+03 1.35-05 1.93-05 3.19-05 4.21-05 5.44-05 6.44-05 6.74-05 6.80-05 6.81-05 6.82-05 6.81-05
  15   2 3.12+04 3.19-04 4.53-04 7.50-04 9.85-04 1.27-03 1.49-03 1.54-03 1.55-03 1.56-03 1.56-03 1.56-03
  -1
  -1  -1
C-----------------------------------------------------------------------------
C
C QASIRELATICISTIC PLANE-WAVE BORN     28 INIT.CONF. ->   24 FIN.CONF.
C
C NAME: BOGDANOVICH P.
C DATE: 06/10/11
C
C-----------------------------------------------------------------------------
```

Table 4.7 gives an example of more complicated calculation. The results present the $4d^4$–$4d^35p$ transition calculations in the quasirelativistic approach for the W^{+2} ion. Since these configurations have a very large number of energy levels, we present only results for the excitation from the lowest level ^5D of the ground configuration to the 8 lowest levels of the excited configuration. In this case the octupole excitations were calculated along with the dipole ones.

Our presented examples demonstrate that the devised computer codes enable us to calculate successfully the electron-impact excitation in plane-wave Born approximation by using the data of the energy level spectra obtained in the quasirelativistic approach. This approach was developed in the Department of Atomic Theory of Institute of The-

Table 4.6: Breit-Pauli results of Fe^{+21} ion for ADAS

```
Fe+21        26        22
    1 2s2 2p1           (2)1( 0.5)              0.00000
    2 2s2 2p1           (2)1( 1.5)         115432.68724
    3 2s1 2p2           (4)1( 0.5)         398738.23497
    4 2s1 2p2           (4)1( 1.5)         453464.89503
    5 2s1 2p2           (4)1( 2.5)         506066.16268
    6 2s1 2p2           (2)2( 1.5)         730928.46678
    7 2s1 2p2           (2)2( 2.5)         753651.55422
    8 2s1 2p2           (2)1( 0.5)         848573.45839
    9 2s1 2p2           (2)0( 0.5)         971777.96213
   10 2s1 2p2           (2)1( 1.5)         984967.72961
   11 2p3               (4)0( 1.5)        1242638.85879
   12 2p3               (2)2( 1.5)        1384587.81368
   13 2p3               (2)2( 2.5)        1414528.10521
   14 2p3               (2)1( 0.5)        1556572.31209
   15 2p3               (2)1( 1.5)        1613420.19456
   -1
22.00    1       1.10+00 1.20+00 1.55+00 2.00+00 3.00+00 5.50+00 1.00+01 2.00+01 5.50+01 1.00+02
   2   1 1.38+04 2.64-04 3.89-04 7.26-04 1.10-03 1.84-03 3.48-03 5.87-03 9.44-03 1.39-02 1.50-02 1.53-02
   3   1 8.19+07 1.98-03 2.74-03 4.29-03 5.43-03 6.88-03 8.56-03 9.86-03 1.11-02 1.29-02 1.39-02-1.70-03
   3   2 1.35+07 9.27-04 1.29-03 2.02-03 2.57-03 3.27-03 4.11-03 4.76-03 5.38-03 6.19-03 6.66-03-7.82-04
   4   1 1.89+06 6.15-05 8.53-05 1.33-04 1.68-04 2.13-04 2.64-04 3.03-04 3.43-04 3.98-04 4.30-04-5.34-05
   4   2 8.39+06 6.73-04 9.34-04 1.46-03 1.86-03 2.36-03 2.95-03 3.41-03 3.85-03 4.44-03 4.78-03-5.72-04
   5   1 0.00+00 0.00+00 0.00+00 0.00+00 0.00+00 0.00+00 0.00+00 0.00+00 0.00+00 0.00+00 0.00+00 0.00+00
   5   2 6.99+07 5.40-03 7.49-03 1.17-02 1.48-02 1.88-02 2.34-02 2.70-02 3.05-02 3.52-02 3.80-02-4.63-03
   6   1 1.05+10 7.78-02 1.08-01 1.67-01 2.10-01 2.62-01 3.22-01 3.70-01 4.21-01 4.94-01 5.36-01-7.07-02
   6   2 2.50+07 3.15-04 4.36-04 6.79-04 8.54-04 1.07-03 1.32-03 1.51-03 1.72-03 2.01-03 2.18-03-2.82-04
   7   1 0.00+00 0.00+00 0.00+00 0.00+00 0.00+00 0.00+00 0.00+00 0.00+00 0.00+00 0.00+00 0.00+00 0.00+00
   7   2 5.89+09 1.00-01 1.39-01 2.15-01 2.71-01 3.40-01 4.18-01 4.80-01 5.45-01 6.37-01 6.91-01-8.95-02
   8   1 3.78+10 8.79-02 1.22-01 1.88-01 2.36-01 2.94-01 3.61-01 4.15-01 4.73-01 5.57-01 6.06-01-8.15-02
   8   2 9.41+07 3.52-04 4.87-04 7.58-04 9.54-04 1.20-03 1.47-03 1.69-03 1.92-03 2.24-03 2.43-03-3.14-04
   9   1 2.10+09 3.21-03 4.44-03 6.87-03 8.59-03 1.07-02 1.31-02 1.51-02 1.72-02 2.03-02 2.22-02-3.02-03
   9   2 3.33+10 7.52-02 1.04-01 1.61-01 2.02-01 2.52-01 3.08-01 3.54-01 4.05-01 4.76-01 5.19-01-6.99-02
  10   1 6.10+09 1.78-02 2.45-02 3.79-02 4.74-02 5.90-02 7.22-02 8.32-02 9.52-02 1.12-01 1.23-01-1.68-02
  10   2 4.37+10 1.88-01 2.61-01 4.03-01 5.05-01 6.30-01 7.72-01 8.88-01 1.01+00 1.19+00 1.30+00-1.75-01
  11   1 5.65+03 2.24-05 3.21-05 5.45-05 7.38-05 9.98-05 1.25-04 1.35-04 1.37-04 1.37-04 1.37-04 1.38-04
  11   2 5.31+03 2.11-05 3.01-05 5.09-05 6.81-05 9.04-05 1.09-04 1.14-04 1.15-04 1.15-04 1.16-04 1.16-04
  12   1 3.06+04 2.28-04 3.26-04 5.48-04 7.33-04 9.71-04 1.18-03 1.26-03 1.27-03 1.27-03 1.27-03 1.28-03
  12   2 1.52+04 9.86-05 1.41-04 2.37-04 3.18-04 4.23-04 5.17-04 5.48-04 5.54-04 5.55-04 5.56-04 5.57-04
  13   1 9.21+03 1.05-04 1.50-04 2.52-04 3.36-04 4.44-04 5.38-04 5.69-04 5.75-04 5.76-04 5.76-04 5.77-04
  13   2 2.69+04 3.97-04 5.69-04 9.62-04 1.29-03 1.73-03 2.15-03 2.29-03 2.32-03 2.33-03 2.33-03 2.34-03
  14   1 1.85-07 9.68-05 1.37-04 2.22-04 2.85-04 3.53-04 3.94-04 4.00-04 4.02-04 4.03-04 4.03-04 4.01-04
  14   2 3.73+04 9.95-05 1.42-04 2.38-04 3.17-04 4.17-04 5.05-04 5.34-04 5.40-04 5.41-04 5.41-04 5.42-04
  15   1 4.18+03 1.36-05 1.94-05 3.22-05 4.24-05 5.49-05 6.51-05 6.81-05 6.87-05 6.88-05 6.88-05 6.88-05
  15   2 3.04+04 3.42-04 4.85-04 8.02-04 1.05-03 1.34-03 1.57-03 1.63-03 1.64-03 1.64-03 1.64-03 1.64-03
  -1
  -1  -1
C-----------------------------------------------------------------------------
C
C BREIT-PAULI (Hartree-Fock)   PLANE-WAVE BORN     30 INIT.CONF. ->   24 FIN.CONF.
C
C NAME: BOGDANOVICH P.
C DATE: 06/10/11
C
C-----------------------------------------------------------------------------
```

oretical Physics and Astronomy, Vilnius University. Several exploratory calculations were performed for the tungsten ions. Consequently, we consider that the first task of the Project was completed in full.

Table 4.7: Some quasirelativistic results of W^{+2} ion $4d^4$ - $4d^3 5p$ transitions for ADAS

```
W + 2        74         3
    1 5p6 5d4            (5)2( 0.0)              0.00000
    2 5p6 5d4            (5)2( 1.0)           1895.38300
    3 5p6 5d4            (5)2( 2.0)           4003.21745
    4 5p6 5d4            (5)2( 3.0)           5917.91421
    5 5p6 5d4            (5)2( 4.0)           7574.06985
.....................................................
   66 5p6 5d3 6p1        (5)4( 2.0)          60202.77182
   67 5p6 5d4            (1)2( 2.0)          62267.80872
   68 5p6 5d3 6p1        (3)2( 1.0)          63578.95022
   69 5p6 5d3 6s1        (1)3( 3.0)          63663.00901
   70 5p6 5d3 6p1        (5)4( 3.0)          63668.27640
   71 5p6 5d3 6p1        (5)3( 2.0)          66050.01520
   72 5p6 5d2 6s2        (3)3( 2.0)          66463.94437
   73 5p6 5d3 6p1        (5)4( 4.0)          67129.39148
   74 5p6 5d2 6s2        (3)3( 3.0)          69046.28299
   75 5p6 5d3 6s1        (3)2( 1.0)          69331.60002
   76 5p6 5d3 6s1        (3)2( 2.0)          69332.91687
   77 5p6 5d3 6p1        (5)3( 3.0)          69965.66226
   78 5p6 5d3 6p1        (5)4( 5.0)          70308.70112
   79 5p6 5d2 6s2        (3)3( 3.0)          70393.19886
   80 5p6 5d3 6p1        (5)3( 2.0)          70808.22541
   -1
 3.00    1       1.10+00 1.20+00 1.55+00 2.00+00 3.00+00 5.50+00 1.00+01 2.00+01 5.50+01 1.00+02
  66   2 3.48+05 6.59-02 9.22-02 1.41-01 1.64-01 1.77-01 1.81-01 1.85-01 1.90-01 1.96-01 1.99-01 -5.78-03
  66   3 2.29+05 7.00-02 9.85-02 1.52-01 1.79-01 1.93-01 1.97-01 2.00-01 2.03-01 2.07-01 2.10-01 -4.25-03
  66   4 5.05+05 2.61-02 3.69-02 5.81-02 7.03-02 7.94-02 8.66-02 9.32-02 1.01-01 1.11-01 1.17-01 -1.04-02
  66   5 0.00+00 3.22-03 4.57-03 7.21-03 8.61-03 9.33-03 9.41-03 9.45-03 9.46-03 9.46-03 9.46-03  9.60-03
  68   1 2.70+08 6.53-01 9.38-01 1.61+00 2.22+00 3.14+00 4.45+00 5.72+00 7.18+00 9.28+00 1.05+01 -2.07+00
  68   2 5.40+07 1.49-01 2.13-01 3.63-01 4.97-01 6.99-01 9.88-01 1.27+00 1.59+00 2.05+00 2.32+00 -4.54-01
  68   3 2.31+06 1.83-02 2.57-02 4.07-02 5.07-02 6.19-02 7.58-02 8.91-02 1.04-01 1.26-01 1.39-01 -2.16-02
  68   4 0.00+00 7.56-03 1.06-02 1.62-02 1.88-02 2.00-02 2.01-02 2.02-02 2.02-02 2.02-02 2.02-02  2.07-02
  68   5 0.00+00 3.69-03 5.20-03 8.01-03 9.41-03 1.01-02 1.01-02 1.02-02 1.02-02 1.02-02 1.02-02  1.04-02
  70   1 0.00+00 4.31-02 5.96-02 8.77-02 9.97-02 1.04-01 1.05-01 1.05-01 1.05-01 1.05-01 1.05-01  1.09-01
  70   2 0.00+00 1.86-03 2.58-03 3.83-03 4.39-03 4.61-03 4.64-03 4.66-03 4.66-03 4.66-03 4.66-03  4.80-03
  70   3 2.28+06 8.29-02 1.16-01 1.79-01 2.16-01 2.47-01 2.79-01 3.10-01 3.45-01 3.96-01 4.25-01 -4.94-02
  70   4 2.99+06 1.10-01 1.55-01 2.42-01 2.93-01 3.38-01 3.86-01 4.31-01 4.81-01 5.54-01 5.97-01 -7.16-02
  70   5 8.37+05 2.58-02 3.64-02 5.75-02 7.08-02 8.38-02 9.81-02 1.12-01 1.27-01 1.49-01 1.63-01 -2.19-02
  71   2 2.52+08 9.79-01 1.41+00 2.43+00 3.34+00 4.73+00 6.72+00 8.63+00 1.08+01 1.40+01 1.59+01 -3.14+00
  71   3 1.08+07 5.41-02 7.73-02 1.30-01 1.76-01 2.43-01 3.38-01 4.29-01 5.34-01 6.85-01 7.74-01 -1.49-01
  71   4 1.17+07 7.17-02 1.02-01 1.70-01 2.26-01 3.06-01 4.19-01 5.28-01 6.52-01 8.31-01 9.37-01 -1.77-01
  71   5 0.00+00 2.81-03 3.93-03 5.96-03 6.92-03 7.34-03 7.38-03 7.41-03 7.42-03 7.42-03 7.42-03  7.61-03
  73   2 0.00+00 6.45-02 8.89-02 1.30-01 1.47-01 1.53-01 1.54-01 1.54-01 1.54-01 1.54-01 1.54-01  1.60-01
  73   3 0.00+00 1.06-04 1.46-04 2.16-04 2.46-04 2.57-04 2.59-04 2.60-04 2.60-04 2.60-04 2.60-04  2.68-04
  73   4 1.83+07 2.71-01 3.82-01 6.18-01 7.92-01 1.02+00 1.32+00 1.61+00 1.94+00 2.42+00 2.70+00 -4.72-01
  73   5 5.98+06 1.29-01 1.81-01 2.88-01 3.61-01 4.46-01 5.55-01 6.58-01 7.76-01 9.47-01 1.05+00 -1.68-01
  77   1 0.00+00 1.65-02 2.26-02 3.22-02 3.58-02 3.70-02 3.72-02 3.74-02 3.74-02 3.74-02 3.74-02  3.87-02
  77   2 0.00+00 1.87-03 2.57-03 3.69-03 4.13-03 4.29-03 4.31-03 4.33-03 4.33-03 4.33-03 4.33-03  4.48-03
  77   3 3.41+08 1.66+00 2.39+00 4.15+00 5.74+00 8.14+00 1.16+01 1.50+01 1.88+01 2.43+01 2.76+01 -5.47+00
  77   4 9.22+05 9.04-03 1.27-02 2.05-02 2.63-02 3.40-02 4.44-02 5.43-02 6.57-02 8.21-02 9.18-02 -1.62-02
  77   5 2.71+07 1.79-01 2.56-01 4.34-01 5.89-01 8.19-01 1.15+00 1.46+00 1.82+00 2.35+00 2.65+00 -5.14-01
  78   3 0.00+00 5.67-02 7.80-02 1.13-01 1.27-01 1.33-01 1.33-01 1.34-01 1.34-01 1.34-01 1.34-01  1.39-01
  78   4 0.00+00 1.11-02 1.54-02 2.26-02 2.56-02 2.67-02 2.69-02 2.70-02 2.70-02 2.70-02 2.70-02  2.79-02
  78   5 7.25+07 8.42-01 1.20+00 2.00+00 2.68+00 3.64+00 4.99+00 6.29+00 7.79+00 9.95+00 1.12+01 -2.13+00
  80   2 9.51+07 2.90-01 4.19-01 7.29-01 1.01+00 1.43+00 2.03+00 2.61+00 3.28+00 4.26+00 4.83+00 -9.57-01
  80   3 2.69+07 9.53-02 1.37-01 2.36-01 3.23-01 4.54-01 6.42-01 8.23-01 1.03+00 1.33+00 1.51+00 -2.97-01
  80   4 1.07+06 1.75-02 2.44-02 3.72-02 4.45-02 5.15-02 5.98-02 6.78-02 7.68-02 8.98-02 9.75-02 -1.28-02
  80   5 0.00+00 2.51-02 3.48-02 5.13-02 5.84-02 6.12-02 6.15-02 6.17-02 6.18-02 6.18-02 6.18-02  6.37-02
  -1
  -1  -1
C-----------------------------------------------------------------------------
C
C QUASIRELATICISTIC PLANE-WAVE BORN LAMDmax= 3    6 INIT.CONF. ->    8 FIN.CONF.
C
C NAME: BOGDANOVICH P.
C DATE: 04/11/11
C
C-----------------------------------------------------------------------------
```

4.3 Peculiarities of spectroscopic properties of W^{+8}

4.3.1 Theory

We have adopted different *ab initio* methods, namely the multiconfiguration Hartree-Fock (MCHF) and multiconfiguration Dirac-Fock (MCDF) approximations taking into account relativistic and QED corrections [B3]. In the multiconfiguration Dirac-Fock approximation, an atomic state function (ASF) of parity P, angular momentum L and spin S, $\Psi(\gamma PJ)$, is given by a linear combination of symmetry-adapted configuration state functions (CSFs) with the same parity, $\Phi(\gamma_i PJ)$, i.e.

$$\Psi(\gamma PJ) = \sum_i c_i \Phi(\gamma_i PJ), \tag{4.8}$$

where J is the total angular momentum of the configuration. The multiconfiguration energy functional is based on the Dirac-Coulomb Hamiltonian, given by (in a.u.),

$$H_{\rm DC} = \sum_{j=1}^{N} \left(c\boldsymbol{\alpha}_j \boldsymbol{p}_j + (\boldsymbol{\beta}_j - 1)c^2 + V(r_j) \right) + \sum_{j<k} \frac{1}{r_{jk}}, \tag{4.9}$$

where $\boldsymbol{\alpha}$ and $\boldsymbol{\beta}$ are the fourth-order Dirac matrices, $\boldsymbol{p}$ is the momentum operator, and $V(r_j)$ is the electrostatic electron-nucleus interaction. In all the calculations reported here, the nuclear charge distribution was modeled by the two-component Fermi function.

The relativistic configuration interaction (RCI) method was used to include the transverse Breit interaction at the low-frequency limit (describing the transversely polarized photon contributions to the electron-electron interactions in Coulomb gauge), and the QED corrections (including self-energy and vacuum polarization) [B4]. The MCDF calculations were performed with the GRASP2K relativistic atomic structure package [B4], [B5] in which the second quantization method in coupled tensorial form and quasispin technique [B3] was adopted for calculations of spin-angular parts of matrix elements. This allowed to achieve the breakthrough in the field, to essentially increase the efficiency and the speed of the calculations, opening the possibilities to consider extremely complex electronic configurations.

4.3.2 Large scale calculations

We used a multi-reference set for the construction of the ASFs. In this approach the configuration state functions of the multiconfigurational calculations include, in Eqs. 4.8, single and double substitutions from the valence $4f$ and $5p$ shells. Restricted active spaces of the CSF's are generated using the orbitals of the following atomic states (AS):

$$\begin{aligned}
AS_0 &= 1s^2 2s^2 2p^6 3s^2 3p^6 3d^{10} 4s^2 4p^6 4d^{10} 4f^{14} 5s^2 5p^4 \\
&+ 1s^2 2s^2 2p^6 3s^2 3p^6 3d^{10} 4s^2 4p^6 4d^{10} 4f^{13} 5s^2 5p^5 \\
&+ 1s^2 2s^2 2p^6 3s^2 3p^6 3d^{10} 4s^2 4p^6 4d^{10} 4f^{12} 5s^2 5p^6, \\
AS_5 &= AS_0 + \{5d, 5f, 5g\}, \\
AS_6 &= AS_5 + \{6s, 6p, 6d, 6f, 6g, 6h\}.
\end{aligned}$$

At all steps only new orbitals were optimized. In order to reduce the size of the multiconfiguration expansion for the $n = 5$ and $n = 6$, the jj- reduction technique was applied [B3].

In case of the MCDF expansions of the even ASFs for the energy spectrum calculations, we used a multireference (MR) set of CSFs based on the $[\mathrm{Kr}]4d^{10}4f^{14}5s^25p^4$, $[\mathrm{Kr}]4d^{10}4f^{13}5s^25p^5$ and $[\mathrm{Kr}]4d^{10}4f^{12}5s^25p^6$ even configurations. The state functions of these three configurations form the basis for the zero-order wave function (MR set). The

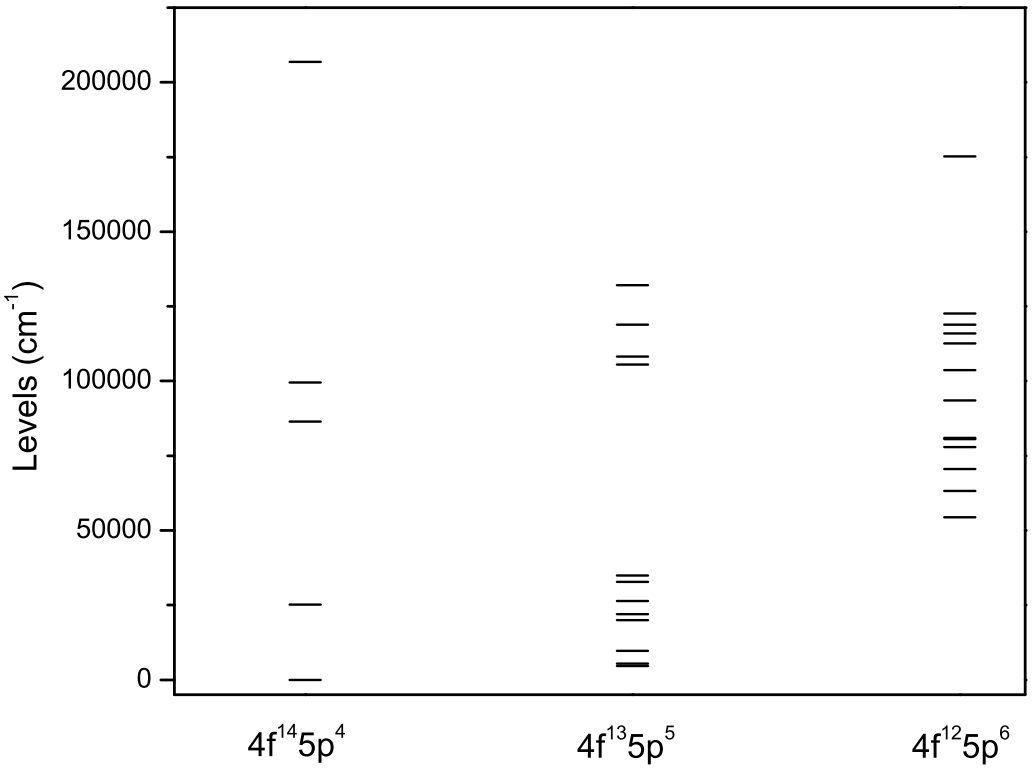

Figure 4.1: The lowest configurations of W^{+8}

energy functional on which the orbitals were optimized was defined according to an extended optimal level (EOL) scheme, where a linear combination of atomic states, corresponding to the lowest two J = 0,...,6 states, was used. An admixed CSFs were obtained from single and double substitutions from all open-shell orbitals to an increasing active set (AS) of orbitals.

Fig. 4.1 displays energies of 30 lowest levels of W^{+8} belonging to [Kr]$4d^{10}4f^{14}5s^25p^4$ (5 levels), [Kr]$4d^{10}4f^{13}5s^25p^5$ (12 levels) and [Kr]$4d^{10}4f^{12}5s^25p^6$ (13 levels) configurations. Analyzing the preliminary results (see Fig. 4.1), we conclude that, on the one hand, the ground electronic configuration is clearly split into relativistic subconfigurations and, on the other hand, the lowest excited configurations are strongly mixed with the ground one. Therefore, here we have the unique situation, when the real electronic configuration is the linear combination of several configurations, having almost equal weights, and, thus, the single-configuration approximation is absolutely unfit.

In Table 4.8 we list the leading percentage compositions exceeding 10% for the lowest 30 energy levels of the W^{+8} ion calculated using MCDF+B+QED. The expansion coefficients c_i from the relation (4.8) for the intermediate coupling wavefunctions are obtained by diagonalizing the Dirac-Coulomb-Breit matrix. The indices N for the levels provided in the first column of Table 4.8 are used in all subsequent tables. In the second column (*State*) of Table 4.8 levels are represented in $LS-$coupling.

Table 4.9 displays the computed energy levels of 3 lowest configurations [Kr]$4d^{1}04f^{1}45s^25p^4$, [Kr]$4d^{1}04f^{1}35s^25p^5$ and [Kr]$4d^{1}04f^{1}25s^25p^6$ of W^{+8}. The fully relativistic calculations were performed using large scale MCDF and RCI approaches with the GRASP2K code and with the AS_6 MR set of the atomic state function expansion.

Table 4.8: The leading percentage compositions (> 10%) of W^{+8} levels in the MCDF+B+QED approach with AS_6 (single-double excitation)

N	State	Leading configuration in jj-coupling			Composition
		Configuration	J P	Contr.	
1	$4f^{14}5p^4\ ^3P_2$	$4f_-^6 4f^8 5p_-^2 5p^2$	2+	88%	
2	$4f^{13}5p^5\ ^3F_4$	$4f_-^6 4f^7 5p_-^2 5p^3$	4+	93%	
3	$4f^{13}5p^5\ ^1F_3$	$4f_-^6 4f^7 5p_-^2 5p^3$	3+	94%	
4	$4f^{13}5p^5\ ^3G_5$	$4f_-^6 4f^7 5p_-^2 5p^3$	5+	97%	
5	$4f^{13}5p^5\ ^3F_3$	$4f_-^5 4f^8 5p_-^2 5p^3$	3+	94%	
6	$4f^{13}5p^5\ ^1D_2$	$4f_-^6 4f^7 5p_-^2 5p^3$	2+	81%	
7	$4f^{14}5p^4\ ^1S_0$	$4f_-^6 4f^8 5p_-^2 5p^2$	0+	93%	
8	$4f^{13}5p^5\ ^3F_2$	$4f_-^5 4f^8 5p_-^2 5p^3$	2+	89%	
9	$4f^{13}5p^5\ ^3G_4$	$4f_-^5 4f^8 5p_-^2 5p^3$	4+	93%	
10	$4f^{13}5p^5\ ^3D_1$	$4f_-^5 4f^8 5p_-^2 5p^3$	1+	97%	
11	$4f^{12}(^3H)5p^6\ ^3H_6$	$4f_-^6 4f^6(J=6)5p_-^2 5p^4$	6+	89%	
12	$4f^{12}(^3F)5p^6\ ^3F_4$	$4f_-^6 4f^6(J=4)5p_-^2 5p^4$	4+	96%	
13	$4f^{12}(^3H)5p^6\ ^3H_5$	$4f_-^5 4f^7(J_{12}=5)5p_-^2 5p^4$	5+	96%	
14	$4f^{12}(^1G)5p^6\ ^3G_4$	$4f_-^5 4f^7(J_{12}=4)5p_-^2 5p^4$	4+	86%	
15	$4f^{12}(^1D)5p^6\ ^1D_2$	$4f_-^6 4f^6(J=2)5p_-^2 5p^4$	2+	57%	+ 27% $4f_-^5 4f^7(J_{12}=2)5p_-^2 5p^4$ + 11% $4f_-^4(J=2)4f^8 5p_-^2 5p^4$
16	$4f^{12}(^3F)5p^6\ ^3F_3$	$4f_-^5 4f^7(J_{12}=3)5p_-^2 5p^4$	3+	96%	
17	$4f^{14}5p^4\ ^3P_1$	$4f_-^6 4f^8 5p_- 5p^3$	1+	94%	
18	$4f^{12}(^3H)5p^6\ ^3H_4$	$4f_-^4(J=4)4f^8 5p_-^2 5p^4$	4+	86%	
19	$4f^{14}5p^4\ ^1D_2$	$4f_-^6 4f^8 5p_- 5p^3$	2+	69%	+ 14% $4f_-^4(J=2)4f^8 5p_-^2 5p^4$
20	$4f^{12}(^1D)5p^6\ ^1D_2$	$4f_-^6 4f^6(J=2)5p_-^2 5p^4$	2+	37%	+ 30% $4f_-^5 4f^7(J_{12}=2)5p_-^2 5p^4$ + 17% $4f_-^4(J=2)4f^8 5p_-^2 5p^4$
21	$4f^{13}5p^5\ ^3D_3$	$4f_-^6 4f^7 5p_-(J_{13}=3)5p^4$	3+	96%	
22	$4f^{13}5p^5\ ^3G_4$	$4f_-^6 4f^7 5p_-(J_{13}=4)5p^4$	4+	95%	
23	$4f^{12}(^1I)5p^6\ ^1I_6$	$4f_-^5 4f^7(J_{12}=6)5p_-^2 5p^4$	6+	89%	
24	$4f^{12}(^1S)5p^6\ ^1S_0$	$4f_-^6 4f^6(J=0)5p_-^2 5p^4$	0+	68%	+ 28% $4f_-^4(J=0)4f^8 5p_-^2 5p^4$
25	$4f^{12}(^3P)5p^6\ ^3P_1$	$4f_-^5 4f^7(J_{12}=1)5p_-^2 5p^4$	1+	94%	
26	$4f^{13}5p^5\ ^3G_3$	$4f_-^5 4f^8 5p_-(J_{13}=3)5p^4$	3+	94%	
27	$4f^{12}(^3F)5p^6\ ^3F_2$	$4f_-^4(J=2)4f^8 5p_-^2 5p^4$	2+	50%	+ 35% $4f_-^5 4f^7(J_{12}=2)5p_-^2 5p^4$
28	$4f^{13}5p^5\ ^3F_2$	$4f_-^5 4f^8 5p_-(J_{13}=2)5p^4$	2+	75%	+ 12% $4f_-^6 4f^8 5p_- 5p^3$
29	$4f^{12}(^3P)5p^6\ ^3P_0$	$4f_-^4(J=0)4f^8 5p_-^2 5p^4$	0+	53%	+ 22% $4f_-^6 4f^6(J=0)5p_-^2 5p^4$ + 21% $4f_-^6 4f^8 5p^4$
30	$4f^{14}5p^4\ ^3P_0$	$4f_-^6 4f^8 5p^4$	0+	72%	+ 15% $4f_-^4(J=0)4f^8 5p_-^2 5p^4$

Table 4.9: The fine structure of W^{+8} levels in the MCDF+B+QED approach with AS_6 (single-double excitation)

N	State	Level (-16111.3239249 a.u.)
1	$4f^{14}5p^4\ ^3P_2$	0.00
2	$4f^{13}5p^5\ ^3F_4$	4276.10
3	$4f^{13}5p^5\ ^1F_3$	4970.34
4	$4f^{13}5p^5\ ^3G_5$	9286.78
5	$4f^{13}5p^5\ ^3F_3$	19617.52
6	$4f^{13}5p^5\ ^1D_2$	21564.44
7	$4f^{14}5p^4\ ^1S_0$	25181.52
8	$4f^{13}5p^5\ ^3F_2$	25971.95
9	$4f^{13}5p^5\ ^3G_4$	32420.30
10	$4f^{13}5p^5\ ^3D_1$	34540.16
11	$4f^{12}(^3H)5p^6\ ^3H_6$	53915.33
12	$4f^{12}(^3F)5p^6\ ^3F_4$	62742.32
13	$4f^{12}(^3H)5p^6\ ^3H_5$	70144.75
14	$4f^{12}(^1G)5p^6\ ^3G_4$	77451.71
15	$4f^{12}(^1D)5p^6\ ^1D_2$	80129.06
16	$4f^{12}(^3F)5p^6\ ^3F_3$	80511.90
17	$4f^{14}5p^4\ ^3P_1$	86403.59
18	$4f^{12}(^3H)5p^6\ ^3H_4$	93050.66
19	$4f^{14}5p^4\ ^1D_2$	99341.48
20	$4f^{12}(^1D)5p^6\ ^1D_2$	103262.26
21	$4f^{13}5p^5\ ^3D_3$	105128.27
22	$4f^{13}5p^5\ ^3G_4$	107795.93
23	$4f^{12}(^1I)5p^6\ ^1I_6$	112195.18
24	$4f^{12}(^1S)5p^6\ ^1S_0$	115516.38
25	$4f^{12}(^3P)5p^6\ ^3P_1$	118434.83
26	$4f^{13}5p^5\ ^3G_3$	118494.90
27	$4f^{12}(^3F)5p^6\ ^3F_2$	122129.28
28	$4f^{13}5p^5\ ^3F_2$	131717.26
29	$4f^{12}(^3P)5p^6\ ^3P_0$	174698.58
30	$4f^{14}5p^4\ ^3P_0$	206586.72

4.4 Multiple ionization of tungsten ions

4.4.1 Multiple electron ionisation rate coefficients, with special emphasis on 4d, 4f and 5d, 5f open-shell systems

The double ionization cross sections by electron impact from the ground levels were investigated for W^{+1}, W^{+3} and W^{+5} ions. The energy level spectra, cross sections of single ionization and excitation by electron impact as well as rates of Auger transitions have been obtained by employing the Flexible Atomic Code [J1]. The mixing of all relativistic configurations corresponding to the same nonrelativistic configuration is taken into account. The direct single electron-impact ionization is calculated in the distorted-wave approximation for W^{+5} ion. However, binary-encounter-dipole model [J2] is employed for W^{+1} and W^{+3} ions because distorted-wave approximation tends to overestimate experimental cross sections [J3] for near-neutrals.

The double ionization of the ions was considered as a two-step process: the initial single ionization by electron impact and the following autoionization:

$$e^- + A^{q+} \rightarrow (A^{(q+1)+})^* + e^- + e^- \rightarrow A^{(q+2)+} + e^- + e^- + e^-. \tag{4.10}$$

In addition, the study included the electron-impact excitation with a further decay through the autoionization channels to the next ionization stage:

$$e^- + A^{q+} \rightarrow (A^{(q)+})^* + e^- \rightarrow (A^{(q+1)+})^* + e^- + e^- \rightarrow A^{(q+2)+} + e^- + e^- + e^-. \tag{4.11}$$

However, in previous work [J4] we have obtained that the influence of excited levels of the initial ion to the double ionization process is negligible. On the other hand, the decay of the excited levels of the initial ion gives rise for the significant population to the levels of the next ionization stage through autoionization process.

Energy levels of W^{+3}, W^{+4} and W^{+5} ions included in calculations of the double-ionization of W^{+3} are shown in Fig. 4.2. In current study, the configurations having the largest relative populations have been determined after electron-impact excitation and ionization from the ground level of the initial ion. Only the configurations with relative populations exceeding 1% are considered for the analysis of double-ionization process. The largest relative populations after the electron-impact excitations are gained by the levels of $5d^26p$ and $5p^55d^4$ configurations, for example, 26.4% and 23.5%, respectively, for incident electron energy of 120 eV. However, the Auger transitions are allowed only from the levels of $5p^55d^4$ configuration. One can see that only the levels of $5p^55s^25d^3$ and $5s5d^3$ configurations can decay to the levels of W^{5+} ion by the Auger transitions. The relative population of $5p^55s^25d^3$ configuration is by two orders of magnitude larger than that of $5s5d^3$ configuration. Consequently, the Auger transitions from the levels of $5p^55s^25d^3$ configuration are responsible for the contribution to the $W^{+3} \rightarrow W^{+5}$ double-ionization cross sections.

Comparison of theoretical and experimental results for electron-impact double-ionization cross section is presented in Fig. 4.3. The total calculated double-ionization cross section of W^{+3} is smaller than the cross section from the experimental data [J5]. The peak of experimental curve is underestimated more than four times by our theoretical calculations. Similar results have been obtained in the previous work [J4] for the double-ionization cross sections of W^{+2}, W^{+4} and W^{+6} ions. It demonstrates that the direct double ionization may play the main role in producing doubly-ionized ions. Good agreement obtained with the experimental values for the single-ionization cross sections suggests that correlation effects will not have significant influence on double ionization. Present calculations of double-ionization cross sections of W^{+1} and W^{+5} ions have the same tendency – theoretical values are too small. An approximate evaluation of the direct double ionization by using sudden-perturbation model in the previous work [J4] did not help to obtain data close to experimental values. On the other hand, our model included only additional ionization due to the sudden perturbation of electronic shells after single ionization. Further analysis is necessary to estimate the contribution of shake-off and shake-up processes to double-ionization cross sections following electron-impact excitation. Those processes can have significant effect on the double ionization because the electron-impact excitation cross sections are approximately by an order of magnitude larger than the cross sections of the direct single ionization.

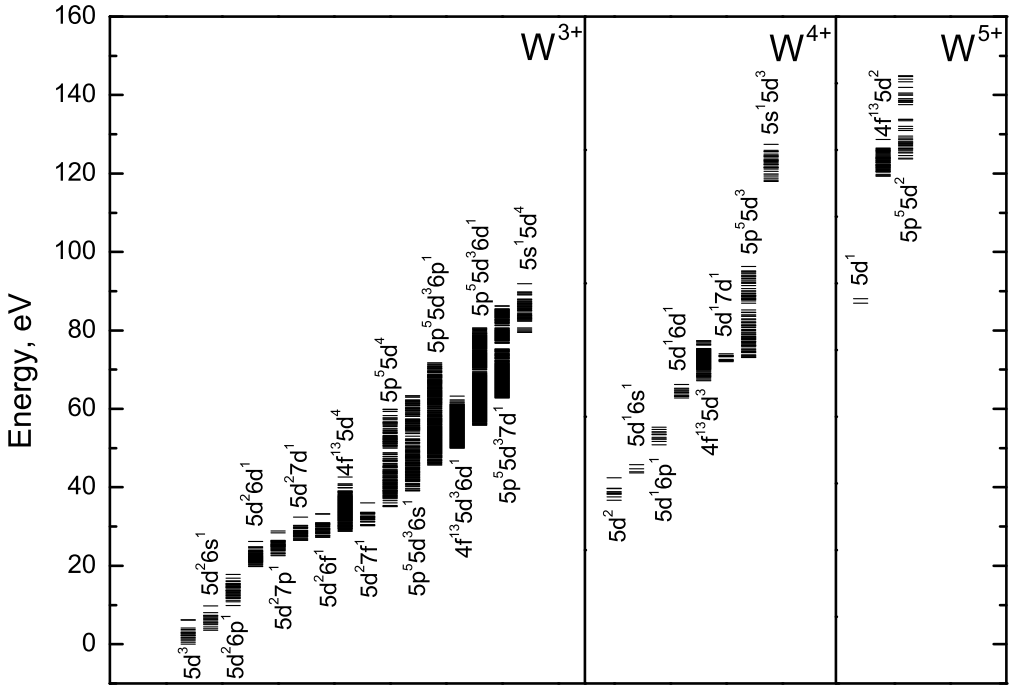

Figure 4.2: Energy levels of W^{+3}, W^{+4} and W^{+5} ions for the configurations included in the calculations of double-ionization cross section of W^{+3} ion.

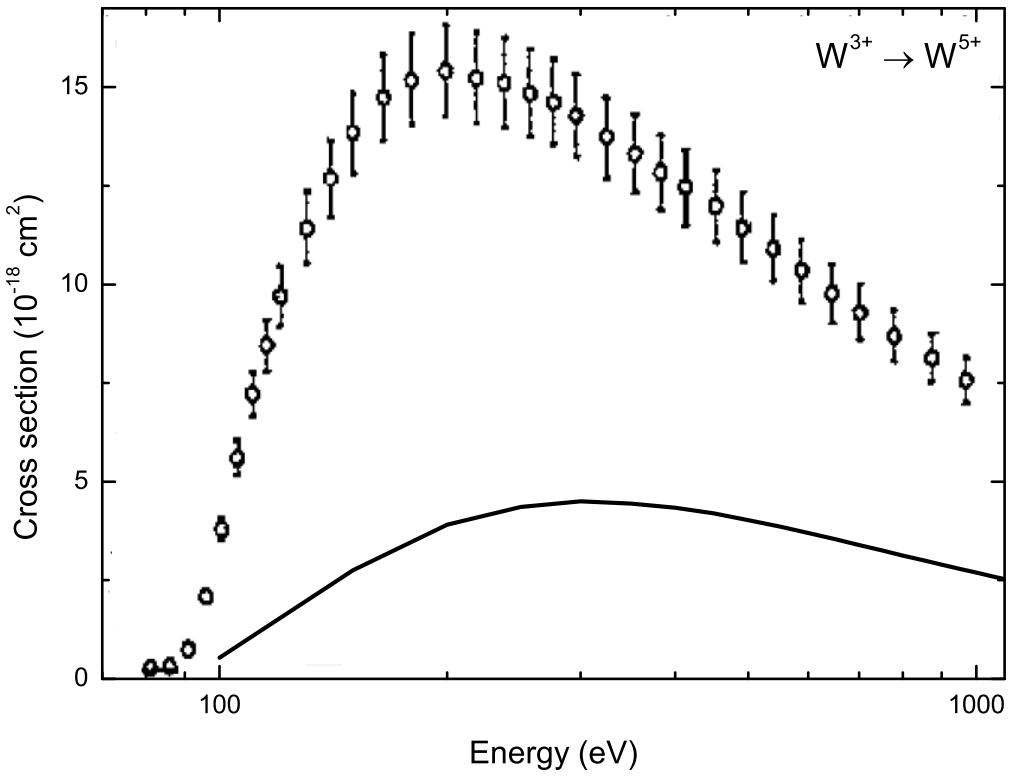

Figure 4.3: Comparison of electron-impact double-ionization cross section for W^{+3} ion. Solid line represents theoretical values, circles with error bars are experimental data [J5].

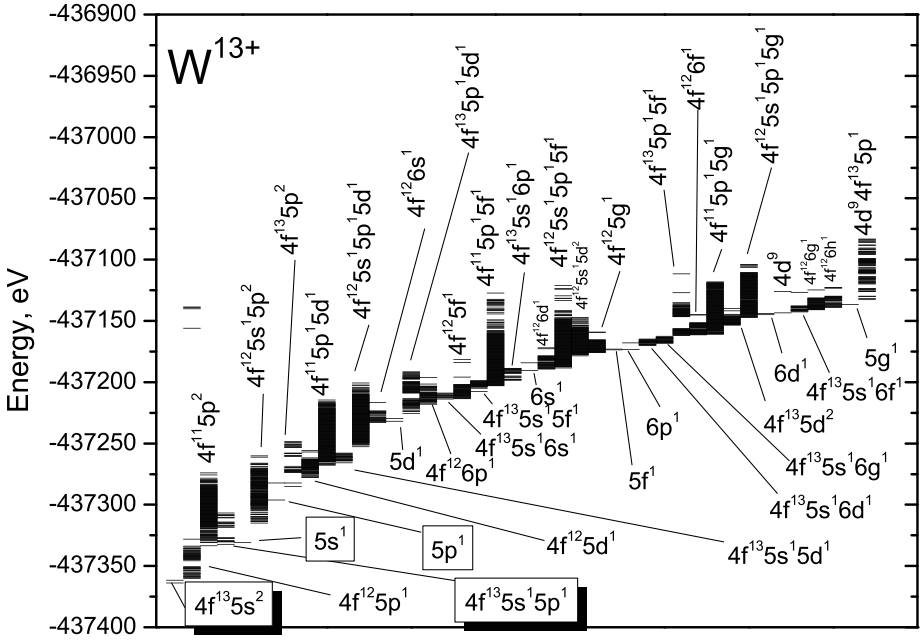

Figure 4.4: Energy levels of W^{+13}ion.

4.4.2 Exploitation of ITPA special studies of key complex ion configuration interactions (such as symmetric exchanger of symmetry), with special emphasis on 4d, 4f and 5d, 5f open-shell systems

W^{+13} ions

Using Berlin EBIT facilities, Hutton et al. [J6] have measured spectra of the tungsten ions at electron-beam energies corresponding to the maximum production of W^{+13} ions in the EBIT plasma. It was expected to observe the resonance lines corresponding to the $5p \rightarrow 5s$ transition which could be used for the fusion plasma diagnostics. They expected that two prominent resonance lines would be produced in the spectrum if the collapse of orbitals would have occurred in the ion. In their work [J6], two intense lines at 258.2 Å and 365.3 Å have been assigned to the resonance transition. Later, the detailed investigation of transitions for W^{+13} by employing the relativistic multireference many-body perturbation theory has been performed in [J7]. The calculations presented therein demonstrated that the ground state of the ion corresponds to the $4f^{13}5s^2$ configuration and it does not coincide with the earlier predictions obtained from the quasirelativistic calculations [J8] stating that the Pm-like ions with the nuclear charge Z larger than 73 have alkali-metal-like structure with the ground configuration being $4f^{14}5s$. The Pm-like W spectra simulated using a collisional-radiative model for the low-density conditions did not help to identify the observed lines from the experimental spectra [J9]. Vilkas et al [J7] stressed that their study did not show one or two dominant resonance lines in the spectra. Therefore the situation with the interpretation of the lines from the EBIT plasma spectra corresponding to the radiative transition in W^{+13} ion was named as a *class of unsolved mysteries* [J10].

We have studied configuration interaction (CI) effects in the W^{+13} ion by employing the extended basis of interacting configurations. Flexible Atomic Code [J1] was employed to obtain the energy levels of W^{+13} using the configuration interaction method. The exploited CI basis consists of 32661 levels which arise from 65 non-relativistic configurations presented in Fig. 4.4: $4f^{13}5s^2$, $4f^{14}5s$, $4f^{14}5l$, $4f^{14}6l'$, $4f^{13}5s5l$, $4f^{13}5s6l'$, $4f^{12}5s^25l$, $4f^{12}5s^26l'$, $4d^94f^{14}5s^2$, $4d^94f^{14}5s5l$, $4d^94f^{13}5s^25l$, $4f^{12}5s5p^2$, $4f^{12}5s5p5l''$, $4f^{12}5s5d^2$, $4f^{12}5s5d5f$, $4f^{12}5s5d5g$, $4f^{12}5s5f^2$, $4f^{12}5s5f5g$, $4f^{12}5s5g^2$, $4f^{11}5s^25p^2$, $4f^{11}5s^25p5l''$, $4f^{13}5p^2$, $4f^{13}5p5l''$, $4f^{13}5d^2$, $4f^{13}5d5f$, $4f^{13}5d5g$, $4f^{13}5f^2$, $4f^{13}5f5g$, $4f^{13}5g^2$ $(l = p, d, f, g; l' = s, p, d, f, g, h; l'' = d, f, g)$.

The configuration interaction for the levels of the ground configuration is not very significant. An addition of the $4f^{12}5s^25f$ configuration does not exceed 6 %. It should be noted that the energy levels of those configurations do not

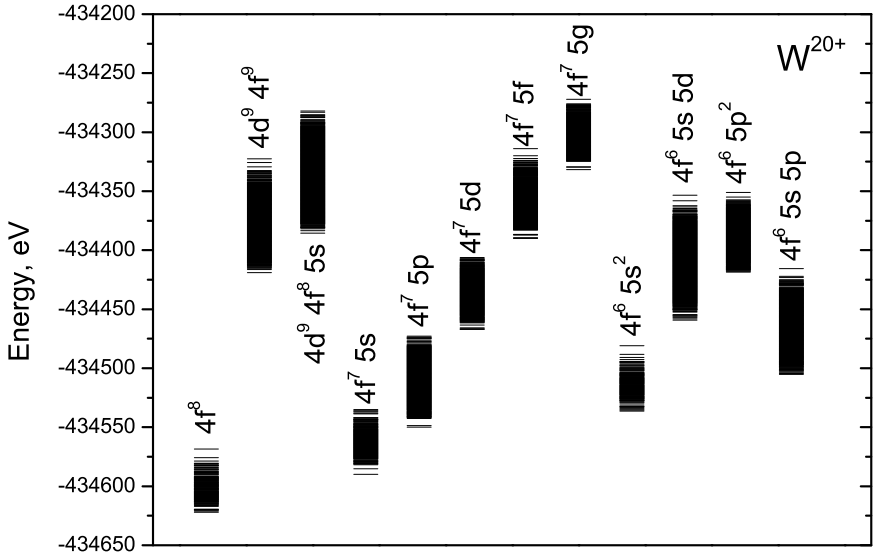

Figure 4.5: Energy levels of W^{+20}ion.

overlap. On the other hand, there is a large number of other levels (30039) with the main percentage compositions in the intermediate wave functions smaller than 50 %. The largest mixing corresponds to the strong interaction of configurations with a symmetric exchange of symmetry: $4f^{12}5s^25d+4f^{12}5s5p^2$; $4f^{13}5s5d+4f^{13}5p^2$; $4f^{11}5s^25p5d+4f^{12}5s^26s+4f^{13}5s5f+4f^{13}5p5d$; $4f^{12}5s5p5d+4f^{12}5s^25f+4f^{12}5s^26p+4f^{13}5s6s$. Many energy levels of these configurations are positioned close energetically and there exists a pronounced mixing among them. The number of the levels with the main percentage composition smaller than 50 % totals to 1809 when the first two configuration state functions in jj-coupling with the largest expansion coefficients belong to the different configurations.

W^{+20} ions

Calculations of energy levels were performed for the $4f^8$, $4f^75l$ ($l \leq 4$), $4d^94f^9$, $4d^94f^85s$, $4f^65s^2$, $4f^65p^2$, $4f^65s5p$ and $4f^65s5d$ configurations of the W^{+20} ion in Dirac-Fock-Slater approximation using Flexible Atomic Code [J1]. In our calculation, the CI basis is contructed from 35779 levels. The theoretical energy levels of these configurations are presented in Fig. 4.5. A very large configuration interaction is observed for the configurations with a symmetric exchange of symmetry, namely $4f^75p+4f^65s^2$; $4f^75d+4f^65s5p$; $4f^75f+4f^65p^2+4f^65s5d+4d^94f^85s$. There are 3067 levels having the main percentage compositions in the configuration-interaction wave functions smaller than 50% and with the first two configuration state functions having the largest expansion coefficients which belong to different non-relativistic configurations.

4.5 references

[6] R. D. Cowan 1981 The theory of atomic structure and spectra, (Berkeley CA, University of California Press) p. 731.
[7] P. Bogdanovich and O. Rancova 2002 Lithuanian. J. Phys. 42, 257.
[8] P. Bogdanovich and O. Rancova 2006 Phys. Rev. A 74, 052501.
[9] P. Bogdanovich and O. Rancova 2007 Phys. Rev. A 76, 012507.
[10] P. Bogdanovich and O. Rancova 2003 Lithuanian. J. Phys. 43, 177.
[11] P. Bogdanovich, V. Jonauskas and O. Rancova 2005 Nucl. Instr. Meth. B 235, 145.
[12] P. Bogdanovich and O. Rancova 2008 Phys. Scr. 78, 045301.
[13] A. Hibbert, R. Glass and C. Froese Fischer 1991 Comput. Phys. Commun. 64, 455
[14] C. Froese Fischer, M. R. Godefroid and A. Hibbert 1991 Comput. Phys. Commun. 64, 486.

[15] C. Froese Fischer and M. R. Godefroid 1991 Comput. Phys. Commun. 64, 501.
[16] P. Bogdanovich P and R. Karpuškienė 1999 Lithuanian J. Phys. 39, 193.
[17] P. Bogdanovich 2005 Nucl. Instr. Meth. B 235, 92.
[18] R. Karpuškienė and P. Bogdanovich 2003 J. Phys.B: At. Mol. Opt. Phys. 36 2145.
[19] P. Bogdanovich, R. Karpuškienė and A. Udris 2004 J. Phys. B: At. Mol. Phys 37, 2067.
[20] P. Bogdanovich and R. Karpuškienė 2009 At. Data Nucl. Data Tables 95, 533.
[21] P. Bogdanovich and R. Karpuškienė 2001 Comp. Phys. Commun. 134, 321.
[22] P. Bogdanovich, R. Karpuškienė and A. Momkauskaitė 2005 Comp. Phys. Commun. 172, 133.
[23] O. Rancova, P. Bogdanovich and R. Karpuškienė 2009 J. Physics: Conf. Ser. 163, 012011.
[24] R. Karpuškienė, O. Rancova and P. Bogdanovich 2010 J. Phys. B: At. Mol. Opt. Phys. 43, 085002.
[25] I. I. Sobelman, L. A. Vainshtein and A. E. Yukov 1995 *Excitation of Atoms and Broadening of Spectral Lines* (Springer Series on Atoms and Plasmas vol 15) (Berlin: Springer).
[27] http://physics.nist.gov/PhysRefData/Ionization/
[28] Y.-K. Kim 2001 Phys. Rev. A 64, 0327713.
[29] P. M. Stone, Y.-K. Kim and J. P. Desclaux 2002 J. Res. Natl. Inst. Stand. Technol. 107, 327.
[30] I. Bray and Y. Ralchenko 2001 http://atom.murdoch.edu.au/CCC-WWW/index.html.
[31] W. B. Westerveld, H. G. M. Heideman and J. van Eck 1979 J. Phys. B 12, 115.
[32] D. E. Shemansky, J. M. Ajello, D. T. Hall and B. Franklin 1985 Astrophysical Journal 296, 774.
[33] H. Merabet, M. Bailey, R. Bruch, J. Hanni, S. Bliman, D. V. Fursa, I. Bray, K. Bartschat, H. C. Tang and C. D. Lin 2001 Phys. Rev. A 64, 012712.
[34] S. Trajmar, J. M. Ratliff, G. Csanak and D. C. Cartwright 1992 Z. Phys. D 22, 457.
[35] J. Schweinzer, R. Brandenburg, I. Bray, R. Hoekstra, F. Aumayr, R. K Janev and H. P. Winter 1999 ADNDT 72, 239.
[36] D. Leep and A. Gallagher 1974 Phys. Rev. A 10, 1082.
[37] W. Williams, S. Trajmar and D. Bozinis 1976 J. Phys. B 9, 1529.
[38] L. Vuskovic, S. Trajmar and D. F. Register 1982 J. Phys. B 15, 2517.
[B3] P. Jönsson, X. He, C. Froese Fischer and I. P. Grant 2007 Comput. Phys. Commun. 177, 597.
[B4] B. J. McKenzie, I. P. Grant and P. H. Norrington 1980 Comput. Phys. Commun. 21, 233.
[B5] C. Froese Fischer, G. Gaigalas and Y. Ralchenko 2006 Comput. Phys. Commun. 175, 738.
[J1] M. F. Gu 2003 Astrophys. J. 582, 1241.
[J2] D.-H. Kwon, Y.-J. Rhee and Y.-K. Kim 2006 Int. J. Mass Spectrom. 252, 213.
[J3] S. D. Loch J. Ludlow, M. Pindzola, A. Whiteford and D. Griffin 2005 Phys. Rev. A 72, 052716.
[J4] V. Jonauskas, S. Kučas and R. Karazija 2009 Lith. J. Phys. 49, 415.
[J5] M. Stenke , K. Aichele, D. Hathiramani, G. Hofmann, M. Steidl, R. Volpel, V. Shevelko, H. Tawara and E. Salzborn 1995 J. Phys. B: At. Mol. Opt. Phys 28, 4853.
[J6] R. Hutton, Y. Zou, J. R. Almados, C. Biedermann, R. Radtke, A. Greier and R. Nieu 2003 Nucl. Instr. Meth. B205, 114.
[J7] M. J. Vilkas, Y. Ishikawa and E. Träbert 2008 Phys. Rev. A77, 042510.
[J8] L. J. Curtis and D. G. Ellis 1980 Phys. Rev. Lett. 45, 2099.
[J9] E. Träbert, M. J. Vilkas and Y. Ishikawa 2009 J. Phys. Conf. Series 163, 012017.
[J10] S. Wu and R. Hutton 2008 Can. J. Phys. 86, 126.

Chapter 5

Atomic data and models for neutral beam diagnostics

The authors of this chapter are Friedrich Aumayr, Katharina Igenbergs, Martin O'Mullane and Hugh Summers. It incorporates the brief report on ADAS-EU sub-contract 4 prepared by the Institute of Applied Physics, Technische Universität Wien,Austria (K. Igenbergs and F. Aumayr) dated 2 January 2012. See also appendix D.

This report is presented to describe the item delivered by the authors from Institute of Applied Physics (IAP) of Vienna University of Technology (TU Wien) to the ADAS group of the University of Strathclyde. After a few introductory remarks, we first describe the method applied and then the data delivered under the subcontract.

5.1 Introduction

Charge exchange (CX) in collision processes between neutral hydrogen isotopes and fully stripped ions has been the subject of a large number of studies in the past (Fritsch & Lin 1991, Bransden et al. 1980) and is of special interest for diagnostics of hot magnetically con.ned fusion plasmas in particular by charge exchange recombination spectroscopy (CXRS) (Isler 1994). CXRS is a standard plasma diagnostic tool to measure radial pro.les of the ion temperature and density by using a heating or diagnostic neutral beam as the local source of neutral hydrogen isotopes inside the plasma. In principle CX from neutral hydrogen into any impurity ion species in the plasma can be used. However, best CXRS results are achieved for those with the highest abundance and using fully stripped ions facilitates the analysis. For many years fully stripped carbon was the dominant impurity in many fusion devices. Due to the change in choice of wall material replacing carbon with tungsten and/or beryllium (ASDEX Upgrade, JET and ITER) the abundance of carbon decreased (Gruber et al. 2009). In addition, the use of metallic walls and in particular the divertor tiles in present and future fusion devices makes the intentional pu. of impurity (seeding) gases mandatory in order to keep heat loads to exposed elements of the metallic wall below technical limits. Impurities like N, Ne and Ar are particularly good candidates to convert a considerable fraction of the heat .ux into radiation leading to a more uniform power distribution over the inner walls of the fusion machine. This technique of controlling the heat exhaust in fusion devices with ITER- and reactor-relevant .rst walls is currently a focus of the worldwide fusion relevant plasma research. For applying the CXRS method in such plasmas the most promising multiply charged ions depend not only on intrinsic impurities (wall material), but also on the radiator used to cool the plasma edge (Kallenbach et al. 2010). To calculate both charge exchange (CX) and ionisation (ION) cross sections, we applied the well-known atomic-orbital close-coupling (AOCC) method described in section 2. The neutral heating beam at current fusion experiments consists mainly of ground state D, but a fraction of the beam enters the plasma in an exited (metastable) state or becomes excited in collisions with plasma particles (electrons) when penetrating the plasma edge. Although this fraction is small, its contribution to the intensity of the observed spectral lines is substantial because the involved CX cross sections are about an order of magnitude larger than those for ground state hydrogen and electron capture from the excited state leads to population of higher n-shells, much closer to the observed transition lines in the visible range. (Hoekstra et al. 1998) At impact energies above 30 keV/amu, it is utterly important to take also ION into account, because it is strongly competing

with CX. This is particularly the case for collisions with H(n = 2). Especially in our AOCC calculations it became necessary to include a large number of ionisation states on the hydrogen centre. We give a very short description of the used theoretical approaches and then quickly present the delivered data. Atomic units are used unless otherwise stated.

5.2 Applied theoretical approach: atomic-orbital close-coupling

We applied the AOCC formalism (Fritsch & Lin 1991, Bransden & McDowell 1992, Gieler et al. 1993) in its impact parameter description. In this semiclassical approach, the total electron wavefunctions are expanded into target-and projectile-centred traveling atomic orbitals (AO). The time-dependent Schrodinger equation is solved in the truncated Hilbert space following the procedure by (Nielsen et al. 1990, Wallerberger et al. 2011). The appropriate choice of atomic basis states re.ects the physical problem to be treated. The calculations are done in the so-called collision frame (impact parameter,b, parallel to x-axis, impact velocity, v, parallel to the quantization axis z). Real spherical harmonics are used for the angular part of the basis states. With this choice only states with the same symmetry with respect to a reflection on the scattering plane couple in the AOCC approach. Thus an initial state of positive reflection symmetry ($l = 0$, $m_l = 0$) does not couple with states of negative reflection symmetry ($l = 1$, $m_l < 0$) and vice versa leading to basis sets of minimal size. In particular, the basis sets using the collision frame for calculations with initial states of negative reflection symmetry become small because all states with positive reflection symmetry can be omitted. The modus operandi is described in much greater detail in (Igenbergs et al. 2009). For convergent calculations, we used basis sets consisting of up to 286 states on the ion centre ($1 \leq n \leq 11$). Depending on the incident ion 54 (C^{+6} ,N^{+6}) or 73 (N^{+7}) states on the hydrogen center were used. The 54-state basis consists of 20 pure hydrogen states ($1 \leq n \leq 4$) and 34 unbound pseudostates representing the ionisation continuum. The 73-state hydrogen basis is made of 10 pure hydrogen states with Laguerre-type radial parts ($1 \leq n \leq 3$) and 63 unbound pseudostates. The used bases differ because for N^{+7} + H more pseudostates were necessary to achieve converging results for ionisation cross sections. For collisions of N^{+7} with ground state H(1s), a number of experimental and theoretical studies have been performed and published by several groups (Meyer et al. 1985, Dijkkamp et al. 1985, Fritsch & Lin 1984, Illescas & Riera 1999). Additionally the Atomic Data and Analysis Structure (ADAS) software package features a scaling algorithm (called ADAS315) that can quickly produce state-resolved CX cross section for any desired incident ion (Foster 2008). This algorithm also works for excited state H(n = 2) targets, but remained the only source we could compare our AOCC cross sections to since no other data for this collision system could be found in the literature. Our delivered data include total CX and ION cross sections as well as n-and nf-resolved CX cross sections. Additionally a parameter a is tabulated that can be used to extrapolate cross sections for n-shells with $n > nmax = 11$ according to

$$\sigma_n(E_i) = \left(\frac{n_{max}}{n}\right)^{\alpha(E_i)} \sigma_{n_{max}}(E_i) \tag{5.1}$$

5.3 Delivered data for Be^{+4} + H(n = 1, 2)

The delivered data are an improvement of the data published in Igenbergs et al. (2009). Here, we used the same basis as in our recently submitted paper on N7+,N6+, C6+ + H collisions. This basis includes more n-shells on the ion center (previously nmax = 8, now nmax = 11 and a better description for the continuum where all unbound pseudostates are located on the H center. Fig. 5.1 shows total CX and ION cross sections for an H(1s) target as well as an H(n = 2) target. Fig.5.2 shows n-resolved cross sections. In particular, data for the following reactions have been delivered:

- $Be^{+4} + H(1s) \rightarrow Be^{+3}(nl) + H^+$, for $1 \leq n \leq 11,\ 0 \leq l \leq n-1$
- $Be^{+4} + H(1s) \rightarrow Be^{+4} + H^+ + e^-$
- $Be^{+4} + H(n = 2) \rightarrow Be^{+3}(nl) + H^+$, for $1 \leq n \leq 11,\ 0 \leq l \leq n-1$
- $Be^{+4} + H(n = 2) \rightarrow Be^{+4} + H^+ + e^-$

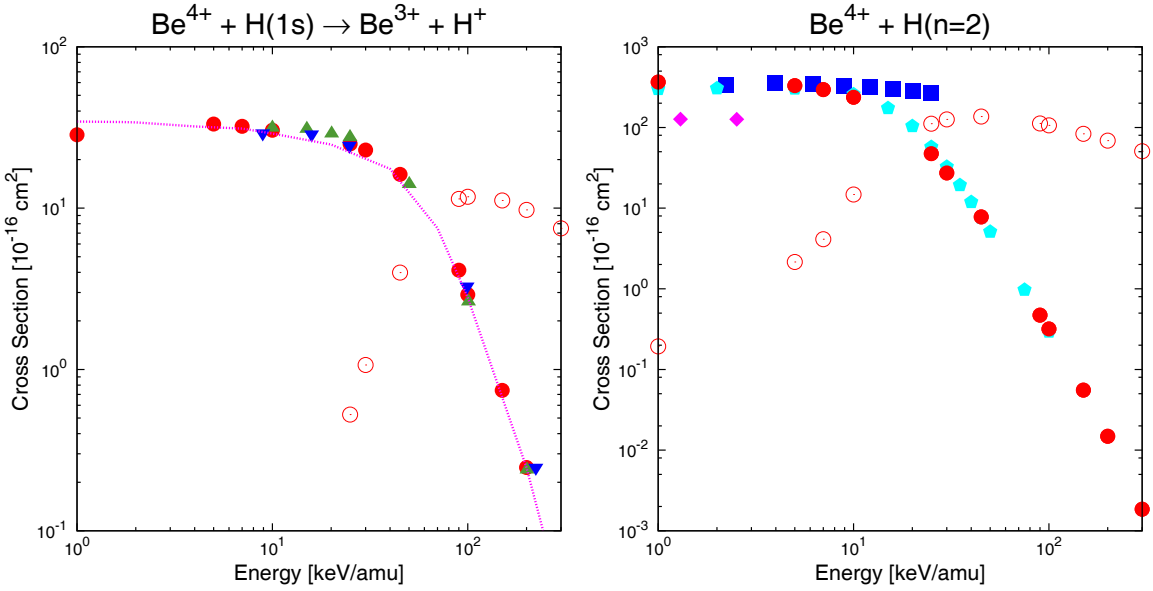

(a) (b)

Figure 5.1: Total CX (closed circle) and ION (open circle) cross sections for collisions of Be4+ and (a) H(1s). For comparison also data from (Minami et al. 2006) (closed triangle) and (Illescas & Riera 1999) (inverted closed triangle) are shown, as well as the recommended cross section for C4+ - H(1s) from (Janev et al. 1988) (dotted line). (b) H(n = 2) target compared to data from (Errea et al. 1998) (closed square), (Casaubon 1993) (closed diamond) and (Hoekstra et al. 1998) (closed pentagon).

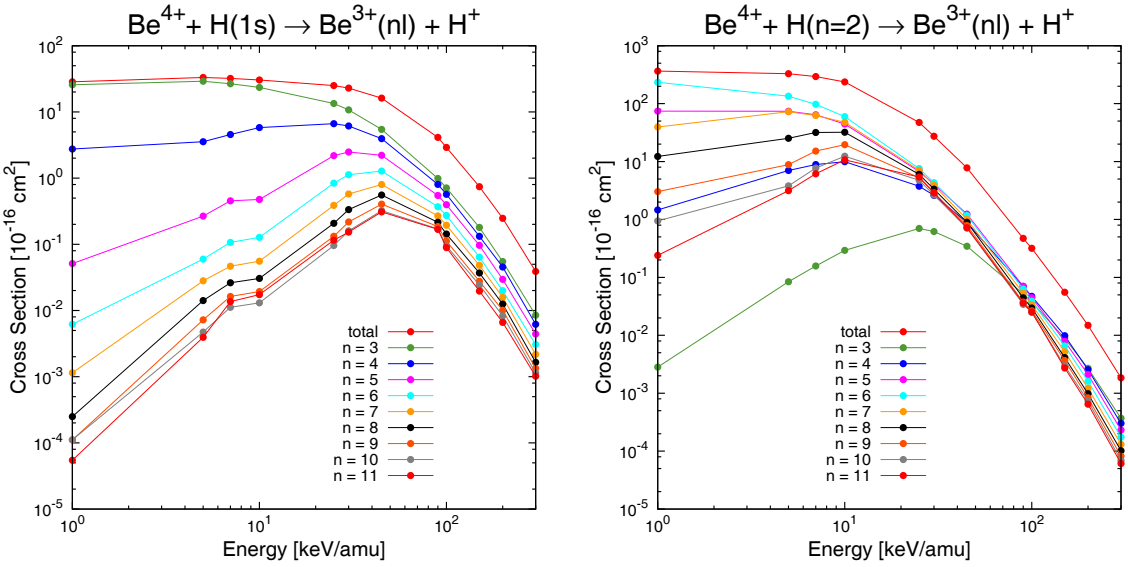

(a) (b)

Figure 5.2: Figure 2: n-resolved cross sections for Be4+ + (a) H(1s) and (b) H(n = 2).

5.4 Delivered data for N^{+7} + H(n = 1, 2)

Fig.5.3(a) shows total CX and ION cross sections for an H(1s) target, fig. 5.3(b) for an H(n = 2) target. The cross section in the latter case is the statistically weighted sum of the cross sections of the four di.erent n = 2 substates (Igenbergs et al. 2009). Figs.4 and 5 show n-resolved cross sections for the respective targets for the main capture channel and the n-shells of interest for CXRS. For a more detailed analysis please refer to our paper submitted to *J. Phys. B: At. Mol. Phys* and *arXiv.org* (Igenbergs et al. 2011).

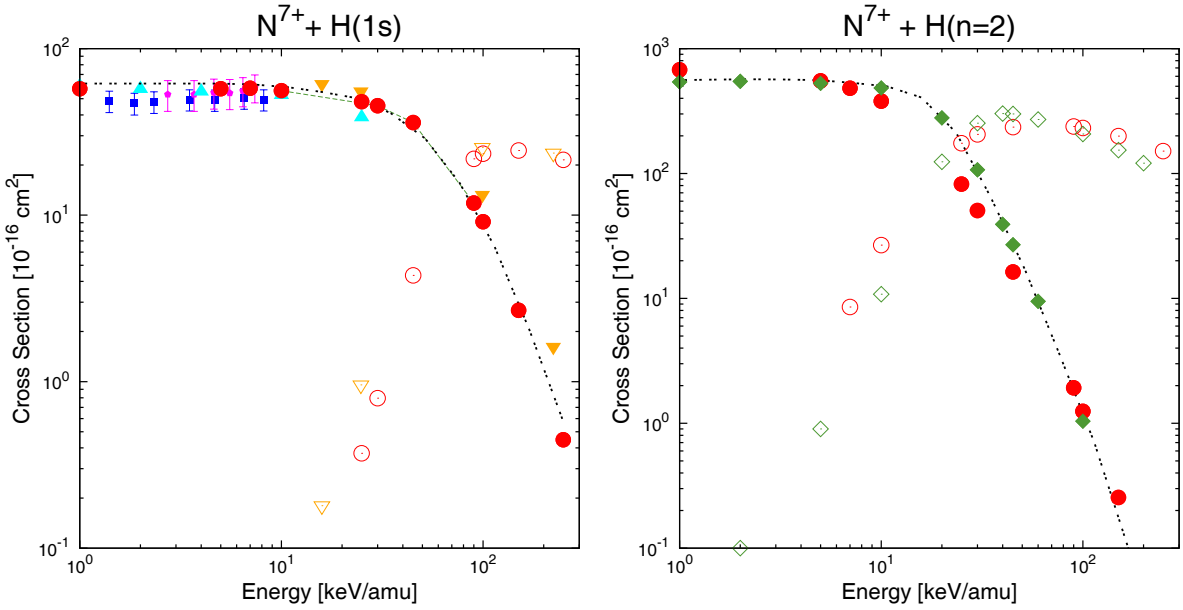

Figure 5.3: Figure 3: Total cross sections for CX (full symbols) and ION (open symbols). (a) H(1s) target. Delivered AOCC cross sections are plotted using solid circles and open circles resepctively. For reference purposes we show experimental CX data from Meyer et al. (1985) ( ) and Dijkkamp et al. (1985) ( ) as well as results from various theoretical approaches: AO+ CX cross sections from Fritsch & Lin (1984) ( ), CTMC results for CX ( ) from Illescas & Riera (1999), scaled CX data ( ) calculated with ADAS315(Foster 2008) and ION ( ) again from Illescas & Riera (1999). (b) H(n = 2) target including CTMC calculations CTMC from (Igenbergs et al. 2011)

In particular, data for the following reactions have been delivered:

- $N^{+7} + H(1s) \rightarrow N^{+6}(nl) + H^{+}$, for $1 \leq n \leq 11, 0 \leq l \leq n-1$
- $N^{+7} + H(1s) \rightarrow N^{+7} + H^{+} + e^{-}$
- $N^{+7} + H(n=2) \rightarrow N^{+6}(nl) + H^{+}$, for $1 \leq n \leq 11, 0 \leq l \leq n-1$
- $N^{+7} + H(n=2) \rightarrow N^{+7} + H^{+} + e^{-}$

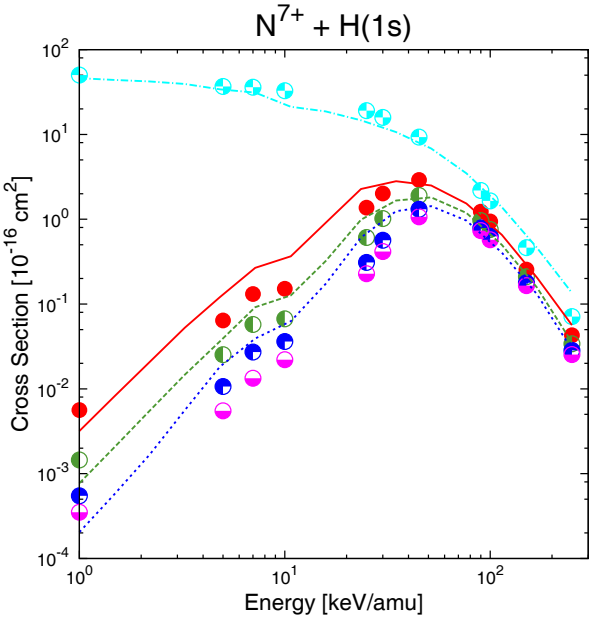

Figure 5.4: Figure 4: n-resolved cross sections for electron capture from the H(1s) target. Circle symbols are used for AOCC data from (Igenbergs et al. 2011) and lines for ADAS315 (Foster 2008) data. σ(n = 5) (cyan), σ(n = 8) (red), σ(n = 9) (green), σ(n = 10) (blue), and σ(n = 11) (magenta).

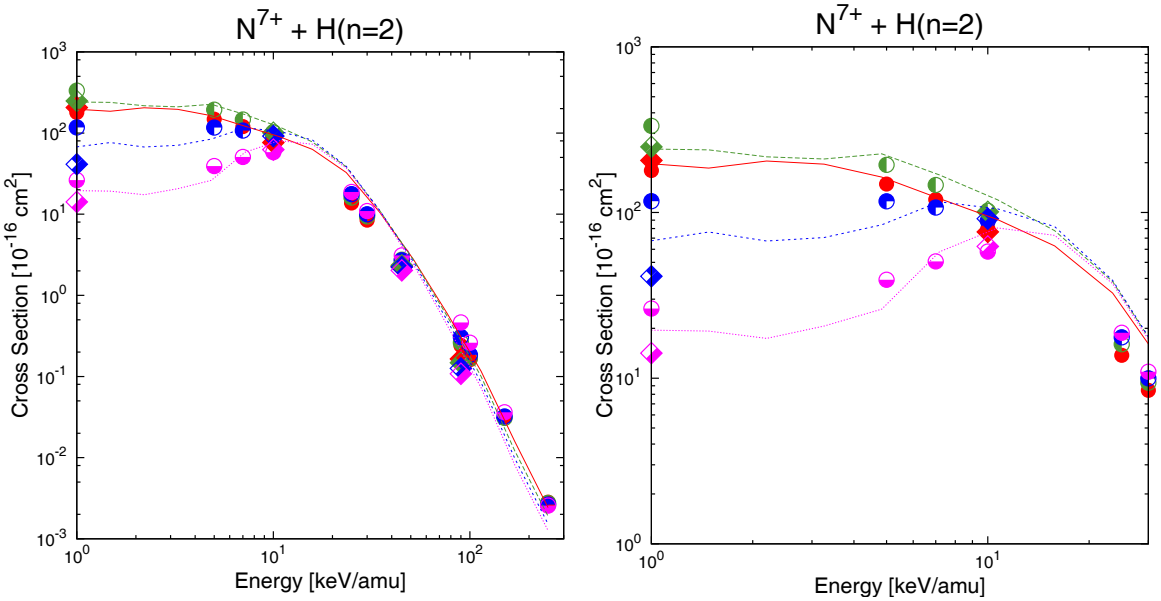

(a) (b)

Figure 5.5: Figure 5: n-resolved cross sections for electron capture from an H(n = 2) target. Circle symbols are used for AOCC data, rhombic symbols for CTMC (Igenbergs et al. 2011), and lines for ADAS315 (Foster 2008) data. σ(n = 8) (red), σ(n = 9) (green), σ(n = 10) (blue), and σ(n = 11) (magenta) (a) total energy range (b) 1-30 keV/amu.

5.5 Cross section data bases for neutral lithium and sodium beam diagnostics

In addition to our AOCC results, we also delivered our databases for neutral lithium or sodium beam diagnostics. These data bases have both been published in Atomic Data and Nuclear Data Tables (Schweinzer et al. 1999, Igenbergs et al. 2008) and include .t formulae and parameters for Li/Na collisions with electrons, protons, and multiply charged ions. In particular, the transitions include

- Electron-impact target excitation of Li($nl \rightarrow n'l$); n, n' =2 - 4 & Na($nl \rightarrow n'l'$); n, n' =3 - 5
- Electron-impact target ionization of Li(nl); n = 2 - 3 & Na(nl); n =3 - 5
- Proton-impact target excitation of Li($nl \rightarrow n'l'$); n =2 - 3, n' =2 - 4 & Na($nl \rightarrow n'l'$); n, n' =3 - 5
- Proton-impact target electron loss of Li(nl); n =2 - 4 & Na(nl); n =3 - 5

5.6 References

[1] Bransden B H, Newby C W & Noble C J 1980 Journal of Physics B: Atomic and Molecular Physics 13(21), 42454255. URL: http://stacks.iop.org/0022-3700/13/4245.
[2] Bransden B & McDowell M 1992 Charge-Exchange and the Theory of Ion-Atom Collisions Vol. 82 of The International Series of Monographs on Physics Oxford Science Publications.
[3] Casaubon J I 1993 Phys. Rev. A 48(5), 36803683.
[4] Dijkkamp D, Ciric D & Heer F J d 1985 Phys. Rev. Lett. 54(10), 10041007.
[5] Errea L F, Harel C, Jouin H, Mendez L, Pons B & Riera A 1998 Journal of Physics B: Atomic, Molecular and Optical Physics 31(16), 35273545. URL: http://stacks.iop.org/0953-4075/31/3527.
[6] Foster A 2008 On the Behaviour and Radiating Properties of Heavy Elements in Fusion Plasmas PhD thesis University of Strathclyde. online at http://www.adas.ac.uk/theses.php.
[7] Fritsch W & Lin C 1991 Physics Reports (Review Section of Physics Letters) 202, 197.
[8] Fritsch W & Lin C D 1984 Phys. Rev. A 29(6), 30393051.
[9] Gieler M, Aumayr F, Schweinzer J, Koppensteiner W, Husinsky W, Winter H P, Lozhkin K & Hansen J P 1993 Journal of Physics B: Atomic, Molecular and Optical Physics 26(14), 2137. URL: http://stacks.iop.org/0953-4075/26/i=14/a=014
[10] Gruber O, Sips A, Dux R, Eich T, Fuchs J, Herrmann A, Kallenbach A, Maggi C, Neu R, Putterich T, Schweinzer J, Stober J & the ASDEX Upgrade Team 2009 Nuclear Fusion 49(11), 115014. URL: http://stacks.iop.org/0029-5515/49/i=11/a=115014
[11] Hoekstra R, Anderson H, Bliek F W, von Hellermann M, Maggi C F, Olson R E & Summers H P 1998 Plasma Physics and Controlled Fusion 40(8), 1541. URL: http://stacks.iop.org/0741-3335/40/i=8/a=007
[12] Igenbergs K, Schweinzer J & Aumayr F 2009 Journal of Physics B: Atomic, Molecular and Optical Physics 42(23), 235206 (8pp). URL: http://stacks.iop.org/0953-4075/42/235206
[13] Igenbergs K, Schweinzer J, Bray I, Bridi D & Aumayr F 2008 Atomic Data and Nuclear Data Tables 94, 981 1014.
[14] Igenbergs K, Schweinzer J, Veiter A, Perneczky L, Fruhwirth E, Wallerberger M, Olson R & Aumayr F 2011. URL: http://arxiv.org/abs/1112.3513v1
[15] Illescas C & Riera A 1999 Phys. Rev. A 60(6), 45464560.
[16] Isler R 1994 Plasma Physics and Controlled Fusion 36, 171208.
[17] Janev R K, Phaneuf R A & Hunter H T 1988 Atomic Data and Nuclear Data Tables 40(2), 249 281. URL: http://www.sciencedirect.com/science/article/B6WBB-4DBJ6F14F/2/f9a54a89457cae893e96623880653c74
[18] Kallenbach A, Dux R, Fuchs J C, Fischer R, Geiger B, Giannone L, Herrmann A, Lunt T, Mertens V, McDermott R, Neu R, Putterich T, Rathgeber S, Rohde V, Schmid K, Schweinzer J, Treutterer W & Team A U 2010 Plasma Physics and Controlled Fusion 52(5), 055002. URL: http://stacks.iop.org/0741-3335/52/i=5/a=055002
[19] Meyer F W, Howald A M, Havener C C & Phaneuf R A 1985 Phys. Rev. A 32(6), 33103318.
[20] Minami T, Pindzola M S, Lee T G & Schultz D R 2006 Journal of Physics B: Atomic, Molecular and Optical Physics 39(12), 2877. URL: http://stacks.iop.org/0953-4075/39/i=12/a=020

[21] Nielsen S E, Hansen J P & Dubois A 1990 Journal of Physics B: Atomic, Molecular and Optical Physics 23(15), 25952612. URL: http://stacks.iop.org/0953-4075/23/2595
[22] Schweinzer J, Brandenburg R, Bray I, Hoekstra R, Aumayr F, Janev R & Winter H 1999 72, 239273. Article ID adnd. 1999.0815.
[23] Wallerberger M, Igenbergs K, Schweinzer J & Aumayr F 2011 Computer Physics Communications 182(3), 775 778. URL: http://www.sciencedirect.com/science/article/pii/S0010465510004285

Chapter 6

Charge exchange and ion impact data for fusion plasma spectroscopy

The authors of this chapter are Luis Méndex, Luis Errea, Clara Illescas, Martin O'Mullane and Hugh Summers. It incorporates the brief report on ADAS-EU sub-contract 5 prepared by the Departamento de Química, Universidad Autónoma de Madrid (Luis Méndex) dated 16 December 2011. See also appendix E.

The participation of the Universidad Autnoma de Madrid (UAM) as a subcontractor of the ADAS-EU Euratom/ Framework 7 Support Action had the objective of providing atomic data to be implemented in the Atomic Data and Analysis Structure (ADAS) Project, and, in particular, the calculation of charge exchange (CX) for their use in plasma diagnostics. The calculations have been carried out by the group of atomic collisions (TCAM) formed by Luis Errea, Clara Illescas, Luis Méndez and Ismanuel Rabadán, permanent members of the staff of the UAM, and the recent incorporation of Jaime Suárez as postdoctoral researcher. As stated in the Programme of Work, the ADAS-EU strategy involved a first step in which a modest number of high-precision calculations are sought, to be used either directly or suggesting scaling laws which permit the extension to heavy elements, out of the capability of existing computational techniques. In this respect, universal curves for n-partial cross sections have been suggested in Ref. [1], whose validation for a few benchmark systems is required. The previous experience of the TCAM group includes the use of close-coupling and classical methods, most of them developed by the TCAM group, to study ion-atom and ion-molecule collisions, which have been extended and applied to evaluate the required cross sections. In this respect, the group has a wide experience in the use of molecular expansions together with either semiclassical or quantum-mechanical treatments for many electron systems. This kind of methods is particularly suitable to evaluate cross sections relevant to edge plasma modeling and diagnostics. In the last few years we have considered the CX reaction H+ (D+, T+) + Be. H(D, T) + Be+, which is important because Be is a plasma facing material of ITER. The most conspicuous result of our research is the high isotopic effect found, which has led us to investigate the potential importance of the isotope effect in other collision systems. The analysis, which may be relevant to tritium inventory in ITER, can be found in Ref. [2]. Similar calculations have been carried out for C^{+4} and B^{+5} collisions with H(1s) [3], and the corresponding cross sections and reaction rate coefficients have been made available to the ADAS-EU staff.

The high-energy calculations were carried out by employing the CTMC method, which permits to evaluate total and state-selective cross sections for ion-atom collisions at energies above 15 keV/u, where target ionization becomes dominant. The accuracy of the methodology is supported by the comparison with close-coupling results at low energies. This study was performed for Ne^{+10} + H(1s) in Ref. [4], where it was pointed out that the critical point is the use of an improved initial distribution, which is required to accurately describe the population of highly-excited states of the ion formed after the CX reaction (Ne^{+9} in this example). This methodology, based on the use of the so-called hydrogenic initial distribution, is appropriate to evaluate nl partial cross sections in one-electron systems, which are the data needed in CX diagnostics of core plasma. The technique has been extended to study collisions with excited targets. In particular, we have considered collisions of B^{+5} with H(n=2, n=3) [5]. In this work we have evaluated effective emission coefficients to check the influence of the presence of excited states.In particular, we have pointed out that n=3 donors can be relevant inthe diagnostic of high density plasmas as those of the Alcator C-Mod tokamak [6]. The calculation has also allowed to check the relevance of using the improved initial distribution in the CTMC

calculation.We have compared the effective emission coefficient (see Ref. [7]) q7.6 for n=1, 2 donors, evaluated with both the new cross sectionsand the data previously stored in ADAS, obtained by means of a CTMC method with the conventional microcanonical initial distribution. It was found that the microcanonical data significant significantly underestimates q7.6 for H(1s), while the influence is practically unnoticeable for n=2 donors for ASDEX-U plasma conditions. Although diagnostics based on B4+ emission are of critical importancewhen the wall is coated with boron (boronization), CX diagnostics aremainly focused on noble gases puffed in the divertor region. In thelast few years, we have extended the calculation to consider Ar andKr ions. In the first case, some comparisons, at the level of total crosssections were performed with molecular close-coupling calculations inRef. [8], and an important conclusion of our work was the inadequacyof the microcanonical distribution to accurately evaluate both total(for ionization and CX) and partial CX cross sections for high-n levels. The situation is particularly worrying because of two reasons: First,the CX diagnostic is based on Ar XVIII emission from n=14-17. Second, the data stored in ADAS were produced in Oak Ridge with themicrocanonical distribution1. Recent calculations by Igenbergs [10], using a large-scale atomic close-coupling expansion, confirm our results and further support the application of the hydrogenic initialdistribution. In order to fill up the data base, we have employed similar techniques to evaluate nl partial cross sections for Ar18+ collisions with H(n=2), and we have started the calculations for partially stripped species Ar17+ and Ar16+. The success of the improved CTMC approach for B5+, Ne10+ and Ar18+ collisions with hydrogen has led us to consider collisions involvingheavier species. We have recently evaluated CX cross sections for Kr36+ collisions with H(1s) in the energy range 15 ¡ E ¡ 250 keV/u 1 The details of this calculation have been recently published [9] (preliminary results were presented in the 10th ECAMP Conference). We have found that the n-partial cross sections fulfill the Oppenheimer n-3 rule at energies above 200 keV/u, and the l-partialcross sections exhibit a behaviour similar to that found for Arq+ + H(1s) collisions with the maximum cross section at l=n-1 in this energy range. The calculated cross sections have been delivered toADAS, and incorporated to the data base by the ADAS-EU staff in theadf01 format. Work is in progress to extend the calculation to Xe54+ W60+ collisions with H. As a first approximation, which has been proved to be valid for Ar ions, the system is described without takinginto account the projectile core. A final contribution of the Madrid group is the calculation of excitationcross sections that were not included in the ADAS data bases; theyinfluence the population of excited donors in CX diagnostics and might be also relevant in passive diagnostics. As a first step in thisdirection, Francisco Guzmn, from ADAS-EU, has collected the data produced in Madrid and Bordeaux using classical and semiclassicalmethods [11] for the reactions: Xq+ + H(1s) . Xq+ + H(n), with Xq+ =Li3+, Ne10+ and Ar18+. He has interpolated the data to providea set of recommended data, which are available as adf01 files. Our codes can evaluate excitation cross sections for other systems if needed.

References

[1] A. R. Foster. PhD thesis, University of Strathclyde (2008) [2] P. Barragn, L. F. Errea, L. Mndez, and I. Rabadn Phys. Rev. A 82 030701 (2010) [3] P. Barragn, L. F. Errea, F. Guzmn, L. Mndez, I. Rabadn, and I.Ben-Itzhak Phys. Rev. A 81 062712 (2010) [4] L.F. Errea, C. Illescas, L. Mndez, B. Pons, A. Riera and J. SurezPhys. Rev. A 70 52713 (2004) [5] F. Guzmn , L F Errea , C. Illescas , L. Mndez and B. Pons J. Phys. B43 144007 (2010) [6] I.O. Bespamyatnov , W. L Rowan, R. S. Granetz and D.F. Beals Am. Inst. Phys. 77 10F123 (2006) [7] H. P. Summers, W. J. Dickson. M.G. OMullane, N. R. Badnell, A.D. Whiteford, D.H. Brooks, J. Lang, S.D. Loch and D.C. Griffin Plasma Phys. Control. Fusion 48 263 (2006) [8] L. F. Errea, C. Illescas, L. Mndez, B. Pons, A. Riera and J. Surez J.Phys. B 39 L91 (2006) [9] D.R. Schultz, Teck-Ghee Lee and S.D. Loch J. Phys. B 43 140201 (2010) [10] K. Ingenbergs, Dissertation TU Wien (2011) [11] L.F. Errea, L. Mndez, B. Pons, A. Riera. I. Sevila and J. Surez Phys. Rev. A 74 012722 (2006)

Chapter 7

Positive ion impact data for fusion applications

The authors of this chapter are Ronnie Hoekstra, Martin O'Mullane and Hugh Summers. It incorporates the brief report on ADAS-EU sub-contract 6 prepared by the Atomic Physics group, KVI, University of Groningen, Netherlands (R. Hoekstra) dated 10 January 2012. See also appendix F.

Appendix A

ADAS-EU: Sub-contract 1

ATOMIC STRUCTURE AND ELECTRON DATA FOR HEAVY ELEMENT IONS: The tungsten ions W^{+0} to W^{+4} and adjacent element systems.

Summary: It is proposed to commission a set of atomic structure calculations and measurements from Prof. Emile Biémont, Department of Physics, University Mons-Hainaut, Belgium. This reference quality sixth-period fundamental data will benchmark iso-nuclear and iso-electronic sequence data available in the ADAS database and guide further large scale production. It will extend the scope of collisional-radiative data and model support provided under the ADAS-EU Project to the European magnetic confinement fusion community. The data, which supports influx studies and spectral measurements on low ionisation states of heavy species, will be interfaced to spectral measurements on fusion devices at EURATOM Associated laboratories through tailored spectral line scripts within the Atomic Data and Analysis Structure, ADAS. The work will make extensive use of the methods and codes developed by Prof. Biémont, Dr. Palmeri, Dr. Quinet and co-workers. The calculations will be performed at University Mons-Hainaut and LIF lifetime measurements at Lund and at CRYRING, Stockholm, Sweden. The data will be organised and relayed from Mons to ADAS in established specific ion data formats with the assistance of ADAS-EU staff. Conversion to spectrum line photon efficiencies and similar derived data will take place at UKAEA/JET Facility and University of Strathclyde. The fundamental and derived data in appropriate ADAS data format collections will be released after assessment and validation to the public domain via OPEN-ADAS [1]. The duration of the project will be eighteen months (Sept. 2009 - Jan. 2011).

Background: The strategy, originated at the JET Facility and now followed by fusion laboratories throughout the world participating in the ADAS Project, for the description of the radiation emission of impurity ions has been the establishment of an integrated atomic data and analysis structure (ADAS). ADAS seeks to provide at appropriate quality, all the derived data required for global modelling and quantitative spectroscopic diagnosis and analysis [2]. The system is based on the initial preparation of collections of fundamental atomic transition probability and excitation rate data for specific ions called specific ion files. Various ADAS computer codes then prepare all the derived data such as net power loss coefficients, spectral line contribution functions etc. in a form directly usable in experimental analysis and in plasma models. The fundamental and derived databases are centrally maintained and accessible by standard routines for modelling and diagnostic applications (eg. edge studies, VUV and XUV spectroscopy). The effectiveness and precision in the applications depends on the quality and availability of fundamental data. In this context a specific need is enhanced provision for low ionisation stages of heavy elements up to and including tungsten. Such enhancement is a central theme of the ADAS-EU Euratom/Framework 7 Support Action. Recognizing the complexity of some of the fusion relevant heavy element ions and current bounds on atomic reaction computability, ADAS-EU policy falls into two parts. Firstly a modest number of high precision reference calculations and/or measurements at the front edge of current capability are sought. Secondly, as well as direct embedding of the associated precise data in the databases, the data should be exploited as fiducials which can suggest adjustments or global/regional scalings to the large scale semi-automated mass production calculations of the ADAS heavy element baseline. This *lift of the baseline* is the central objective and the primary delivery. One of the main sources of spectroscopic properties of atoms and low ionisation stage ions of heavy elements is the group of Prof. Bimont. This group has steadily developed and systematised their methods which use underpinning atomic structure calculations to analyse observed LIF spectra at the Lund Laser Centre (LLC) (Lund, Sweden) and possibly at CRYRING (Stockholm, Sweden). The adjustment and optimising of

theory to observations provides identified reference energy levels and transition probabilities, along with insight into the controlling configuration interactions and orbital characteristics [3]. The group has worked on many systems, specialising in lanthanides, but including ions touching [4] and adjacent to the present fusion interest [5]. Additionally the group developed and maintains the DREAM database [6] of energy levels and parameters for lanthanides and also the DESIRE database (database for sixth row elements) [7]. The approach of Prof. Biemont is ideally suited for matching to and strengthening the ADAS atomic modelling system along the manner described in the first paragraph of this section. The groups theoretical structure calculations are principally based on the Cowan code - exploiting the semi-relativistic Hartree-Fock (HFR) variant, but exploiting also multi-configuration Dirac-Fock (MCDF) [8]. It is noted that baseline mass production in ADAS principally uses the Cowan code. However the extended special techniques used by the group such as model potentials for core polarisation and correction factors for core-penetration - along with optimising to experimental spectra, lift the analysis and description to reference level. In the fusion domain, the neutral and near neutral ions of elements are inflowing from inner wall surfaces contacted by the plasma. They ionise rapidly as they enter the relatively high (albeit divertor or edge) temperature plasma dispersing from their source as the ions become entrained in parallel transport along the magnetic field lines. Detection of the species and deduction of its influx is the main diagnostic and this is ideally inferred from spectrum lines in the visible. For heavy elements, the deduction is difficult due to the lack of strong identified lines and the presence of metastables. Thus for example, the only useful line at this time for WI is the transition 5d5(6S) 6s 7S3 - 5d5(6S) 6p 7P4 (ΔE=24938.39 cm-1) which is not in the ground state spin system. Fully validated influx requires matching of influx in two successive ionisation stages, summed over the various metastable contributors [9]. This is demanding in spectroscopy and in the theoretical provisions of identifications, generalised collisional-radiative modelling and photon efficiencies - especially for heavy species. The proposal directly targets the fundamental specialist atomic data critical points in enabling this diagnostic capability for the ITER scenario. In doing so it is recognised that the highest precision methods for electron impact excitation cross-sections are not yet computationally feasible for the systems W+0-W+4. But the plasma regime is highly ionising with principal cross-sections in the Born-Bethe regime. Availability of high-grade theoretical atomic structure allows evaluation of the Born-Bessel integrals. Also the lowest intersystem transitions, omitted in Born approximation, may be accessible to restricted R-matrix study. The block of ions, W+5- W+15, occurring in the tokamak divertor, have individually narrow shells and small emission measures, but collectively influence the local radiated power balance. Comprising partially filled d- and f-shell systems, these rare-earth-like configurations have been extensively analysed by the group of Prof. Bimont. This sub-contract provides an opportunity, through guided mapping of data across databases, to lift the quality of ADAS radiated power modelling of such intermediate heavy ions.

The proposed work: The work falls into four parts, namely lifetime measurement and transition probability analysis, Born-Bessel integral incorporation and re-calculation, inter-database mapping of selected ion parameters, guided adoption of structure parameters in ADAS baseline modelling - including static dipole polarisabilities. (1) Extension of analysed 6th period ions by selective studies from the ions Ta+0-Ta+3,, W+0-W+3, Re+0-Re+3 (2) Implementation of Born-Bessel integral and Born cross-section evaluation using Mons-Hainaut wavefunctions generated from energy level and oscillator strength analyses. (3) Production of ADAS adf04 data sets mapped from Mons-Hainaut analyses and databases, spanning the ion group of (1) and selections from the lanthanide systems. (4) Establishment of preferred parameters for Cowan code calculations, in the 6th period ion region, as an extrapolation and interpolation of Mons-Hainaut analyses. Generation of dipole polarisabilities for ground and excited states of the above systems at configuration average resolution or beyond as feasible.

Integration of data into ADAS will be executed by staff of ADAS-EU, including the conversion to the key derived data format adf11, adf13, and adf15. ADAS-EU staff will pay working visits to Mons-Hainaut to assist with execution of the above tasks as appropriate. A copy of ADAS software will be made available on a workstation at the Department of Physics, University of Mons-Hainaut at no charge for local use.

References:

[1] http://www.adas.ac.uk/openadas.php
[2] http://www.adas.ac.uk
[3] E Biémont and P Quinet (2003) Physica Scripta T105, 38.
[4] P Palmeri, P Quinet, V Fiver, E. Biémont et al. (2008) Physica Scripta 78, 015304.
[5] P Quinet, P Palmeri, V Fiver, E. Biémont et al. (2008) Phys. Rev. A 77, 022501.
[6] http://w3.umh.ac.be/ astro/dream.shtml
[7] V. Fivet, P. Quinet, P. Palmeri, E. Biémont and H.L. Xu, 2007, J. Electron. Spectrosc. Related Phenomena 156-158, 250

[8] E. Biémont , V Fivet and P Quinet (2004) J. Phys.B 37, 4193.
[9] K H Behringer, H P Summers et al. (1989) Plasma Physics & Control. Fusion 31, 2059.

Appendix B

ADAS-EU: Sub-contract 2

ELECTRON IMPACT CROSS-SECTION DATA FOR FUSION APPLICATIONS: Ionisation and recombination of heavy element ions.

Summary: It is proposed to commission selected ionisation and recombination measurements and associated evaluations from Prof. Alfred Mller, University of Giessen, Germany. This reference quality sixth-period fundamental data will benchmark iso-nuclear and iso-electronic sequence data available in the ADAS database and guide further large scale production. It will extend the scope of collisional-radiative data and model support provided under the ADAS-EU Project to the European magnetic confinement fusion community The data, which supports deduction of the ionisation state of heavy species, will be interfaced to plasma transport models and to diagnostic spectral measurements on fusion devices at EURATOM Associated laboratories and ITER through tailored data formats within the Atomic Data and Analysis Structure, ADAS. The work will make extensive use of the methods and measurement techniques developed by Prof. Mller, Prof. Schippers and co-workers. The ionisation cross-section measurements will be from the crossed-beams apparatus and ECR source at Giessen, combining animated-beams and high resolution energy-scan methods. The recombination cross-section measurements will focus on dielectronic recombination exploiting the merged beam method in the electron cooler of the Heidelberg heavy ion storage ring. The data will be organised and relayed from Giessen to ADAS with the assistance of ADAS-EU staff. Conversion to derived data formats through collisional-radiative modelling data will take place at UKAEA/JET Facility and University of Strathclyde. The fundamental and derived data in appropriate ADAS data format collections will be released after assessment and validation to the public domain via OPEN-ADAS [1]. The duration of the project will be eighteen months (Sept. 2009 - Jan. 2011).

Background: The strategy, originated at the JET Facility and now followed by fusion laboratories throughout the world participating in the ADAS Project, for the description of the radiation emission of impurity ions has been the establishment of an integrated atomic data and analysis structure (ADAS). ADAS seeks to provide at appropriate quality, all the derived data required for global modelling and quantitative spectroscopic diagnosis and analysis [2]. The fundamental and derived databases are centrally maintained and accessible by standard routines for modelling and diagnostic applications (eg. edge studies, core plasma, XUV spectroscopy). The effectiveness and precision in the applications depends on the quality and availability of fundamental data. In this context a specific need is enhanced provision for low ionisation stages of heavy elements up to and including tungsten. Such enhancement is a central theme of the ADAS-EU Euratom/Framework 7 Support Action. Recognizing the complexity of some of the fusion relevant heavy element ions and current bounds on atomic reaction computability, ADAS-EU policy falls into two parts. Firstly a modest number of high precision reference calculations and/or measurements at the front edge of current capability are sought. Secondly, as well as direct embedding of the associated precise data in the databases, the data should be exploited as fiducials which can suggest adjustments or global/regional scalings to the large scale semi-automated mass production calculations of the ADAS heavy element baseline. This lift of the baseline is the central objective and the primary delivery. One of the main sources of ionisation and recombination cross-section measurements of both low and high ionisation stage ions of heavy elements is the group of Prof. Mller. The group has focussed on ionisation and recombination (both radiative and dielectronic) cross-sections with special attention to the delineation of resonant structures and to absolute measurements [3]. The group has established and maintained very strong collaborations with theoretical groups who calculate electron impact ionisation and recombination [4]. This engagement has led to important clarifications, to calculation extensions and has pointed the way forward, for example in low temperature

DR [5], excitation-autoionisation, REDA [6] etc. The group has worked on many systems, including ions touching and adjacent to the present fusion interest [7, 8]. The approach of Prof. Mller is ideally suited for matching to and strengthening the ADAS atomic modelling system along the manner described in the first paragraph of this section. On dielectronic recombination, inter alia, the theoretical point of comparison includes the AUTOSTRUCTURE code (IPIR approximation) [9] and developments there from. It is noted that the large scale production of dielectronic recombination in ADAS uses the AUTOSTRUCTURE code. Similarly on ionisation, inter alia, the theoretical point of comparison includes the CADW code (configuration average distorted wave approximation) [10] as used by ADAS. In the fusion domain, a principal concern is the behaviour of heavy element impurities in particular tungsten in the plasma environment. Tungsten inner wall components will be present at the locations of high thermal load in the divertor/strike-zones of ITER and so will be the subject of intensive study at current machines, such as JET and AUG in the preparations for ITER. From an atomic physics perspective, tungsten is particularly challenging for lower ionisation stages W+0 - W+25 with active inner and outer d- and f-shells. For dielectronic recombination, it is expected that the many resonant series will produce an unresolved quasi-continuum in the cross-section, a complexity compounded by possibly several metastable initial capturing ion states. State selective dielectronic coefficient calculations, such as those generated by AUTOSTRUCTURE (currently up to about Mg-like systems) must be abbreviated for the very complex systems above and experimental fiducials are required for this new territory. For electron impact ionisation of W+0 - W+25 it is anticipated that excitation-auto-ionisation will dominate direct ionisation, however the completeness of the current CADW approach and its convergence towards experimental values as z increases is not yet demonstrated. There are experimental indications that REDA resonances may be substantial. Semiempirical adjustments to ADAS baseline, large coverage, theoretical methods for such effects do need benchmarking. Also, in the relatively highly ionising plasma environment for an inflowing near neutral tungsten ion, multiple ionisation (as a correction to successive single ionisations) needs to be quantified. The group of Prof. Mller has a demonstrated capability for experimental measurements which bear on the above issues and experience with similar systems to those of direct concern for fusion. This sub-contract provides an opportunity for benchmark measurements, choice of broad-coverage computational methods and guided use of global parametric scaling adjustments of data, to lift the quality of ADAS ionisation state modelling for such low to intermediate charge state heavy ions.

The proposed work: The work falls into four parts, namely dielectronic recombination cross-section measurements and analysis, ionisation cross-section measurements and analysis, assessment of calculations and definition of global/zonal, parametric (generally z-scaled) adjustments for recombination and ionisation. (1) Selective dielectronic recombination cross-section measurements of 6th period element ions from ions W+0-W+25 or isoelectronically equivalent adjacent element ions focussing on d- and f-shell (as inner and outer shells) parent transition contributions. (2) Assessment and comparison of results in terms of Burgess-Bethe (BBGP) approximations. Identification/recommendation of global/zonal parametric adjustments. (3) Selective ionisation cross-section measurements of 6th period element ions from ions W+0-W+25 or isoelectronically equivalent adjacent element ions focussing on excitation-autoionisation and REDA resonances for active inner d- and f-shells. Measurements will include multiple ionisation cross-sections. (4) Assessment and comparison of results in terms of distorted wave approximations and BBGP type adjustments for REDA. Identification/recommendation of global/zonal parametric adjustments.

Integration of data into ADAS will be executed by staff of the ADAS-EU, including incorporation of fiducials and adjustments into the key fundamental data formats adf09 and adf23 and re-processing for the derived data formats adf07 and adf11. ADAS-EU staff will pay working visits to Giessen to assist with execution of the above tasks as appropriate. A copy of ADAS software will be made available on a workstation at the Department of Physics, University of Giessen at no charge for local use.

References:

[1] http://www.adas.ac.uk/openadas.php
[2] http://www.adas.ac.uk
[3] A Müller (2008) Adv. At. Mol. Opt. Phys. 55, 293. [4] E W Schmidt, S Schippers et al. (2008) Astron. Astrophys. 492, 265.
[5] D W Savin, T Bartsch et al. (1997) Astrophys. J. 489, L115.
[6] K Aichele, D Hathiramani et al. (2001) Phys. Rev. Lett. 86, 620.
[7] M. Lu, M. F. Gharaibeh et al. (2006) Phys. Rev. A 74, 012703.
[8] B. Fabian, A. Müller et al. (2005) J. Phys. B 38, 2833.
[9] http://amdpp.phys.strath.ac.uk/autos/
[10] S D Loch, M S Pindzola et al. (2002) Phys. Rev. A 66, 052708.

Appendix C

ADAS-EU: Sub-contract 3

ATOMIC STRUCTURE AND ELECTRON DATA FOR HEAVY ELEMENT IONS: (1) Configuration interaction and relativisitic/quasi-relativistic structure. (2) Auger/cascade, multiple ionisation and shake-off.

Summary: It is proposed to contract with Dr Alicija Kupliauskiene, acting for the Department of the Theory of an Atom, Institute for Theoretical Physics and Astronomy, University of Vilnius, Vilnius, Lithuania, to provide a set of calculations of atomic structure together with associated reaction quantities and prescriptions. The reference quality data and studies will establish characteristics of homologous and iso-electronic systems of fourth, fifth and sixth long period elements at low and medium charge states. They will include specification of key configuration interactions and elucidate precision in ab initio quasi-relativistic and relativistic calculations. These patterns and the selected specific data will benchmark iso-nuclear and iso-electronic sequence data available in the baseline ADAS database and guide adjustments for further large scale production. The studies will include evaluation of Auger/cascade and shake-off pathways leading to multiple electron - sequential and simultaneous - loss. The latter will be targetted on a selection of heavy species, including tungsten, in moderate states of ionisation (z 5 - 15) to predict corrections to simple stage-to-stage ionisation in the divertor environment of fusion devices. The work will make extensive use of the methods and codes developed by Prof. Bogdanovich, Prof. Karazija, Prof. Gaigalas, Prof. Rudzikas and co-workers. The calculations will be performed at the Institute for Theoretical Physics and Astronomy, University of Vilnius, Vilnius. The data will be organised and relayed from Vilnius to ADAS in established specific ion data formats with the assistance of ADAS-EU staff. Conversion to spectrum line photon efficiencies and similar derived data will take place at the EFDA-JET Facility and University of Strathclyde. The fundamental and derived data in appropriate ADAS data format collections will be released after assessment and validation to the public domain via OPEN-ADAS [1]. The duration of the project will be eighteen months (Aug. 2010 Jan. 2012) at a fixed price of 10,000.

Background: The strategy, originated at the JET Facility and now followed by fusion laboratories throughout the world participating in the ADAS Project, for the description of the radiation emission of impurity ions has been the establishment of an integrated atomic data and analysis structure (ADAS). ADAS seeks to provide at appropriate quality, all the derived data required for global modelling and quantitative spectroscopic diagnosis and analysis [2]. The system is based on the initial preparation of collections of fundamental atomic transition probability and excitation rate data for specific ions called specific ion files. Various ADAS computer codes then prepare all the derived data such as net power loss coefficients, spectral line contribution functions etc. in a form directly usable in experimental analysis and in plasma models. The fundamental and derived databases are centrally maintained and accessible by standard routines for modelling and diagnostic applications (eg. edge studies, VUV and XUV spectroscopy). The effectiveness and precision in the applications depends on the quality and availability of fundamental data. In this context a specific need is enhanced provision for low and medium ionisation stages of heavy elements up to and including tungsten. Such enhancement is a central theme of the ADAS-EU Euratom/Framework 7 Support Action. Recognizing the complexity of some of the fusion relevant heavy element ions and current bounds on atomic reaction computability, ADAS-EU policy falls into two parts. Firstly a modest number of high precision reference calculations and/or measurements at the front edge of current capability are sought. Secondly, as well as direct embedding of the associated precise data in the databases, the data should be exploited as fiducials which can suggest adjustments or global/regional scalings to the large scale semi-automated mass production calculations of the ADAS heavy element baseline. This lift of the baseline is the central objective and the primary delivery. The Department of the Theory of

an Atom at the Institute for Theoretical Physics and Astrophysics, has a long history of research in complex atomic structure, very large multi-configuration approaches and efficient algebraic methods, stemming from the original work of Prof. Yutsis on through the work of Prof. Rudzikas through to the present day and the work of Profs. Kupliauskiene, Karazija, Bodganovich and Gaigalas. Their associated research groups exploit these broad methods in specific unique areas which can be of special value to the magnetic confinement fusion program as it seeks to model, analyse and exploit heavy species such as tungsten for ITER. Thus the modified radial orbital (RO) approach combined with the very large multi-configuration approach with virtual excitations of Prof. Bogdanovich and Dr Rancova, extended to quasi-relativistic transformed radial orbitals (TROs) [3, 4], allows ab initio access to systems as complex as WII with good precision. The team of Prof. Karazija evaluates global characteristics [5] which rank the key configuration interactions, such as symmetric exchange of symmetry influencing accurate theoretical atomic structure [6]. These effects can constrain the spread and relative intensities of individual components of very large transition arrays. This team has special expertise in Auger/cascade, shake-down and shake-off, originally applied to photoionisation [7], but more recently to multiple electron loss in electron impact ionisation of low ionisation stages of tungsten. The group of Prof. Gaigalas works with very large scale multi-configuration Hartree-Fock and Dirac-Fock calculations of fine structure, tackling very difficult cases such as transuranic elements [8]. The group has special interests in efficient coding of spin algebra for Dirac-Fock codes and the correct handling of f-states. These advanced theoretical capabilities connect well with the layered precision approach of ADAS and ADAS-EU for bringing all relevant heavy elements into effective modelling and analysis for ITER. Of principal concern is modelling and diagnostic spectroscopy of heavy elements within the divertor and scape-off-layer, which spans charges states from neutral to ¡ 20. The baseline ADAS database for ionisation state, excited population state, radiated power and emissivities centres on automatic creation of configuration sets for each ion, optimised on contributors to total radiated power. This approach, suited to superstaging and general 2-D divertor modelling, should be selectively improved for specific radiators and in particular specific homologous systems and iso-electronic sequences dictated by spectroscopy. The configuration selection prescriptions, evaluated for heavy element ions of the Department of the Theory of an Atom can directly modify/extend the promotional rule sets of the ADAS baseline. Secondly the explicit atomic structure and transition probability outputs for selected ions from the Department of the Theory of an Atom may be routed through the ADAS processing steps to specific ion datasets of fundamental ADAS data format adf04. At this point, automatic passage through ADAS derivative processing is enabled, lifting the baseline systematically. It is this chain of exploitation, suitably supported by close engagement for ADAS-EU staff with researchers of the Department of the Theory of an Atom, which the subcontract in broad terms intends to achieve. This sub-contract is concerned with using theoretical methods to lift the quality of the ADAS databases. It links to other sub-contracts providing experimental measures of energies, transition probabilities, ionisation cross-sections and recombination rate coefficients. Collectively these benchmarking studies on reference elements and ion will guide parametric adjustments globally to ADAS derived data. The enhanced theoretical relativistic and quasi-relativistic structures of the targetted systems will provide in turn the stepping-off point for the highest grade electron impact collision cross-section calculations in due course and completion of the heavy element theme of ADAS-EU.

The proposed work: The work falls into four parts, ab initio structure and transition probability calculations in the large scale multi-configurational approach with virtual excitations and TROs, global characteristics and CI prescriptions, Auger/cascade pathways and multiple ionisation, selected Dirac-Fock calculations for neutral/near neutral very heavy systems. (1) Multiple electron ionisation rate coefficients, with special emphasis on 4d, 4f and 5d, 5f open shell systems. The study should be based on contiguous sets of iso-nuclear ions of selected elements from which approximate general prescriptions can be inferred. This will include design of an extension of ADAS data formats adf23 and adf07. (2) Exploitation of ITPA special studies of key complex ion configuration interactions (such as symmetric exchanger of symmetry), by inclusion in ADAS data format adf54, tuned to primary resonance line spectroscopy, with special emphasis on 4d, 4f and 5d, 5f open shell systems.. (3) A benchmark study for WI, WII, and WIII using the Bogdanovich quasi-relativisitic (TRO) approach. The structure and transition probability study will be extended to implement plane wave Born cross-sections so that delivery can be in the form of ADAS adf04 datasets. Professor Nigel Badnell for ADAS-EU will collaborate with Professor Bogdanovitch and his co-workers and provide support procedures and sub-routines so that the link from structure to plane-wave Born can be made. (4) A benchmark study in Dirac-Fock approximation of a selected lanthanide-like ion in a low charge state (6-12). The study is designed to assess the possibility of more extensive use of such heavy elements as markers (observed in low ionisation stages in divertor regimes) and edge transport studies and cross-reference other approximate studies of low charge state tungsten ions. Suitable ions would be W+8 (Dy-like) or Au+8 (Yb-like).

Integration of data into the ADAS system will be executed by staff of ADAS-EU. ADAS-EU staff will engage closely with ITPA in the study, assisting in the passage of the general prescriptions and results into the ADAS data

formats [9], especially adf04, adf07, adf23 and adf54. ADAS-EU staff will pay working visits to University of Vilnius to assist with execution of the above tasks as appropriate. A copy of ADAS software will be made available on a workstation at the Department of Physics, University of Vilnius at no charge for local use.

References:

[1] http://www.open.adas.ac.uk
[2] http://www.adas.ac.uk
[3] P. Bogdanovich , D. Majus and T. Pakhomova (2006) Phys. Scr. 74, 558.
[4] P. Bogdanovich and O. Rancova (2008) Phys. Scr. 78, 045301.
[5] V. Jonauskas, S. Kucas et al. (2007) Phys. Scr. 75, 237.
[6] S. Kucas, R. Karazija et al. (2009) J. Phys. B 42, 205001.
[7] V. Jonauskas, R. Karazija and S. Kucas (2008) J. Phys. B 41, 215005.
[8] G. Gaigalas, E. Gaidamauskas and Z. Rudzikas (2009) Phys. Rev. A 79, 022511.
[9] H. P. Summers (2010) The ADAS-Manual (http://www.adas.ac.uk/manual.php).

Appendix D

ADAS-EU: Sub-contract 4

ATOMIC DATA AND MODELS FOR NEUTRAL BEAM DIAGNOSTICS: (1) Lithium and sodium beam models and data.(2) CCAO calculations for h (n=1,2) targets.

Summary: It is proposed to contract with Prof. Friedrich Aumayr, Institute of Applied Physics, Technische Universitt Wien, Vienna, Austria to make available in ADAS a comprehensive set of atomic rate coefficient data for the use of neutral lithium and sodium for beam diagnostics. These relate to processes determining the state of excitation of the beam species and to its action as a donor to plasma impurity ions. The TU Wien group will assist ADAS-EU staff in installing a pedagogical tool within the interactive IDL-ADAS system as a guide to the diagnostic method and to assist in data verification and maintenance. Additional theoretical state selective charge exchange data in the CCAO approximation for neutral hydrogen as a donor to selected full stripped impurities in the nuclear charge range 4-18 will be added to the ADAS database. In association with ADAS-EU staff, these latter data will be merged with other data in the ADAS database to provide new preferred data collections for application. The work will make extensive use of the methods and codes developed by Prof. Winter, Prof. Aumayr and Ms Igenbergs at the Technische Universitt Wien in close collaboration with Dr. Schweinzer at the Max Planck Institut fr Plasmphysik, Garching-bei-Munchen, Germany. The data will be organised and relayed from Vienna to ADAS in established specific ion data formats with the assistance of ADAS-EU staff. Conversion to charge exchange effective emission coefficients and similar derived data will take place at EFDA-JET Facility and University of Strathclyde. The fundamental and derived data in appropriate ADAS data format collections will be released after assessment and validation to the public domain via OPEN-ADAS [1]. The duration of the project will be twelev months (Jul. 2010 - Jun. 2011) at a fixed price of 10,000.

Background: The strategy, originated at the JET Facility and now followed by fusion laboratories throughout the world participating in the ADAS Project, for the description of the radiation emission of impurity ions has been the establishment of an integrated atomic data and analysis structure (ADAS). ADAS seeks to provide at appropriate quality, all the derived data required for global modelling and quantitative spectroscopic diagnosis and analysis [2]. The system is based on the initial preparation of collections of fundamental atomic transition probability and excitation rate data for specific ions called specific ion files. Various ADAS computer codes then prepare all the derived data such as net power loss coefficients, spectral line contribution functions etc. in a form directly usable in experimental analysis and in plasma models. The fundamental and derived databases are centrally maintained and accessible by standard routines for modelling and diagnostic applications (eg. edge studies, charge exchange spectroscopy and beam emission spectroscopy). Additionally beyond the original scope of ADAS, in EXTENDED-ADAS, codes such as CXSFIT which are more linked to diagnostic analysis are developed and supported by ADAS/ADAS-EU staff in close collaboration with fusion laboratories. In this context there is a specific need to fill a gap in the ADAS beam modelling provision for neutral lithium and sodium beams, used for diagnosis of edge plasma parameter profiles especially density, but also temperature and impurity concentrations [3]. Continued development and enhancement of neutral beam emission and charge exchange emission diagnostic capabilities are central themes of the ADAS-EU Euratom/Framework 7 Support Action. The effectiveness and precision in the applications depend on the quality and availability of fundamental data. Recognizing current bounds on computability of certain fusion relevant collision data such as ion impact on neutral targets, ADAS-EU policy falls into two parts. Firstly a modest number of high precision reference calculations and/or measurements at the front edge of current methodologies are sought. These, in their regions of validity, are assessed and combined to provide preferred data which are comprehensive and of extended

energy range span. Secondly, as well as direct embedding of the associated precise data in the databases, the data should be exploited as fiducials which can suggest adjustments or global/regional scalings to the large scale semi-automated mass production calculations of the ADAS baseline. This managed lift of the baseline is a central objective and a primary delivery. The group at the Institute of Applied Physucs, Technische Universitt Wien, originally lead by Prof. H-P. Winter and now by Prof. F. Aumayr has been at the centre of development and implementation of neutral lithium beams as an edge plasma diagnostic [3] in Europe for nearly two decades. They have worked closely in the exploitation and validation of the diagnostic at fusion laboratories including IPP Garching and FZ-Juelich. Also they have given careful attention to procurement of necessary fundamental atomic data for the diagnostics including preparation of key data collections for lithium [4] and sodium [5]. Diagnostic analysis codes for both the lithium and sodium beams were developed at Technische Universitt Wien. These codes are now in a frozen state with new code development exploiting Bayesian methods underway at IPP Garching under the guidance of Dr J. Schweinzer [6]. The original codes, with suitable interfacing within IDL-ADAS can fulfil the pedagogical and validation needs for ADAS. In recent years, the Technische Universitt Wien group, in close association with Dr J. Schweinzer, have focussed their attention on in-house calculation of key ion impact cross-section data for neutral beams. These calculations are based on the close-coupled atomic orbital method. This, potentially high precision method is particularly suited to the energy region 50keV/amu typical of current neutral hydrogen heating beams and complements the classical trajectory Monte Carlo and close coupled molecular orbital methods valid at higher and lower energies respectively. The group is extending the scope of CCAO to handle the very many levels sets required by colliders such as Ar+18 [7]. Completed calculations include Be+4 + H(n=1, 2) [8] and N+7 + H(n=1, 2) [9]. ADAS used collisional-radiative modelling, operating on collections of fundamental data, to convert them into the derived data used for plasma models and plasma diagnostic analysis. The collisional-radiative modelling for beam driven charge exchange and beam emission spectroscopic analysis is elaborate. Charge exchange spectroscopy of highly charged species such as Ar+18require nl-resolved and n-resolved models to very high n-shells to describe adequately the redistribution, cascade and re-ionisation leading to the effective emission in useful (normally visible-range) spectrum lines. Also, current models, to allow detailed analysis of neutral hydrogen beam emission, must operate in field disturbed (Stark/Paschen-Back) manifolds with oriented collisions and polarised directional emission. One key to enhanced precision in such models is state selective ion impact excitation and charge transfer by highly charged ions as described above. ADAS machinery allows rapid exploitation of such enhancements to the benefit of the fusion community. In the spatial and temporal non-equilibrium domains, usual ADAS practice (focussed on hydrogen and helium beams) separates metastable and excited populations [10]. The iterative forward modelling with unrelaxed excited states, tied to experimental measurement, as used by Technische Universitt Wien, is complementary to the ADAS use. On the other hand, ADAS very high n-shell methods complement Technische Universitt Wien collisional-radiative modelling. This sub-contract provides an opportunity, through guided mapping of data across databases, to extend the scope and lift the quality of ADAS charge exchange and beam emission spectroscopy modelling. The development will have strong synergy with ADAS and other ADAS-EU sub-contracts (cf. Madrid and Groningen) concerned with fundamental ion-atom collision data improvement. It will ensure the preparedness and completeness of ADAS/ADAS-EU for ITER.

The proposed work: The work falls into four parts, namely database extension for lithium and sodium beams, pedagogical diagnostic model implementation, reference charge exchange/target excitation ion impact cross-sections and assembly of preferred data. (1) Entry and verification of Technische Universitt Wien databases for inelastic collisions of lithium and sodium atoms with electrons, protons and multiply charged ions into ADAS data format adf01 and adf02 (revised). (2) Assisting ADAS-EU staff in preparation of the Technische Universitt Wien/MPI Garching forward modelling lithium/sodium beam density profile determining code and sample data as an ADAS series 3 implementation, with IDL graphical user interface. (3) Preparation of CCAO state selective charge exchange cross-sections and associated state selective charge exchange cross-sections in ADAS adf01 and adf02 (revised) format for available colliders to include Be+4 and N+7 (Ar+18 to be included if extended calculations, currently underway, reach suitable completion). (4) Establishment of preferred adf01 and adf02 (revised) data as above, in agreement with ADAS-EU staff.

Integration of data into ADAS will be executed by staff of ADAS-EU, including the conversion to the key derived data formats, adf12, adf21 and adf22. ADAS-EU staff will pay working visits to Technische Universitt Wien to assist with execution of the above tasks as appropriate. A copy of ADAS software will be made available on a workstation at the Institute of Applied Physics, Technische Universitt Wien at no charge for local use.

References:
[1] http://www.open.adas.ac.uk
[2] http://www.adas.ac.uk

[3] E. Wolfrum, F. Aumayr et al. (1993) Rev. Sci. Instrum. 64, 2285.
[4] J. Schweinzer, R Brandenburg et al. (1999) At. Data and Nucl. Data Tables 72, 239.
[5] K. Igenbergs, J. Schweinzer et al. (2008) At. Data and Nucl. Data Tables 94, 981.
[6] E. Wolfrum (2007) ADAS Workshop, Ringberg, Germany Current state of Li-beam at AUG (http://www.adas.ac.uk/talks207.php).
[7] K. Igenbergs (2009) ADAS Workshop, Ringberg, Germany Atomic orbital close-coupling calculations of CXRS relevant cross-sections (http://www.adas.ac.uk).
[8] K. Igenbergs, J. Schweinzer and F. Aumayr (2009) J. Phys. B 42, 235206.
[9] K. Igenbergs, J. Schweinzer and F. Aumayr - in preparation.
[10] H. P. Summers (2010) The ADAS-Manual (http://www.adas.ac.uk/manual.php).

Appendix E

ADAS-EU: Sub-contract 5

CHARGE EXCHANGE AND ION IMPACT DATA FOR FUSION PLASMA SPECTROSCOPY: State-selective charge transfer and excitation for low/medium charge projectiles and neutral hydrogen targets

Summary: It is proposed to commission a set of charge transfer and associated target excitation and ionisation cross-section calculations from TCAM group [1] (Prof. Luis Mndez, Prof. Luis Errea, Dr. Clara Illescas, Dr. Ismanuel Rabadn and coworkers, Departamento de Qumica, Universidad Autnoma de Madrid, Spain). These high quality, fundamental state selective data for neutral hydrogen isotope targets and representative low - high mass, highly ionised projectiles will benchmark iso-nuclear and iso-electronic sequence interpolated and extrapolated data available in the ADAS database and guide further large scale production. It will extend the scope of collisional-radiative data and model support provided under the ADAS-EU Project to the European magnetic confinement fusion community The data, which supports charge exchange studies and spectral measurements with hydrogen, both in neutral beams and in thermal plasma, will be interfaced to spectral measurements on fusion devices at EURATOM Associated laboratories through tailored spectral line scripts within the Atomic Data and Analysis Structure, ADAS. The work will make extensive use of the methods and codes developed by Prof. Riera, Prof. Mndez, Prof. Errea and co-workers. The calculations will be performed at Universidad Autnoma de Madrid. The data will be organised and relayed from Madrid to ADAS in established ADAS data formats with the assistance of ADAS-EU staff. Conversion to spectrum line effective emission coefficients, stopping coefficients and similar derived data will take place at UKAEA/JET Facility and University of Strathclyde. The fundamental and derived data in appropriate ADAS data format collections will be released after assessment and validation to the public domain via OPEN-ADAS [2]. The duration of the project will be eighteen months (Sept. 2009 - Jan. 2011) at a fixed price of 10,000.

Background: The strategy, originated at the JET Facility and now followed by fusion laboratories throughout the world participating in the ADAS Project, for the description of the radiation emission of impurity ions has been the establishment of an integrated atomic data and analysis structure (ADAS). ADAS seeks to provide at appropriate quality, all the derived data required for global modelling and quantitative spectroscopic diagnosis and analysis [3]. The system is based on the initial preparation of collections of fundamental atomic data for specific ions typically including energy levels, transition probabilities and ion and/or electron impact coefficients. Various ADAS computer codes then prepare all the derived data such as net power loss coefficients, spectral line contribution functions etc. in a form directly usable in experimental analysis and in plasma models. The fundamental and derived databases are centrally maintained and accessible by standard routines for modelling and diagnostic applications (eg. edge studies, beam-penetrated plasma studies, visible and VUV spectroscopy). The effectiveness and precision in the applications depends on the quality and availability of fundamental data. In this context a specific need is enhanced provision of state selective charge transfer and excitation data for neutral hydrogen, present both in fast beams and in thermal plasma, in interaction with selected impurity species. Such enhancement is a central theme of the ADAS-EU Euratom/Framework 7 Support Action. Recognizing the complexity of handling some of the fusion relevant heavier element ions and current bounds on atomic reaction computability, ADAS-EU policy falls into two parts. Firstly a modest number of high precision reference calculations and/or measurements at the front edge of current capability are sought. Secondly, as well as direct embedding of the associated precise data in the databases, the data should be exploited as fiducials which can suggest adjustments or global/regional scalings to the large scale semi-automated mass production calculations of the ADAS medium-heavy element baseline. This lift of the baseline is the central objective and the primary delivery. One

of the main sources of calculations of state selective ion impact cross-sections with neutral hydrogen targets is the group established by Prof. Riera. This group has steadily developed and systematised their methods which span from the low energy to high energy regimes and encompass a wide range of both fully ionised and partially ionised colliders. For the low energy regime, the group is a principal exponent of the close-coupled molecular orbital method capable of delivering benchmark quality calculations [4]. These benchmarks can include state-selective charge transfer cross-sections from neutral hydrogen to partially stripped ions of fusion relevant light elements such as carbon or oxygen [5] in the near edge thermal environment as well as total charge transfer. The group has also an wide experience in ion-molecule collisions; in particular, H+ + H2 collisions have been studied in several works (see [6] and references therein). The TCAM group has also applied the method at higher energies towards the range of neutral hydrogen heating beams for detailed comparisons with simpler high-energy-specific methods [7]. The group has special interest in developing and exploiting classical trajectory Monte Carlo methods, primarily applying to the high energy regime but extending towards lower energies through sophisticated microcanonical superpositions [8]. The group has worked on many systems, but has specialised recently on the requirements of charge exchange spectroscopy in magnetic confinement fusion. In particular, they have focussed on extended precision calculations for the light elements beryllium and boron as the fully stripped receivers Be+4 [9] and B+5 [10] as well as the important medium weight rare gas argon as a fully stripped Ar+18 and the partially stripped Ar+16 receivers [11]. The group has also extended the calculations to include the excited hydrogen, H(2s), as a donor to B+5 and Ne+10 [12]. The approach of the TCAM group is ideally suited for matching to and strengthening the ADAS atomic modelling system along the manner described in the first paragraph of this section. In the fusion domain, charge transfer from neutral hydrogen isotopes is of importance near the plasma edge where ebullient thermal neutral hydrogen from the walls interacts with low ionisation stages of impurity elements. State selective charge transfer directly modifies the excited populations which emit observed spectrum lines as well as modifying the balance of ionisation state. Then in fast neutral beam penetrated plasma, plasma and impurity ion impact is the dominant process determining the beam stopping and the state of excitation of the beam atoms. Beam emission spectroscopy, that is analysis of the emission by the excited neutral beam atoms is a key diagnostic closely linked to and influenced by the motional Stark effect in magnetic confinement fusion. The charge transfer part of beam stopping to the plasma impurity ion colliders is the initiating mechanism of charge exchange spectroscopy - another central diagnostic. Neutral beams are usually of neutral hydrogen isotopes for plasma heating but may be specifically diagnostic beams and on occasions may be of neutral helium isotopes or of hydrogen with helium admixture. Both positive ion and negative ion beam sources are relevant to fusion and ITER. The ion-atom collision cross-section data (excitation, ionisation and charge transfer) requirements for these two diagnostic approaches are large since each requires sophisticated collisional-radiative population modelling and the characteristic energy ranges of each beam type in interaction with thermal plasma ion colliders must be spanned. In the experimental spectroscopic diagnostic analysis of the beams/plasma interaction zone, multichord visible spectroscopy is used principally Stark resolved Balmer alpha for the beam emission and high transitions between sub-dominant levels for the charge exchange spectroscopy. The polarisation/directional characteristics of the beam emission is a key part of the beam emission diagnostic application. The planning for ITER has focussed attention on heavier impurity elements such as argon and above as charge exchange spectroscopy emitters. This development has potentially important implications for transport studies since CXS from an ion succession such as Ar+18, Ar+17 and Ar+16 may be observed spatially resolved along the beam-line. Although elements substantially heavier than argon produce a more grass-like CXS spectrum, weak and unsuited to conventional spectrum-line CXS, it has an implications for other planned measurements such as detection of slowing alpha particle emission against the (apparent) Bremsstrahlung continuum. Also it is noted that the cross-section database for impurity ion impact excitation of beam atoms is less complete and assured than that of charge exchange. These issues may be directly addressed by the particular capabilities of the TCAM group. In this respect, the use of both CTMC and one-centre close-coupling expansions is specially suited to be applied in collaboration with Prof. Bernard Pons (CELIA, Universit de Bordeaux I, France). This sub-contract provides an opportunity, through selected ion studies, to lift the quality of ADAS ion impact cross-section database and thereby increase the precision and completeness of the charge exchange and beam emission application support.

The proposed work: The work addresses ion impact collision cross-section data in both in the higher energy fast neutral beam regime and in the low energy thermal plasma regime and falls into four parts, namely, improved CTMC calculations of nl-resolved CX data from fast hydrogen isotope beams and associated hydrogen target excitation data, examination and recommendation of global parametric forms for nl-resolved data interpolation and extrapolation, studies of low energy transfer from neutral hydrogen to partially stripped ionisation stages of light elements and recommendation of total charge exchange cross-sections for collisional-radiative modelling of ionisation state in thermal edge plasma. (1) Extension of existing CTMC and improved CTMC calculations to include complete nl-selective charge exchange cross-section data from H(1s) targets and associated H(1s) target excitation to l-resolved levels with n?4 in interaction with selected fully stripped projectiles up to Kr+36 at energies above 10keV/amu. The collision

data will be assembled in ADAS adf01 format. (2) Extension of CTMC calculations to evaluate nl-resolved charge exchange cross sections for collisions of selected ions with H(n=2). (3) Assessment of global parametric fitting forms for total, n- and nl-resolved charge exchange data as a function of z for interpolation and extrapolation. Parametric forms will be optimised by fitting to the selected data of (1) above and used to provide an adf01 baseline for arbitrary charged projectiles for the fast hydrogen beam target and energy range. (4) Incorporation of selected bench mark CCMO calculations for partially stripped light impurity ion in interaction with thermal neutral hydrogen in ADAS specific ion files of format adf04. (5) Review and recommend total charge transfer approximations and rate coefficients for thermal neutral hydrogen donors in interaction with arbitrary low charge state (principally residual charge ¡4) thermal impurity ion receivers. The thermal ranges will correspond with the electron temperature range of significant fractional abundance of the impurity ions in fusion plasma. The data will be incorporated as CCD and PRC category data in the ADAS data format adf11 baseline.

Integration of data into ADAS will be executed by staff of the ADAS-EU, including the conversion to the key derived data format adf11, adf12, adf21 and adf22. ADAS-EU staff will pay working visits to Universidad Autnoma de Madrid to assist with execution of the above tasks as appropriate. A copy of ADAS software will be made available on a workstation at the Departamento de Qumica, Universidad Autnoma de Madrid at no charge for local use.

References:

[1] http://tcam.qui.uam.es
[2] http://www.adas.ac.uk/openadas.php
[3] http://www.adas.ac.uk [3] P Barragan, L F Errea, L Méndez et al. (2006) Phys. Rev A 74, 024701.
[4] C N Cabello, L F Errea et al. (2003) J. Phys. B 36, 307.
[5] L F Errea, C Illescas, L Méndez et al. (2004) Phys. Rev A 70, 052713.
[6] L. F Errea et al. (2009) J. Phys. B 42, 105207.
[7] L F Errea, C Illescas, L Méndez et al. (2004) J. Phys. B 37, 4323.
[8] F Guzmán et al. (2008) Phys. Rev A 77, 012706.
[9] L F Errea, F Guzmán et al. (2006) Plasma Physics and Control. Fusion 48, 1585.
[10] L F Errea, C Illescas, L Méndez et al. (2006) J. Phys. B 39, L91.
[11] L F Errea, F Guzmán et al. (2007) J. Phys. Conf. Ser. 58, 203.
[12] L.F. Errea et al. (2006) Phys. Rev. A 74,012722.

Appendix F

ADAS-EU: Sub-contract 6

POSITIVE ION IMPACT DATA FOR FUSION APPLICATIONS: Data for hydrogen and helium beam stopping and emission

Summary: It is proposed to commission a data review, evaluation of selective database restructuring and initial data filling of new ADAS data formats from Prof. Ronnie Hoekstra, KVI, University of Groningen, Netherlands. These actions centre on the current provisions of ion impact data for neutral hydrogen and helium isotope beam stopping and emission in the range 5keV/amu to 200keV/amu in the ADAS databases. It will extend the scope of collisional-radiative data and model support provided under the ADAS-EU Project to the European magnetic confinement fusion community The data, which supports hydrogen beam stopping and emission due to ion colliders, will be interfaced to spectral measurements and beam and beam-sourced ion transport models for fusion devices at EURATOM Associated laboratories and ITER through tailored data formats within the Atomic Data and Analysis Structure, ADAS. The work will make use of the methods and experience developed by Prof. Hoekstra and co-workers in support of the JET experiment and new experimental capabilities at KVI. Experiments clarifying orientation/alignment and angular differential cross-sections will be performed with the MOTRIMS/COLTRIMS capability at KVI in conjunction with the KVI ECR source and the Heidelberg EBIT. Restructured data formats and new data formats for angular differential cross-sections and dressed ion impact reactions will be designed, organised and initially filled at KVI in engagement with ADAS-EU staff. Conversion to derived data formats through collisional-radiative modelling, especially beam stopping, effective emissivities and appropriate driver/receiver reaction resolved data will take place at UKAEA/JET Facility and University of Strathclyde. The fundamental and derived data in appropriate ADAS data format collections will be released after assessment and validation to the public domain via OPEN-ADAS [1]. The duration of the project will be one and a half year (Oct. 2009 - Apr. 2011) at a fixed price of 10,000.

Background: The strategy, originated at the JET Facility and now followed by fusion laboratories throughout the world participating in the ADAS Project, for the description of the radiation emission of impurity ions has been the establishment of an integrated atomic data and analysis structure (ADAS). ADAS seeks to provide at appropriate quality, all the derived data required for global modelling and quantitative spectroscopic diagnosis and analysis [2]. The fundamental and derived databases are centrally maintained and accessible by standard routines for modelling and diagnostic applications (eg. edge studies, VUV and XUV spectroscopy). The effectiveness and precision in the applications depends on the quality and availability of fundamental data. In this context a specific need is enhanced provision for neutral beam stopping and emission with both hydrogen and helium isotope beam species and plasma ion colliders. Such enhancement is a central theme of the ADAS-EU Euratom/Framework 7 Support Action. Recognizing the importance of diagnostic spectral observations of beam emission for ITER, the use of negative ion-sourced beams and the consolidation of beam and slowing down particle transport models, ADAS-EU policy falls into two parts. Firstly a modest number of related fundamental measurements at the front edge of current capability will be made. Of necessity some of these fundamental measurements are indicative rather than direct since exact matching of reactants to the fusion case is not possible. Secondly, the measurements will be used to guide model and data enhancements as outlined below - an area of considerable experience and success in the earlier collaboration between JET and KVI. The associated upgrade of ADAS beam stopping and emission is the central objective and the primary delivery. One of the main sources of experimental cross-sections for highly charge ion colliders on neutral targets is the group of Prof. Hoekstra. Focussing in the early nineties on spatially resolved spectroscopic measurements along the ion collider

beam line downstream from the target, the work provided benchmark state resolved charge transfer data for fusion neutral beam scenarios, underpinning associated calculations [3]. The group maintained strong engagement with the JET Joint Undertaking and the fusion community throughout the nineties, extending the ADAS charge exchange databases and modelling capability to include helium donors (ground and metastable) and excited hydrogen donors [4] as well as adding beam excitation cross-section data [5]. In recent years, the group has introduced recoil ion momentum spectroscopy and cold atom traps, working extensively with helium and sodium with ion colliders from in-house ECR sources and from external EBIT sources. The studies span from Ar+15 Ar+18 state selective single electron capture from helium [6] through to ionisation and capture in He+2 /Na collisions [7]. Such latter studies which can include differential cross-section measurement and target (Na 3p) alignment are specially noted for this proposal. The group has strong contacts with theoretical groups and has maintained a strong interest in review and assessment of ion/atom collision data. It has participated in many International Atomic Energy Agency sponsored data reviews and collaborative research programs. For magnetic confinement fusion devices penetrated by fast neutral beams for heating or diagnostic purposes, the atomic reactions of the beam and plasma ions are a central issue. They moderate the deposition of energy by the beams into the plasma and initiate the charge transfer and beam excitation reactions which lead to charge exchange spectroscopy (CXS) and beam emission spectroscopy (BES). In the advance towards ITER, ions of heavier species such as argon and beyond become significant for beam stopping. Also the key motional Stark effect (MSE) internal field measurement will become dependent on beam emission spectroscopy rather than polarization. There are then some atomic physics issues for attention. Plasma ion impact dominates electron for excitation of beam atoms and all impurity ion species in the plasma contribute, broadly in proportion to their share of zeff . The primary excitation cross-section data is currently insufficiently precise at all energies to sustain the hoped-for precision of the BES diagnostic, relying in many cases on z-scaled values. Also, along with a required extension to heavier species, it is noted that partially stripped impurity ions may be present in the confined plasma. The collision of an impurity ion with a beam atom state, because of the fast beam speed is essentially directional, the effective cross-sections being only partial angularly integrated cross-sections over a solid angle depending on the beam to thermal speed ratio larger for light thermal nuclei (such as deuterons) and fast ions. The target atom, usually a hydrogen isotope, in an excited shell has Stark alignment and distortion orthogonal to the beam direction. Collisions, from a collisional-radiative modelling perspective may be seen as potentially differentiating in their influence on n, k or m mixing (in Stark quantisation) where the n=2, 3 and 4 shells are the most important. All these effects have not yet been included in beam emission/beam stopping. Attention to the above considerations is the key to increasing the scope of the BES diagnostic and to lifting the ADAS database and modelling to the level of precision sought for ITER.

The proposed work: The work falls into four parts: (1) Assessment, extension and re-specification of ADAS data format adf02. Data sets will be for specific target neutral, will follow the broad pattern of adf04 files and will include excitation, net CX and ionisation data. The data for the light elements colliders He+2, Be+4, B+5, C+6, O+8 and Ne+10 will be considered and updated. The format will remain as a total cross-section type. (2) Assessment of angular differential excitation and ionisation cross-sections for selected ion colliders with He(1s2) target from MOTRIMS/COLTRIMS measurement. Investigate with ADAS-EU staff the structure for a new ADAS data format for ion impact angular differential data for He (1s2) and H(1s) and the possibilities of initial filling with a transfer algorithm from the total cross-section database of (1) and the study above. (3) Assessment of angular differential excitation, ionisation and charge transfer cross-sections for selected ion colliders with Na(3s) and aligned Na(3p) targets from MOTRIMS measurement. Investigate with ADAS-EU staff the possibilities of initial filling the new angular differential cross-section ADAS format for H(n=2) and H(n=3) Stark states with a transfer algorithm from the total cross-section database of (1) and the study above. (4) Investigatation with ADAS-EU staff of the character of Stark nkm mixing for neutral hydrogen beams in the energy range 5-200 keV/amu beam emission studies. . Integration of data into ADAS will be executed by staff of the ADAS-EU, including the conversion to the key derived data format adf12, adf21, and adf22. ADAS-EU staff will pay working visits to Groningen to assist with execution of the above tasks as appropriate. A copy of ADAS software will be made available on a workstation at the KVI, University of Groningen at no charge for local use.

References:

[1] http://www.adas.ac.uk/openadas.php
[2] http://www.adas.ac.uk
[3] R Hoekstra, H Anderson, F W Bliek et al. (1998) Atomic and Molecular Data & their Applications (ed. Mohr, AIP Press) pp37-56
[4] R Hoekstra, H Anderson, et al. (1998) Plasma Physics & Control. Fusion 40, 1541.
[5] H O Folkerts, F W Bliek, et al. (1994) J. Phys. B. (1994) 27, 3475
[6] S Knoop, D Fischer et al. (2008) J. Phys.B 41, 195203.

[7] S Knoop, R E Olson et al. (2005) J. Phys.B 38, 1987.